

**TRACE ELEMENTS IN FLOODPLAIN SOILS -  
EFFECTS OF REDOX CONDITIONS ON THE MOBILITY OF  
TRACE ELEMENTS AND VOLATILIZATION OF MERCURY**

Inaugural-Dissertation

zur

Erlangung des Doktorgrades

der Mathematisch-Naturwissenschaftlichen Fakultät

der Universität zu Köln

vorgelegt von

Iris Hindersmann

aus Lindlar

2013

Berichterstatter: Prof. Dr. Tim Mansfeldt

Prof. Dr. Carsten Munker

Tag der mündlichen Prüfung: 22.01.2014



## ABSTRACT

*Purpose.* Floodplains are characterized by periodic flooding and their soils can contain high concentrations of trace elements. The flooding events lead to varying oxygen contents in the soil. This is accompanied with varying redox conditions that are expressed by strongly fluctuating redox potentials. This study investigated the influence of flooding events on the mobilization of the trace elements arsenic, cadmium, cobalt, chromium, copper, molybdenum, nickel, lead, antimony, and zinc, as well as the volatilization of mercury in laboratory experiments.

*Material and methods.* Multi-contaminated floodplain soils from the Elbe River in Lower Saxony, Germany, and the Wupper River in North Rhine-Westphalia, Germany, were used for the experiments.

The first type of experiment was a microcosm experiment. Soil suspensions were held at fixed redox conditions in these experiments. In the first experiment we investigated the influence of oxidizing (oxygen predominant), weakly reducing (tri- and tetravalent manganese reduction), and moderately reducing (trivalent iron reduction) conditions at three temperatures (7, 15, and 25 °C) on the solubility of ten trace elements. Soil suspensions were sampled at different intervals and analyzed for trace elements and accompanying parameters (iron, bivalent iron, manganese, chloride, sulfate, and dissolved organic carbon). In the second experiment we investigated the distribution of mercury among the solid, dissolved, and gaseous phases under moderately reducing (trivalent iron reduction) and strongly reducing (hexavalent sulfur reduction) conditions. The degassed mercury was trapped in tubes filled with activated carbon in order to determine the total mercury volatilized. On every third day soil suspensions were sampled, filtered, and analyzed for dissolved and solid mercury. The mercury in the three different phases was analyzed with a direct mercury analyzer (DMA-80, MLS, Germany).

The other type of experiment was the soil column experiment with undisturbed soil cores from the topsoil at the Elbe River. Soil columns were incubated at 20 °C with various soil moisture contents (water-saturated for two weeks, 95 and 90% water content for one week each) and the redox potential was recorded. The gaseous mercury that accumulated in the headspace of the flux chamber of the columns was pumped over cooled traps filled with adsorber material and analyzed by gas chromatography/inductively coupled plasma mass spectrometry for the various mercury species.

*Results.* In the microcosm experiments the solubility of the trace elements was low under oxidizing conditions. Reductive dissolution of manganese oxides under weakly reducing conditions was accompanied by a release of cobalt and molybdenum. Reductive dissolution of iron oxides (and of remaining manganese oxides) under moderately reducing conditions also led to a release of arsenic, cadmium, chromium, nickel, and lead, whereas copper and zinc were hardly affected. Antimony revealed different behavior, because after an initial increase a continuous decrease in its concentration was observed soon after the onset of weakly reducing conditions. This could be attributed to the fact that the antimony species changed to a strongly bound species. We conclude that soil temperature should be considered as a master variable when distinguishing between weakly and moderately reducing soil conditions. It is also necessary to keep element specific behavior in mind when dealing with the effects of redox conditions on trace element solubility in soils.

In the second microcosm experiment the dissolution of mercury was highest at the beginning of the experiment and then decreased rapidly. This resulted from the dissolved mercury being reduced to the gaseous species (elemental mercury), which then could evaporate. Mercury volatilization reached its maximum around day 20 and then strongly decreased. Overall, during the course of the experiment only small amounts of mercury were dissolved; hence, only small amounts could volatilize. This resulted from the strong binding of mercury in this soil, as revealed by sequential fractionation.

In the column experiments watering the soil resulted in a rapid decrease in the redox potential and the achievement of strongly reducing conditions (redox potential  $< -100$  mV). Mercury concentrations in the pore water decreased continuously from  $68.3 \mu\text{g L}^{-1}$  mercury in the beginning to  $5.78 \mu\text{g L}^{-1}$  mercury at the end of the experiment. Species analyses revealed that only elemental mercury became volatile. The volatilization rate of mercury was between  $1.73$  and  $824 \text{ ng m}^{-2} \text{ h}^{-1}$ , which is consistent with other studies at the Elbe River site.

*Conclusions.* Lowering the redox potential in all experiments resulted mostly in increased solubility of the trace elements. However, the reactions of the trace elements were element specific. For mercury the increasing solubility under reducing redox conditions led to increased volatilization of mercury, because dissolved mercury in soil solutions can be reduced to gaseous mercury species.

## KURZZUSAMMENFASSUNG

*Einleitung.* Auenböden zeichnen sich durch hohe Kontaminationen von Spurenelementen und variierende Wassergehalte infolge stark schwankender Grundwasserstände aus. Die variierenden Wassergehalte führen zu unterschiedlichen Sauerstoffgehalten im Boden und dieses bedingt Veränderungen im Redoxpotenzial. Die Löslichkeit der Spurenelemente Arsen, Cadmium, Kobalt, Chrom, Kupfer, Molybdän, Nickel, Blei, Antimon und Zink und die Ausgasung von Quecksilber unter variierenden Redoxpotenzialen stehen im Mittelpunkt der hier vorgestellten Arbeit.

*Material und Methoden.* Auenböden der Elbe (Hohnstorf, Niedersachsen) und Wupper (Leichlingen, Nordrhein-Westfalen) wurden für die Studien genutzt. Diese Auenböden weisen erhöhte Spurenelementgehalte gegenüber den natürlichen Hintergrundwerten auf.

Die erste Versuchsreihe wurde mit Mikrokosmen durchgeführt. Bei diesen Versuchen wurden an Bodensuspensionen definierte Redoxpotenziale eingestellt. Die Versuche wurden mit den Redoxstufen oxidierend, schwach reduzierend (Reduktion von drei- und vierwertigem Mangan) und reduzierend (Reduktion von dreiwertigem Eisen) mit den Temperaturvarianten 7, 15 und 25 °C durchgeführt. In unterschiedlichen Intervallen wurde Bodensuspension entnommen, gefiltert und die Spurenelementkonzentrationen und weitere Parameter (Eisen, zweiwertiges Eisen, Mangan, Chlorid, Sulfat und der gelöste organische Kohlenstoff) bestimmt. Weitere Mikrokosmenversuche wurden in einer zweiten Versuchsreihe durchgeführt, um die Verteilung des Quecksilber in der Fest-, Flüssig- und Gasphase zu bestimmen. Hierbei wurden die Redoxstufen oxidierend, reduzierend (Reduktion von dreiwertigem Eisen) und stark reduzierend (Reduktion von sechswertigem Schwefel) bei einer Temperatur von 20 °C angesteuert. Das ausgasende Quecksilber wurde auf Röhrchen, die mit Aktivkohle gefüllt waren, gebunden. In gleichbleibenden Intervallen wurde Bodensuspension entnommen und gefiltert. Das Quecksilber in den Proben wurde mit einem Direktanalysator (DMA-80, MLS, Deutschland) bestimmt.

An ungestörten Bodenproben wurden in einer dritten Versuchsreihe Säulenversuche mit variierenden Wassergehalten (wassergesättigt für zwei Wochen, 95 und 90 % Wassergehalt für jeweils eine Woche) bei 20 °C in einem Inkubator durchgeführt. Das Redoxpotenzial wurde über den gesamten Versuch aufgezeichnet. Das ausgasende Quecksilber wurde unter Glashauben auf den Säulen gesammelt und zur Analyse auf –180 °C gekühlt und mit Quecksilber-Adsorbent gefüllten Röhrchen gebunden. Die Analyse wurde mit einer Gaschromatographie/Massenspektrometrie mit induktiv gekoppeltem Plasma durchgeführt.

*Ergebnisse.* In den ersten Mikrokosmenversuchen zeigte sich unter oxidierenden Bedingungen nur eine sehr geringe Löslichkeit der Spurenelemente. Die reduktive Lösung von Manganoxiden unter schwach reduzierenden Bedingungen führte zu einer erhöhten Löslichkeit von Kobalt und Molybdän. Die verstärkte Löslichkeit von Eisenoxiden unter reduzierenden Bedingungen bedingte eine vermehrte Lösung von Arsen, Cadmium, Chrom, Nickel und Blei. Die Elemente Kupfer und Zink zeigten auch unter diesen Bedingungen keine verstärkte Löslichkeit. Antimon zeigte ein anderes Verhalten, da nach einem ersten Anstieg der Löslichkeit die Konzentration in der Bodensuspension mit der Ansteuerung von reduzierenden Bedingungen abnahm. Ursache für diese Entwicklung kann die Umwandlung der Antimonspezies zu einer stärker gebundenen Spezies sein. Auch die Temperatur zeigte sich als ein wichtiger Einflussfaktor, da sie entscheidend ist für die Geschwindigkeit, mit der sich reduzierende Bedingungen einstellten. Wichtig ist es auf das elementspezifische Verhalten von Spurenelementen bei dem Effekt des Redoxpotenzials auf die Löslichkeit zu achten.

In der zweiten Mikrokosmenversuchsreihe war die Löslichkeit von Quecksilber zu Beginn der Experimente am stärksten und nahm dann rapide ab. Diese Abnahme ist auf die Bildung von gasförmigem Quecksilber zurückzuführen, welches ausgasen kann. Die Ausgasung von Quecksilber erreichte ihr Maximum etwa am 20. Tag des Experiments und nahm dann deutlich ab. Allgemein zeigte sich in diesem Versuch, dass nur sehr wenig Quecksilber gelöst wurde und daher auch nur wenig für die Ausgasung verfügbar war. Zurückzuführen war dieses Verhalten auf die starke Bindung von Quecksilber im Boden, was durch die sequentielle Extraktion bestätigt wurde.

In den Säulenexperimenten führte die Bewässerung der Säulen zu einer Absenkung des Redoxpotenzials, bis stark reduzierende Bedingungen (Redoxpotenzial  $< -100$  mV) erreicht waren. Die Konzentration von Quecksilber in dem Porenwasser des Bodens zeigte eine kontinuierliche Abnahme ( $68.3 \mu\text{g L}^{-1}$  zu  $5.78 \mu\text{g L}^{-1}$ ) bis zum Ende des Experimentes. Die Speziesanalyse zeigte, dass ausschließlich elementares Quecksilber ausgasete. Die Ausgasungsraten variierten zwischen  $1.73$  und  $824 \text{ ng m}^{-2} \text{ h}^{-1}$ . Dieses stand im Einklang mit den Ausgasungsraten anderer Studien, die an der Elbe durchgeführt wurden.

*Fazit.* Die Veränderung des Redoxpotenzials zu reduzierenden Bedingungen führte bei den meisten Spurenelementen zu einer verstärkten Löslichkeit. Es bestanden jedoch metallspezifische Unterschiede. Bei Quecksilber führte die verstärkte Löslichkeit unter reduzierenden Bedingungen zu einer verstärkten Ausgasung von Quecksilber, da mehr gelöstes Quecksilber für die Reduktion zu gasförmigen Quecksilber vorhanden war.

## ACKNOWLEDGEMENT

It would not be possible to write this thesis without the help and support of people around me, to only some of whom it is possible to give a particular mention here.

At first I give a special thank to my advisor Prof. Dr. Tim Mansfeldt for the continuous support of my thesis. I especially acknowledge his numerous encouraging and intensive discussions.

Beside my advisor I would like to thank the rest of my thesis committee Prof. Dr. Carsten Munker, Prof. Dr. Manfred Mühlberg, and Dr. Oliver Bödeker for their encouragement, insightful comments and hard questions.

I thank Dr. Jörg Hippler and Prof. Dr. Alfred V. Hirner from the Institute of Environmental Analytical Chemistry from the University of Duisburg-Essen. Thank you for the measurement, the support, and the inspired discussions.

This thesis was supported by the German Research Foundation (DFG) under the contract no. Ma 2143/9-1 (Einfluss von Bodenwassergehalten und Bodenredoxpotenzialen auf die Löslichkeit und Verflüchtigung von Hg-Spezies aus kontaminierten Böden) and the RheinEnergieStiftung under the contract no. W-09-2-018 (Einfluss von Wassergehalten, Redoxpotenzialen und Temperaturen auf die Verflüchtigung von Quecksilber-Spezies aus kontaminierten Böden in Köln). I gratefully acknowledge the financial support.

Without the active support in field and laboratory measurements of the working group from Prof. Dr. Tim Mansfeldt, this thesis could not have been accomplished. My special thanks go to Svenja Helle, Karin Greef, Katrin Matern, Corinna Földi, Kristof Dorau, Dr. Stefan Schuth, Dr. Mark Overesch, Tobias Matern, Henry Bohn, and Henning Schiedung.

Last but not least, I thank Carsten for his support and love. Many thanks also go to my parents, Elisabeth and Paul, and sisters, Carola and Heike, for supporting me throughout my entire life.

Special thanks go to Lena who has enriched my life enormously.



# TABLE OF CONTENT

<b>List of figures</b> .....	<b>XI</b>
<b>List of tables</b> .....	<b>XIII</b>
<b>List of abbreviations</b> .....	<b>XIV</b>
<b>1 Introduction</b> .....	<b>1</b>
<b>2 Test site and project implementation</b> .....	<b>5</b>
<b>2.1 Test site</b> .....	<b>5</b>
<b>2.2 Project implementation</b> .....	<b>9</b>
<b>3 Trace-element solubility in a multi-contaminated soil as affected by     redox conditions and temperature</b> .....	<b>11</b>
<b>3.1 Introduction</b> .....	<b>11</b>
<b>3.2 Material and methods</b> .....	<b>13</b>
3.2.1 Study site, sampling, and sample preparation.....	13
3.2.2 Soil characteristics .....	14
3.2.3 Contents and fractionation of trace elements.....	14
3.2.4 Soil incubation in microcosms.....	15
3.2.5 Analyses of soil suspensions and extractants.....	16
3.2.6 Modeling and statistical calculations .....	17
<b>3.3 Results and Discussion</b> .....	<b>17</b>
3.3.1 Soil properties and trace element status.....	17
3.3.2 Fractionation of trace elements.....	19
3.3.3 Redox potential, temperature, and pH .....	21
3.3.4 Further redox-sensitive and non-redox sensitive parameters.....	24
3.3.4.1 Manganese .....	24
3.3.4.2 Iron.....	26
3.3.4.3 Sulfate .....	26

3.3.4.4	Dissolved Organic Carbon .....	27
3.3.4.5	Chloride.....	27
3.3.5	Trace elements .....	28
3.3.5.1	Non-redox sensitive and cationic trace elements.....	28
3.3.5.1.1	Cadmium .....	32
3.3.5.1.2	Nickel .....	32
3.3.5.1.3	Lead.....	33
3.3.5.1.4	Zinc.....	34
3.3.5.1.5	Copper .....	34
3.3.5.2	Redox sensitive and/or anionic trace elements .....	35
3.3.5.2.1	Cobalt .....	35
3.3.5.2.2	Molybdenum .....	36
3.3.5.2.3	Arsenic.....	37
3.3.5.2.4	Chromium.....	38
3.3.5.2.5	Antimony.....	39
<b>3.4</b>	<b>Conclusion .....</b>	<b>40</b>
<b>4</b>	<b>Mercury volatilization from a floodplain soil during a simulated flooding event .....</b>	<b>42</b>
<b>4.1</b>	<b>Introduction.....</b>	<b>42</b>
<b>4.2</b>	<b>Material and Methods .....</b>	<b>43</b>
4.2.1	Study site, sampling, and sample preparation.....	43
4.2.2	Soil characteristics .....	44
4.2.3	Soil column experiments.....	45
4.2.4	Analyses of soil solution and extractants.....	47
4.2.5	Species analyses of gaseous mercury .....	48
<b>4.3</b>	<b>Results and discussion .....</b>	<b>48</b>
4.3.1	Soil properties and sequential extraction of mercury .....	48

4.3.2	Redox potential and water content.....	50
4.3.3	Total mercury in the soil columns.....	52
4.3.4	Dissolved mercury in the soil columns.....	53
4.3.5	Gaseous mercury in the headspace of the soil columns.....	53
4.3.5.1	Mercury species .....	53
4.3.5.2	Mercury volatilization during the course of the experiment.....	55
4.3.5.3	Rates of mercury volatilization.....	57
<b>4.4</b>	<b>Conclusion .....</b>	<b>58</b>
<b>5</b>	<b>Phase distribution of mercury under defined redox conditions of a floodplain</b>	
	<b>soil of the Elbe River.....</b>	<b>59</b>
<b>5.1</b>	<b>Introduction.....</b>	<b>59</b>
<b>5.2</b>	<b>Material and Methods .....</b>	<b>60</b>
5.2.1	Study site, sampling, and sample preparation.....	60
5.2.2	Soil characteristics .....	61
5.2.3	Soil incubation in microcosms.....	62
5.2.4	Analyses of soil suspensions, extractants, filter residual and gaseous Hg phase.....	63
5.2.5	Modeling and statistical calculations.....	64
<b>5.3</b>	<b>Results and Discussion.....</b>	<b>64</b>
5.3.1	Soil properties .....	64
5.3.2	Sequential extraction.....	65
5.3.3	Redox potential and pH .....	66
5.3.4	Manganese, iron, sulfate, chloride, and dissolved organic carbon .....	68
5.3.5	Hg in different phases .....	73
5.3.5.1	Hg in filter residual .....	73
5.3.5.2	Hg in soil solution.....	74
5.3.5.3	Volatilization of Hg.....	76
<b>5.4</b>	<b>Conclusions.....</b>	<b>77</b>

<b>6</b>	<b>Conclusions.....</b>	<b>78</b>
<b>7</b>	<b>Literature.....</b>	<b>82</b>

## LIST OF FIGURES

Fig. 2.1: Map of Northern Germany with the two sampling sites; Elbe in Hohnstorf und Wupper in Leichlingen.....	6
Fig. 2.2: Sampling site a at the Wupper in Leichlingen and site b at the Elbe in Hohnstorf .....	7
Fig. 3.1: Scheme of a microcosm and control device .....	15
Fig. 3.2: Development of redox potential ( $E_H$ ) and pH during the microcosm experiments performed at 7, 15, and 25 °C (● 7 °C, ▲ 15 °C, ■ 25 °C).....	22
Fig. 3.3: Development of the concentrations of total Mn, total Fe ( $Fe_{tot}$ ), ferrous Fe ( $Fe^{2+}$ ), sulfate, chloride, and dissolved organic carbon (DOC) during the microcosm experiments performed at 7, 15, and 25 °C (● 7 °C, ▲ 15 °C, ■ 25 °C) with change of conditions from oxidising to weakly reducing und from weakly reducing to moderately reducing at 25 °C —, 15 °C —, and 7 °C — .....	25
Fig. 3.4: Development of the concentration of ten trace elements during the microcosm experiments performed at 7, 15, and 25 °C (● 7 °C, ▲ 15 °C, ■ 25 °C) with change of conditions from oxidising to weakly reducing und from weakly reducing to moderately reducing at 25 °C —, 15 °C —, and 7 °C — .....	29
Fig. 3.5: Relationship between the concentrations of ten trace elements and the redox potential ( $E_{HpH7}$ ) performed at 7, 15, and 25 °C (● 7 °C, ▲ 15 °C, ■ 25 °C).....	30
Fig. 4.1: Scheme of the experimental design for sampling of gaseous Hg including a column with a flux chamber and a gas sampler equipped with an ethanol-filled Dewar flask cooled to -100 °C .....	46
Fig. 4.2: Development of redox potential ( $E_H$ ) during the column experiments (● column A; ▲ column B; ■ column C; ▼ sampling gas probe of the headspace under the flux chambers; ● removal of water) .....	51

Fig. 4.3: Measurement of sampling 3 of column A by GC-ICP-MS (— $^{200}\text{Hg}$ ; and — $^{202}\text{Hg}$ ) .....	54
Fig. 4.4: Development of the amounts of gaseous Hg (■ column A; ■ column B; and ■ column C). On day 1, an amount of 0.4 ng Hg was detected for column C. All other missing values are due to sampling or analytical shortcomings. Removal of water was done on days 14 and 21. ....	56
Fig. 5.1: Scheme of a microcosm and control device .....	62
Fig. 5.2: Development of redox potential ( $E_{\text{H}}$ ) and pH during the microcosm experiments (● moderately reducing, ● strongly reducing) .....	67
Fig. 5.3: Development of the concentrations of total Mn, total Fe ( $\text{Fe}_{\text{tot}}$ ), ferrous Fe ( $\text{Fe}^{2+}$ ), sulfate, chloride, and dissolved organic carbon (DOC) during the microcosm experiments (● moderately reducing, ● strongly reducing).....	70
Fig. 5.4: Development of the concentrations of Hg in the filter residual (solid) ( $\text{Hg}_{\text{s}}$ ), dissolved Hg ( $\text{Hg}_{\text{d}}$ ), and gaseous Hg ( $\text{Hg}_{\text{g}}$ ) (● moderately reducing, ● strongly reducing).....	74

## LIST OF TABLES

Tab. 2.1: General characteristics of the sites from the Wupper in Leichlingen and Elbe in Hohnstorf.....	8
Tab. 3.1: Chemical and physical characteristics of the Ah horizon of a grassland Fluvisol from the Wupper river at Leichlingen, North Rhine-Westphalia, Germany.....	18
Tab. 3.2: Amounts of trace elements as determined by aqua regia in the Ah horizon of a grassland Fluvisol from the Wupper river at Leichlingen, North Rhine-Westphalia, Germany [ $\text{mg kg}^{-1}$ ].....	19
Tab. 3.3: Sequential extraction of trace elements in the Ah horizon of a grassland Fluvisol from the Wupper river at Leichlingen, North Rhine-Westphalia, Germany [ $\text{mg kg}^{-1}$ ] .....	20
Tab. 3.4: Correlation between $E_H$ and the trace element concentrations .....	31
Tab. 4.1: Chemical and physical characteristics of the Ah horizon of a Fluvisol from the Elbe River at the biosphere reserve "Niedersächsische Elbaue" at Hohnstorf, Lower Saxony, Germany .....	49
Tab. 4.2: Sequential extraction of Hg in the Ah horizon of a grassland Fluvisol from the Elbe River in the biosphere reserve "Niedersächsische Elbaue" at Hohnstorf, Lower Saxony, Germany [ $\text{mg kg}^{-1}$ ] .....	50
Tab. 4.3: Concentration of Hg in the soil solution measured after days 14, 21, and 28 ...	53
Tab. 5.1: Chemical and physical characteristics of the Ah horizon of a Fluvisol from the Elbe river at the biosphere reserve "Niedersächsische Elbaue" at Hohnstorf, Lower Saxony, Germany .....	65
Tab. 5.2: Sequential extraction of Hg in the Ah horizon of a grassland Fluvisol from the Elbe river at the biosphere reserve "Niedersächsische Elbaue" at Hohnstorf, Lower Saxony, Germany [ $\text{mg kg}^{-1}$ ] .....	66

## LIST OF ABBREVIATIONS

aAh horizon	soil horizon with humus enrichment with alluvial dynamics	
Ag-AgCl electrode	silver-silver chloride electrode	
Ah horizon	soil horizon with humus enrichment	
Al	aluminum	
As	arsenic	
BBodSchV	Federal Soil Protection Regulation	
BGR	Federal Institute for Geosciences and Natural Resources of Germany	
BrCl	bromine chloride	
C	carbon	
C/N	carbon to nitrogen ratio	
C <sub>6</sub> H <sub>12</sub> O <sub>6</sub>	glucose	
CaCl <sub>2</sub>	calcium chloride	
Cd	cadmium	<i>(Cd<sup>2+</sup>, CdCl<sup>+</sup>)</i>
CH <sub>3</sub> COO <sup>-</sup> /CH <sub>3</sub> COOH	acetic acid	
CH <sub>3</sub> COONH <sub>4</sub>	ammonium acetate	
Cl <sup>-</sup>	chloride	
Co	cobalt	<i>(Co(OH)<sub>3</sub>, Co<sup>2+</sup>, Co<sup>3+</sup>, CoOOH, Co<sup>II</sup>)</i>
CO <sub>2</sub>	carbon dioxide	
Cr	chromium	<i>(Cr<sup>3+</sup>, CrO<sub>4</sub>, HCrO<sub>4</sub><sup>2-</sup>, Cr<sup>III</sup>, Cr<sup>VI</sup>)</i>
Cu	copper	<i>(Cu<sup>0</sup>, Cu<sup>I</sup>)</i>
DMHg	dimethylmercury	<i>((CH<sub>3</sub>)<sub>2</sub>Hg)</i>
DOC	dissolved organic carbon	
DOM	dissolved organic matter	
e <sup>-</sup>	electron	
e. g.	exempli gratia - for example	
E <sub>H</sub>	redox potential	
E <sub>HpH7</sub>	redox potential converted to pH 7	
FAO	Food and Agriculture Organization	



Fe	iron	$(Fe^{2+}, Fe^{3+}, FeOOH, Fe^{II}, Fe^{III}, Fe_{tot}, Fe_xS, Fe(OH)_3)$
Fe <sub>d</sub>	iron dissolved by dithionite extract	
Fe <sub>o</sub>	iron dissolved by oxalate extract	
Fig.	figure	
GC	gas chromatography	
H <sup>+</sup>	hydrogen	
H <sub>2</sub> O	water	
H <sub>2</sub> O <sub>2</sub>	hydrogen peroxide	
HCl	hydrochloric acid	
Hg	mercury	$(Hg^0, CH_3Hg^+, Hg^{2+}, (CH_3)_2Hg)$
HNO <sub>3</sub>	nitric acid	
i. e.	id est - that means	
ICP-MS	inductively coupled plasma mass spectrometry	
IUSS	International Union of Soil Sciences	
KOH	potassium hydroxide	
LABO	Federal/State soil protection working group	
LANUV	Regional Office for Nature, Environment and Consumer Protection	
Mn	manganese	$(Mn^{2+}, Mn^{III}, Mn^{IV}, MnO_2, MnS)$
Mo	molybdenum	
MMHg	monomethylmercury	$(CH_3Hg^+)$
N	nitrogen	$(N^V)$
n	number of samples	
Na <sub>2</sub> SO <sub>4</sub>	sodium sulfate	
NH <sub>4</sub> -EDTA	ammonium ethylene-diamine-tetraacetic acid	
NH <sub>4</sub> NO <sub>3</sub>	ammonium nitrate	
(NH <sub>4</sub> ) <sub>2</sub> C <sub>2</sub> O <sub>4</sub> · H <sub>2</sub> O	ammonium oxalate monohydrate	
NH <sub>2</sub> OH HCl	hydroxylamine hydrochloride	
Ni	nickel	

NO <sub>3</sub> <sup>-</sup>	nitrate	
O <sub>2</sub>	oxygen	
OH <sup>-</sup>	hydroxy ion	
p	significance level	
Pb	lead	
pe	negative decimal logarithm of the electron activity	
pH	negative decimal logarithm of the reciprocal of the hydrogen ion activity	
pK	negative logarithm of the dissociation constant K	
PTFE	polytetrafluorethylen	
PVC	polyvinylchloride	
r	correlation coefficient	
rpm	revolutions per minute	
S	sulfur	<i>(HS<sup>-</sup>, S<sup>2-</sup>, S<sup>VI</sup>, SO<sub>4</sub><sup>2-</sup>)</i>
Sb	antimony	<i>(Sb(OH)<sub>3</sub><sup>0</sup>, Sb<sup>III</sup>, Sb<sup>V</sup>, Sb(OH)<sub>6</sub><sup>-</sup>)</i>
Tab.	table	
TGM	total gaseous mercury	
UV	ultraviolet	
vol	volume	
WRB	world reference base	
Zn	zinc	<i>(Zn<sup>2+</sup>)</i>

## 1 INTRODUCTION

The accumulation of trace elements in the environment arises from natural and anthropogenic sources. Human activities have resulted in increased levels of trace elements in many soils (Kabata-Pendias and Mukherjee, 2007). Trace elements from anthropogenic sources exist mainly in the soil surface (Kabata-Pendias and Mukherjee, 2007). Prominent examples of anthropogenic input are mining and smelting, metal finishing, plastic industry, microelectronics, battery manufacture, landfills/refuse disposal, phosphate fertilizer, sewage sludge, and metal scrapheaps (Adriano, 2001). Floodplain soils in Europe are characterized by high amounts of many trace elements including cadmium (Cd), lead (Pb), and mercury (Hg) (Du Laing et al., 2009). The increased deposition of trace elements in floodplain soils has been recognized ever since the increase in industrialization. Sources of the trace elements include industrial activities, mining activities, agricultural uses, atmospheric deposition, and the sewage disposal of municipal wastewaters (Du Laing et al., 2009). Floodplain soils have frequent flooding and thus permanent delivery of new sediments. With flooding high levels of trace elements can be deposited (Du Laing et al., 2009; Overesch et al., 2007). Currently, only small amounts of trace elements enter the floodplain soils. However, the amount of trace elements is still high and is a result of human activities. The deposited trace elements have the potential of being remobilized and thus maybe entering the food chain.

In our work we investigated the floodplain soils of two rivers in Germany, the Wupper River in Leichlingen, North Rhine-Westphalia, and the Elbe River in Lower Saxony. Pollution of the Elbe River with trace elements is well documented (Devai et al., 2005; Overesch et al., 2007; Wallschläger et al., 1996). For example, until 1996 there were  $1500 \pm 500$  tons of Hg deposited in the floodplains of the Elbe River (During et al., 2009; Wallschläger et al., 1996). Pollution can come from various sources. The main pollution sources are industrial points (Hamburg Port Authority, 2005; Wallschläger et al., 1995). Pollution of the Wupper River is also well documented by Schenk (1994). The river is characterized by former mining activities during the Middle Ages and former intensive industrial use beginning in the middle of the 19<sup>th</sup> century and ending in the middle of the 20<sup>th</sup> century. However, input from agricultural and municipal sewage is also noted in this river.

Analysis of the trace elements in both floodplain soils showed clearly elevated concentrations of all trace elements compared to background values in Germany (BGR, 2008; LANUV, 2003). For example, background values of floodplain soils in environs of agglomerations used as grasslands in the state of North Rhine-Westphalia are  $0.6 \text{ mg kg}^{-1}$  for Cd,  $40 \text{ mg kg}^{-1}$  for Pb and  $0.12 \text{ mg kg}^{-1}$  for Hg (LANUV, 2003).

One trace element that was intensively analyzed in this work was Hg. Pollution of floodplains with Hg is a worldwide problem, especially since Hg is a persistent pollutant, is highly toxic, and accumulates in soils (Devai et al., 2005; Rinklebe et al., 2010). The floodplain soils of the Elbe River showed a clear excess in the concentration of Hg with respect to background values in Germany (BGR, 2008; LANUV, 2003). In comparison, the median of background values for Hg in floodplain soils in environs of agglomerations used as grassland in the state of Lower Saxony is  $0.12 \text{ mg kg}^{-1}$  for Hg (LABO, 2003).

Mercury is a toxic element and may cause serious environmental and health problems (Counter and Buchanan, 2004). The methylated species monomethylmercury (MMHg) ( $\text{CH}_3\text{Hg}^+$ ) and dimethylmercury (DMHg) ( $(\text{CH}_3)_2\text{Hg}$ ) are responsible for major diseases. Methylated Hg is a neurotoxin that is largely present in fish and seafood products and can accumulate in the food chain.

The chemistry of Hg in the environment has been extensively reviewed (Gabriel and Williamson, 2004; Schuster, 1991; Zhang et al., 2003). Unlike other toxic elements, elemental Hg can easily be volatilized. The main gaseous species is elemental Hg ( $\text{Hg}^0$ ) where more than 95% of this species is in the atmosphere (Cobos et al., 2002). Another species that can volatilize is the dimethylated form  $(\text{CH}_3)_2\text{Hg}$  (Schlüter, 2000). Mercury is released into the atmosphere from natural and anthropogenic sources. Typical anthropogenic sources include coal combustion, waste incineration, mining, refining, manufacturing, and chloride-alkali production (Li et al., 2009), whereas geothermal activities, evasion from soils, water bodies, vegetation surfaces, wild fires, as well as re-emissions of deposited Hg are known as natural sources (Li et al., 2009; Schlüter, 2000). Mercury volatilization from soil requires different steps: production of  $\text{Hg}^0$ , mass transport or diffusion of  $\text{Hg}^0$  in the soil, and mass transport or diffusion across the soil-air boundary into the atmosphere (Zhang and Lindberg, 1999).

In addition to the high levels of trace elements, floodplain soils are characterized by various redox states that result from flooding events and various water saturation levels. During water

saturation of floodplain soils there is a change from aerobic to anaerobic conditions. Changes in the redox states can be measured by the redox potential ( $E_H$ ). The  $E_H$  shows whether the soil is dominated by oxidizing or reducing processes (Fiedler and Sommer, 2004). The reduction or oxidation status of soil influences the availability of electrons. The soil redox condition under which oxygen ( $O_2$ ) is available is termed aerobic, and is characterized by low electron availability. The  $O_2$  pool in soils is continuously replenished by  $O_2$  diffusion through soil pores, as long as these pores are filled with air. When the soil pores are filled with water, the  $O_2$  diffusion is extremely slow and, depending on metabolic activity, the soil  $O_2$  pool can be rapidly exhausted. The soil redox condition under which  $O_2$  partial pressure is low or  $O_2$  is absent is termed anaerobic, and is characterized by high electron availability. Under anaerobic soil conditions elements other than  $O_2$  are used as terminal electron acceptors. These elements include pentavalent nitrogen (N) in nitrate, tri- and tetravalent manganese ( $Mn^{III,IV}$ ) in Mn oxides, trivalent iron ( $Fe^{III}$ ) in Fe oxides, and hexavalent sulfur ( $S^{VI}$ ) in sulfate (Alewell et al., 2008; Du Laing et al., 2009). Although some overlap may occur, the use of the different electron acceptors is stepwise and known as the sequential reduction sequence. According to the preferential electron acceptor in use, more precise classifications of the different redox conditions can be deduced. For example, Zhi-Guang (1985) classified the redox status of soils into oxidizing ( $E_H > 400$  mV; oxygen is predominant), weakly reducing ( $E_H$  ranges from 400 to 200 mV; oxygen partial pressure is low; nitrate and manganese ( $Mn^{III,IV}$ ) are reduced), moderately reducing ( $E_H$  ranges from 200 to  $-100$  mV;  $Fe^{III}$  is reduced) and strongly reducing ( $E_H < -100$  mV; sulfate and carbon dioxide are reduced) conditions. However, not only is the fate of carbon (C), nitrogen (N), manganese (Mn), iron (Fe), and sulfur (S) strongly affected by redox reactions, but so is the fate of many trace elements. These effects can be divided into two groups: direct and indirect effects. For example, depending on the redox conditions, As occurs either as the reduced species arsenite or the oxidized species arsenate. This describes the direct effect. The indirect effect is the reductive dissolution of As-hosting Fe oxides with the subsequent release of As.

The redox processes in soils are influenced by many factors. The temperature seems to be one of the main factors (Vaughan et al., 2009). The rate of microbial activity in soils is temperature sensitive in that the activity rate of microorganisms slows with decreasing temperatures (Rabenhorst, 2005). Redox processes are catalyzed by microbes and because the microorganisms are temperature sensitive, the concentration of redox sensitive parameters including reduced N, Mn, and Fe reflect temperature changes (Atlas and Bartha, 1987; Massmann et al.

2006; Vaughan et al., 2009). The temperature dependency of denitrification is documented by David et al. (1997) and Carrera et al. (2001). Olivie-Lauquet et al. (2001) also described correlations between increasing concentrations of dissolved Fe and Mn with increasing temperature.

With reference to the abovementioned discussion, the hypothesis of this work is:

Redox conditions ( $E_H$ ) and temperature influence the solubility and volatilization, respectively, of trace elements.

With reference to this hypothesis, this work addressed the following questions:

- (1) How does the solubility of trace elements react to variations in the  $E_H$ ?
- (2) Does temperature variations have an influence on these reactions?
- (3) Does variations in the  $E_H$  influence the solubility and volatilization of Hg?
- (4) What is the distribution of Hg among the different phases of solid soil, soil solution, and the gaseous phase?
- (5) Can different Hg species be detected in soil solutions and the gaseous phase?

## **2 TEST SITE AND PROJECT IMPLEMENTATION**

### **2.1 Test site**

For this project we searched for sites that met two criteria. First, the site had to be located near a river so that various soil water contents and with that various  $E_H$  could be naturally found. The alluvial soils on floodplains have high microbial activity. Active microorganisms such as manganese-, iron- and sulfate-reducing bacteria can naturally be found in these soils. The second important criterion for choosing a test site was high contamination levels of the soil with trace elements. The soil sites were chosen under the condition that the legislative threshold value for Hg in Germany, which was laid down for precautionary soil protection, was exceeded. The threshold value depends on soil texture, as well as pH. The threshold value for loamy soil is  $0.5 \text{ mg kg}^{-1}$  for Hg (BBodSchV, 1999). Also, the other elements should exceed the mean for background values of floodplain soils in environs of agglomerations.

We selected two sites in Germany. Figure 2.1 shows the positions of the two sites in Germany. They were the Wupper River in Leichlingen, North Rhine-Westphalia, and the Elbe River in Hohnstorf, Lower Saxony.



Fig. 2.1: Map of Northern Germany with the two sampling sites; Elbe in Hohnstorf und Wupper in Leichlingen (Google Earth, 2013a).



Figure 2.2 shows the two sites. Site (a) (Fig. 2.2a) was at the Wupper River in Leichlingen, North Rhine-Westphalia ( $51^{\circ}7'10.65''$  N;  $7^{\circ}0'40.79''$  E) and site (b) (Fig. 2.2b) was at the Elbe River in Hohnstorf, Lower Saxony ( $53^{\circ}21'25.05''$  N;  $10^{\circ}34'42.22''$  E). As both sites are located near rivers, they are characterized by flooding events and subsequent changes in the water content and  $E_H$ .

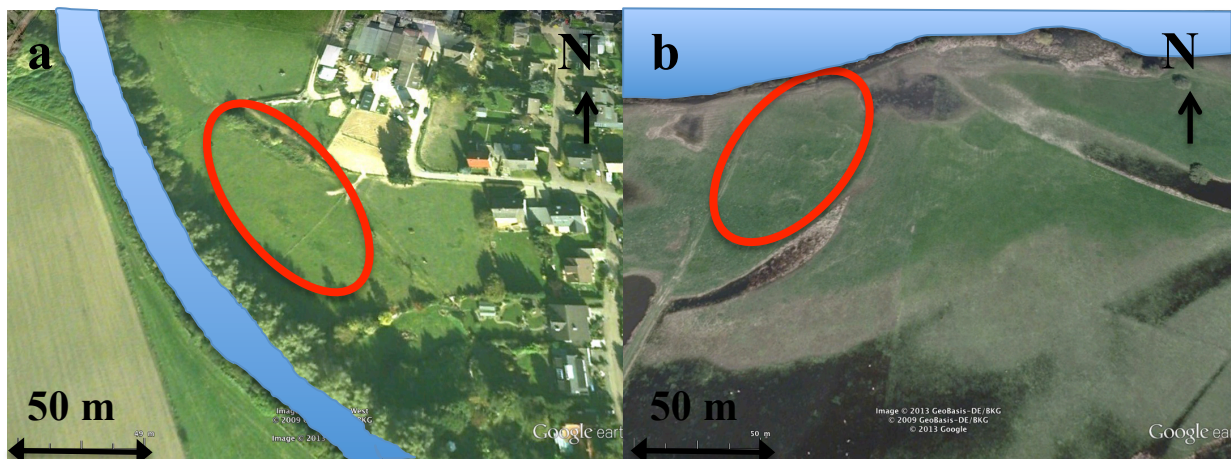


Fig. 2.2: Sampling site a at the Wupper in Leichlingen and site b at the Elbe in Hohnstorf (Google Earth, 2013b)

The general characteristics of the two sites are shown in Tab. 2.1. The first site (Fig. 2.2 a) was located in Leichlingen, North Rhine-Westphalia, at the Wupper River. This site is used as grassland for keeping livestock. The sampling area was located approximately 20 m from the river. The second site (Fig. 2.2 b) was the Elbe River in Hohnstorf, Lower Saxony. This site is part of the biosphere reserve called "Niedersächsische Elbaue". This sampling site was located approximately 30 m from the river.

Tab. 2.1: General characteristics of the sites from the Wupper in Leichlingen and Elbe in Hohnstorf

	<b>Wupper</b>	<b>Elbe</b>
<b>Coordinates</b>	51°7'10.65" N 7°0'40.79" E	53°21'25.05" N 10°34'42.22" E
<b>Site</b>	Leichlingen, North Rhine-Westphalia	Hohnstorf, Lower Saxony
<b>Type of land use</b>	Grassland	Biosphere reserve "Niedersächsische Elbe"
<b>Distance from the river</b>	~ 20 m	~ 30 m
<b>Soil type</b>	Eutric Fluvisol	Eutric Fluvisol
<b>Soil horizon</b>	Ah	aAh
<b>Sampling depth</b>	0 to 15 cm	0 to 15 cm

Both sites are characterized by temporary flooding events. During these flooding events the conditions of the sites are modified in terms of water content and  $E_H$ . Furthermore, flooding transports new sediments to the site.

The soils of both areas are Eutric Fluvisols (Du Laing et al., 2009). These soils are characterized by a high nutrient content. We collected samples from the top horizon of the soils. The top horizons of both areas are characterized by a high humus content.

Before the different experiments were started, the soils were characterized for their physical and chemical soil characteristics including pH and soil texture. The amounts of trace elements were determined by aqua regia extraction. Determination of the chemical binding of the trace elements was established by sequential chemical extractions. For the elements arsenic (As), cadmium (Cd), cobalt (Co), chromium (Cr), copper (Cu), molybdenum (Mo), nickel (Ni), lead (Pb), antimony (Sb), and zinc (Zn) the extraction scheme of Zeien and Brümmer (1989) was used; for Hg the scheme of Bloom et al. (2003) was used.

## **2.2 Project implementation**

The aim of our project was to determine the solubility of the trace elements As, Cd, Co, Cr, Cu, Mo, Ni, Pb, Sb, and Zn, as well as the volatilization of Hg particularly under defined  $E_H$ . The soil water content was crucial for variation in the  $E_H$ . The influence of both interlinked factors was the main object of our study. To reach these aims we performed microcosm and column experiments in the laboratory.

We started with the microcosm experiments. The advantage of these experiments was that the  $E_H$  could be specifically controlled. A wide range of parameters could be analyzed in the soil solution including concentrations of the trace elements, Fe, Mn, dissolved organic carbon (DOC) and anions. Furthermore, permanent monitoring of the parameters  $E_H$ , pH, and temperature was possible.

Microcosms consisted of glass chambers filled with air-dried and sieved soil material, and water. The glass chambers were closed and airtight and tubes were embedded in the cover of the microcosms. These tubes were necessary for monitoring temperature,  $E_H$ , and pH, as well as for providing an inlet for nitrogen or filtered air for controlling the  $E_H$ , and sampling the soil solutions. The tubes were, in part, connected with the control unit for controlling the  $E_H$  and for data recording. The evaporated Hg was collected in tubes filled with activated carbon when the overpressure left the system.

An advantage of this experiment was control of the  $E_H$ . Furthermore, a wide range of parameters could be analyzed in the solid phase and factors that influenced the solubility and evaporation of trace elements could be detected. Any influence from factors such as sunlight radiation and temperature could be minimized and controlled. One disadvantage of these experiments was that the natural soil structure was destroyed.

The second experiment consisted of column experiments. In these experiments the impact of varying water content on the evaporation of Hg in undisturbed soils was investigated. These experiments allowed the determination of Hg species in the gas phase. In these experiments the variation of the  $E_H$  was designated by the change in the water content.

For the column experiments undisturbed soil in columns were watered and the surface of the column was closed with flux chambers. The headspace under the flux chamber was sampled twice a week. The columns were placed in an incubator at 20 °C. The  $E_H$  was constantly measured and was varied by removing water at the bottom of the column.

The advantage of these experiments was that natural undisturbed soil could be used. Furthermore, the complete gas phase could be sampled and the Hg species could be measured. The influence of factors such as wind speed, temperature, and sunlight radiation was minimal. The disadvantages were that additional influencing parameters such as binding partners could only be detected by variation of the water content. In addition, the soil material in the columns could be analyzed at the end of the experiment. In the column experiments the focus was on the gas phase.

### **3 TRACE-ELEMENT SOLUBILITY IN A MULTI-CONTAMINATED SOIL AS AFFECTED BY REDOX CONDITIONS AND TEMPERATURE**

#### **3.1 Introduction**

Trace metals and semimetals (they will be designated as trace elements in the following text) are introduced into the soil environment both by natural and anthropogenic sources (Adriano, 2001; Hooda, 2010). While natural sources seldom lead to harmful levels of trace elements in soils, the semimetal As is a prominent exception (Ravenscroft et al., 2009); anthropogenic activities have resulted in soil pollution with this element group worldwide. Typically, soil pollution is caused by a single or only a few elements. For example, tanning of leather and processing of chromite ores are involved in chromium contamination at related sites (Farmer et al., 2006; Shams et al., 2009), vineyard soils can be contaminated with Cu (Mirlean et al., 2007; Wightwick et al., 2008), and soils at shooting ranges with Pb, Sb, and Cu (Knechtenhofer et al., 2003). However, multiple element soil pollution does sometimes exist, which is a special challenge for risk assessment. Such multiple element pollution can occur at floodplain soils (Du Laing et al., 2009; Schulz-Zunkel and Krueger, 2009).

Floodplains are found worldwide. Their soils are characterized by frequent flooding and the induced permanent delivery of new sediments. With the supply of new sediments through flooding, high amounts of trace elements can be deposited (Du Laing et al., 2009). These trace elements originate from different sources and are transported through the river. The main sources are industrial and mining activities but also agricultural uses, atmospheric deposition, the sewage disposal of municipal wastewaters, and runoff (Du Laing et al., 2009). The increased deposition of trace elements started during industrialization. Nowadays only small amounts of trace elements enter the floodplain soils. However, the amounts of trace elements are still high, and the deposited trace elements have the potential to be remobilized thus may enter the food chain.

One important soil property for the mobilization of trace elements is the availability of electrons, i.e. the reduction–oxidation (redox) status of soils. Redox conditions of soils are classically assessed by measuring the  $E_H$ . The most important source of electrons in soils is the reduced carbon (C) occurring in the soil organic matter. Metabolizing plant roots and microorganisms are able to enzymatically oxidize the reduced C forms. Electrons which are re-

leased during the oxidation of C are transferred to elemental oxygen (O which is occurring as the dioxygen molecule O<sub>2</sub>) which, in turn, is reduced to water (H<sub>2</sub>O). Hence, O<sub>2</sub> acts as the terminal electron acceptor. Soil redox conditions under which O<sub>2</sub> is available are termed aerobic, and are characterized by low electron availability. The O<sub>2</sub> pool of soils is continuously replenished by O<sub>2</sub> diffusion through soil pores as long as they are filled with air. When filled with water, the O<sub>2</sub> diffusion is extremely slow and, depending on metabolic activity, the soil O<sub>2</sub> pool is more or less rapidly exhausted. Soil redox conditions under which O<sub>2</sub> partial pressure is low or O<sub>2</sub> is absent are termed anaerobic, and are characterized by high electron availability. Under anaerobic soil conditions, elements other than O are used as terminal electron acceptors, including pentavalent nitrogen (N<sup>V</sup>) in nitrate, tri- and tetravalent manganese (Mn<sup>III,IV</sup>) in Mn oxides, trivalent iron (Fe<sup>III</sup>) in Fe oxides, and hexavalent sulfur (S<sup>VI</sup>) in sulfate. Although some overlap may occur, the use of different electron acceptors is a stepwise one and known as the sequential reduction sequence (Bartlett and James, 1993). According to the preferential electron acceptor in use, more precise classifications of the different redox conditions can be deduced. Zhi-Guang (1985) classified the redox status of soils into *oxidizing* (E<sub>H</sub> > 400 mV; oxygen is predominant), *weakly reducing* (E<sub>H</sub> ranges from 400 to 200 mV; oxygen partial pressure is low; nitrate, and manganese (Mn<sup>III,IV</sup>) are reduced), *moderately reducing* (E<sub>H</sub> ranges from 200 to -100 mV; Fe<sup>III</sup> is reduced) and *strongly reducing* (E<sub>H</sub> < -100 mV; sulfate and carbon dioxide are reduced) conditions. However, not only is the fate of C, N, Mn, Fe, and S strongly affected by redox reactions but also that of trace elements. Some elements are directly involved in electron transfer and hence occur in different valences like As with its oxidized species arsenate and reduced species arsenite (Smedley and Kinniburgh, 2002). Many, if not all trace elements, are indirectly influenced by redox reactions. For example, under moderately reducing conditions, trace element-hosting Fe oxides can be reductively dissolved, thus releasing sorbed trace elements (Zachara et al., 2001); under strongly reducing conditions, trace elements can be precipitated as metal sulfides (Onstott et al., 2011; Weber et al., 2009).

Patrick and co-workers (1966; 1973) have designed a system by which the E<sub>H</sub> of soil suspensions can be maintained at different levels. This equipment was later adapted by other researchers to study the effect of the E<sub>H</sub> on the solubility of trace elements. Most previous studies focused on one (Masscheleyn et al., 1991) or only a few trace elements (Carbonell et al., 1999). For multiple-element contaminated sites, however, there is a need to study such effects on a larger set of elements because, e.g., they may compete for the same sorption sites.

Most soil redox reactions are catalyzed by microorganisms. The rate of microbial activity, in turn, is temperature sensitive (Paul and Clark, 1996). Hence, apart from saturation with water, the presence of microorganisms and available organic matter, suitable soil temperature must prevail to achieve reducing conditions. For permanently or temporarily water saturated soils of temperate zones, it can be postulated that not only the flooding event itself but also the seasons play an important role in the remobilization of trace elements.

The objective of the current study was to investigate the influence of a sequence of different redox conditions (from oxidizing via weakly reducing to moderately reducing conditions) on the solubility of ten trace elements in a multiple-contaminated floodplain soil. Because the effect of sulfate reduction on the trace element solubility has been well studied in floodplain soil (Weber et al., 2009) and because this site is characterized only by short-term flooding events, strongly reducing conditions were not considered. Instead, we focused on the transition between weakly and moderately reducing soil conditions. This site is in the temperate zone. Hence, the effect of soil temperature was studied by carrying out the laboratory experiments at 7, 15 and 25 °C. Trace elements considered include Sb, As, Cd, Cr, Co, Cu, Pb, Mo, Ni, and Zn.

## **3.2 Material and methods**

### **3.2.1 Study site, sampling, and sample preparation**

Soil samples were taken from a grassland floodplain located close (~ 20 m) to the river Wupper in Leichlingen, North Rhine-Westphalia, Germany (51°7'10.65'' N; 7°0'40.79'' E). This river is characterized by former mining activities during the Middle Age and former intensive industrial use that began in the middle of the 19<sup>th</sup> century and ended in the middle of the 20<sup>th</sup> century. Also, inputs caused by agricultural activities and by municipal sewage affected the river (Schenk, 1994). Twenty-five individual samples were collected by a spade from an area of about 2,000 m<sup>2</sup>, each containing ~1 kg of soil. Sampling was restricted to the humic topsoil (0 to 15 cm, Ah horizon). The soil samples were combined, manually homogenized, air-dried, and sieved (2 mm). Subsamples were ground in an agate ball mill for analysis of total element contents.

### **3.2.2 Soil characteristics**

Soil pH was measured potentiometrically using a glass electrode both in 0.01 mol L<sup>-1</sup> CaCl<sub>2</sub> solution and water (mixed 5:1 with soil (vol/vol)). Particle size distribution was determined by wet sieving and sedimentation using the pipette sampling technique. Prior to analyses, the organic matter was destroyed by H<sub>2</sub>O<sub>2</sub>. Total C and N were quantified with an elemental analyzer (Vario EL, Elementar). Total C equals organic C since the soil was free of carbonates. Contents of Mn and Fe were measured after microwave-induced (Multiwave, Perkin Elmer) aqua regia digestion. Binding forms of Fe were determined by an oxalate extraction according to Schwertmann (1964) and a dithionite extraction according to Mehra and Jackson (1960).

### **3.2.3 Contents and fractionation of trace elements**

The contents of the ten trace elements were measured after microwave-induced aqua regia digestion. Two hundred mg of air-dried and ground sample were weighed into a polytetrafluorethylen (PTFE) liner. Then 6 mL of concentrated HNO<sub>3</sub> (supra pure, Merck) and 2 mL concentrated HCl (supra pure, Merck) were added. After digestion, the samples were filtered through blue ribbon filter (2 µm, Whatman 589/3) and made up to a final volume of 50 mL with demineralized water (Nanopure Diamond, Barnsteadt). Three replications were performed for each sample. The reference material “River Sediment” (LGC 6189, LGC Standards) was used to control the digestion. Recovery rates were between 97 % for Pb and 114 % for Sb.

The trace elements were sequentially extracted according to the extraction scheme of Zeien and Brümmer (1989). One g of soil was weighed into 50 mL PTFE centrifuge tubes, and the tubes were shaken with a bench top shaker (3006, GFL). After each extraction step, the samples were centrifuged for 10 minutes (Rotina 46, Hettich). Then the supernatant was removed and filtered (cellulose acetate syringe filter, 0.22 µm). Steps 2 to 6 were followed by a washing step to collect the remaining extractant solution. The extractant and washing solution were combined for analysis. Three replications were run for each step. The extraction including the hypothetical interpretation were as follows: Fraction 1 (F1): mobile fraction with 1 mol L<sup>-1</sup> NH<sub>4</sub>NO<sub>3</sub> (extraction time 24 h); Fraction 2 (F2): easily mobilizable fraction with 1 mol L<sup>-1</sup> CH<sub>3</sub>COONH<sub>4</sub>, pH 6 (extraction time 24 h) and washing with 1 mol L<sup>-1</sup> NH<sub>4</sub>NO<sub>3</sub> (extraction time 10 min); Fraction 3 (F3): bound to Mn oxides with 0.025 mol L<sup>-1</sup>



$\text{NH}_2\text{OH}\cdot\text{HCl} + 1 \text{ mol L}^{-1} \text{ CH}_3\text{COONH}_4$ , pH 6 (extraction time 30 min) and washing twice with  $1 \text{ mol L}^{-1} \text{ CH}_3\text{COONH}_4$ , pH 6 (extraction time 10 min); Fraction 4 (F4): organic bound fraction with  $0.025 \text{ mol L}^{-1} \text{ NH}_4\text{-EDTA}$ , pH 4.6 (extraction time 90 min) and washing with  $1 \text{ mol L}^{-1} \text{ CH}_3\text{COONH}_4$ , pH 6 (extraction time 10 min); Fraction 5 (F5): bound to weakly crystalline Fe oxides with  $0.2 \text{ mol L}^{-1} (\text{NH}_4)_2\text{C}_2\text{O}_2\cdot\text{H}_2\text{O}$ , pH 3.25 (extraction time 2 h, dark) and washing with  $0.025 \text{ mol L}^{-1} \text{ NH}_4\text{-EDTA}$ , pH 4.6 (extraction time 10 min); Fraction 6 (F6): bound to crystalline Fe oxides with  $0.1 \text{ mol L}^{-1} \text{ C}_6\text{H}_8\text{O}_6 + 0.2 \text{ mol L}^{-1} (\text{NH}_4)_2\text{C}_2\text{O}_2\cdot\text{H}_2\text{O}$ , pH 3.25 (extraction time 2 h in water bath at  $95 \text{ }^\circ\text{C}$ ) and washing with  $0.2 \text{ mol L}^{-1} (\text{NH}_4)_2\text{C}_2\text{O}_2\cdot\text{H}_2\text{O}$ , pH 3.25 (extraction time 10 min, dark); Fraction 7 (F7): residual with aqua regia.

### 3.2.4 Soil incubation in microcosms

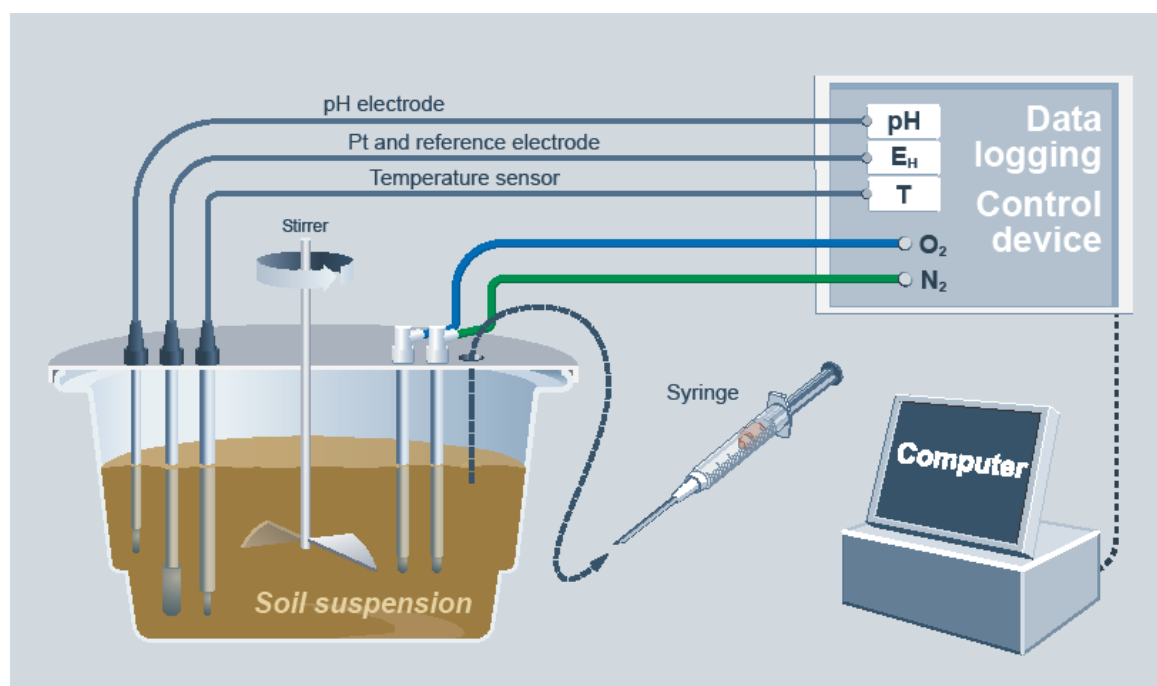


Fig. 3.1: Scheme of a microcosm and control device

To study the behavior of trace elements under different redox and temperature regimes, microcosm experiments at controlled redox potentials and temperatures were performed. The device used was adapted from Patrick et al. (1973). Microcosms were filled with 1.25 kg air-dried soil (< 2 mm) and 6 L deionized water and were continuously stirred (Fig. 3.1).

Soil suspensions were incubated under oxidizing ( $> 400$  mV), weakly reducing ( $\sim 300$  mV) and moderately reducing conditions ( $\sim 100$  mV) in the microcosm system. Regulation of  $E_H$  was achieved by flushing  $N_2$  or filtered ambient air through the microcosms. Redox potentials in the microcosms were kept under oxidizing conditions during the first week, then switched to weakly reducing conditions for the second week, and finally to moderately reducing conditions. The experiments were of different lengths of time, because it took longer to reach moderately reducing conditions at lower temperatures, i.e. 38 days at  $7$  °C, 35 days at  $15$  °C, and 33 days at  $25$  °C. Temperature, pH, and redox potential were recorded every 30 minutes with a data logger. The temperature was determined by temperature probe (PT 100, Meinsberg) and the  $E_H$  as well as pH with combination electrodes (EMC 33, Ag-AgCl, and EGA 153, Meinsberg). The measured redox values were related to the standard hydrogen electrode by adding 207 mV which refer to the Ag-AgCl reference electrode. Redox measurements were converted into values corresponding to pH 7 using the pH of soil suspensions and considering the temperature ( $T$ , in °C) using the equation  $E_H(\text{pH}7) = E_H + (\text{pH} - 7) \cdot 59 - 0.76 (T - 25)$  where  $E_H$  is expressed in mV. Although the value of  $-59$  mV per pH unit is reasonable for most measurements (Bohn et al., 2001) we reported both the measured  $E_H$  and the pH. Temperature control of the microcosms was achieved by setting them into water filled stainless steel tanks connected to a temperature control unit (Fig. 3.1; RP 845, Lauda). Experiments were performed at  $7$ ,  $15$ , and  $25$  °C. Every third day, 50 mL of the soil suspension were taken from the microcosms with a 60 mL sterile syringe (Exelmed, I.M.I.). Soil suspensions were filtered ( $0.45$   $\mu\text{m}$  cellulose-nitrate filter, Sartorius) and aqueous subsamples were stabilized by adding  $\text{HNO}_3$ .

### **3.2.5 Analyses of soil suspensions and extractants**

Ferrous Fe ( $\text{Fe}^{2+}$ ) concentrations of the aqueous phase of the soil suspensions were analyzed spectrophotometrically (Lambda 25, Perkin Elmer) with ferrozine at 562 nm according to Viollier et al. (2000) immediately after sampling. Nitrate, chloride, and sulfate were determined by ion chromatography (ICS-1000, Dionex) using an ultraviolet absorbance detector for nitrate and an electrical conductivity detector for chloride and sulfate, respectively. The stabilized subsamples were used to measure the total concentrations of Fe, Mn, and trace elements. Iron and Mn were determined by flame atomic absorption (iCE 3500, Thermo scientific) using an air-acetylene flame at 248.3 nm and 279.5 nm, respectively. Total dissolved

organic C was determined by high temperature catalytic oxidation. By this procedure, dissolved C was oxidized to CO<sub>2</sub> and quantified by a non-dispersive, infrared analyzer. A Shimadzu TOC-5050 analyzer operating at 680 °C was used. Dissolved inorganic carbon was measured by quantifying the CO<sub>2</sub> generated following phosphoric acid addition and was subtracted from total dissolved C to give DOC. Trace elements were analyzed by inductive coupled plasma mass spectrometry (ICP-MS, X-Series II, Thermo Scientific). To control all measurements with ICP-MS the reference material “fortified water” (TMDA 51.3, CRM) was analyzed. Recovery rates of this measurement were between 100 % for As and 110 % for Pb. Sequential extraction and aqua regia extractions were also quantified by ICP-MS. Recovery for the measurement of the sequential extraction rates between 100 % for As and 109 % for Pb, and for the aqua regia extraction between 99 % for As and 106 % for Pb.

### **3.2.6 Modeling and statistical calculations**

The trace-element species distribution of the divalent metals was modeled with the software Visual Minteq 3.0. Complexation by dissolved organic ligands was considered with the Stockholm Humic Model (Gustafsson, 2001). The model calculation was carried out with the following assumptions as to the composition of dissolved organic matter (DOM): 65 % of DOM is fulvic acid and 35 % is inert, and the DOM concentration was calculated as two times that of DOC (Meers et al., 2006).

All statistical calculations were performed with the program IBM SPSS Statistics 20.

## **3.3 Results and Discussion**

### **3.3.1 Soil properties and trace element status**

Table 3.1 summarizes the main properties of the soil which is according to WRB and IUSS Working Group (2006) a Eutric Fluvisol, often found at loamy terraces (Du Laing et al., 2009). The pH was in the moderately acid range which is typical for floodplain soils of the temperate zone. The texture was dominated by silt and sand with significant amounts of clay and is according to FAO loam. Both the high content of organic C (85 g kg<sup>-1</sup>) and the relatively low ratio of C/N are characteristic of grassland floodplains. About one-third of the Fe is bound in Fe oxides. The ratio of Fe<sub>o</sub>/Fe<sub>d</sub> was 0.60 and indicated a slightly greater proportion of less stable poorly crystalline Fe oxides.

Tab. 3.1: Chemical and physical characteristics of the Ah horizon of a grassland Fluvisol from the Wupper river at Leichlingen, North Rhine-Westphalia, Germany

<b>Property</b>	
pH (in H <sub>2</sub> O), [-]	6.4
pH (in CaCl <sub>2</sub> ), [-]	5.8
Particle size distribution	
Sand [g kg <sup>-1</sup> ]	415
Silt [g kg <sup>-1</sup> ]	435
Clay [g kg <sup>-1</sup> ]	150
Texture	loam <sup>†</sup>
Total Fe [g kg <sup>-1</sup> ]	63.9
Fe <sub>o</sub> [g kg <sup>-1</sup> ]	12.8
Fe <sub>d</sub> [g kg <sup>-1</sup> ]	21.3
Fe <sub>o</sub> /Fe <sub>d</sub>	0.60
Total Mn [g kg <sup>-1</sup> ]	1.0
Total C [g kg <sup>-1</sup> ]	85.3
Total N [g kg <sup>-1</sup> ]	5.20
C/N	16
Chromium reducible S [mg kg <sup>-1</sup> ]	252

<sup>†</sup>according to FAO

Table 3.2 shows the amounts of trace elements as dissolved by aqua regia. The median for background values of floodplain soils in environs of agglomerations used as grassland in the state of North Rhine-Westphalia are 0.6 mg kg<sup>-1</sup> for Cd, 40 mg kg<sup>-1</sup> for Pb, 33 mg kg<sup>-1</sup> for Cr, 18 mg kg<sup>-1</sup> for Cu, 19 mg kg<sup>-1</sup> for Ni, and 99 mg kg<sup>-1</sup> for Zn, respectively (LANUV, 2003). For the other investigated elements, such values do not exist for the state of North Rhine-Westphalia. Recently, the Federal Institute for Geosciences and Natural Resources (BGR) of Germany has performed a survey that considers also the lacking elements. Accordingly, the median for background values of German loamy soils used as grassland are 0.5 to 0.8 mg kg<sup>-1</sup> for Mo, 3.1 to 11.5 mg kg<sup>-1</sup> for As, 9 to 14 mg kg<sup>-1</sup> for Co, and 0.4 to 1.3 mg kg<sup>-1</sup> for Sb (BGR, 2008). Since all background values were clearly exceeded, a considerable contamination for this soil can be inferred, which has been reported elsewhere for German floodplain soils, e.g., at the Elbe (Devai et al., 2005; Overesch et al., 2007; Schulz-Zunkel and Krueger, 2009), Saale (Devai et al., 2005), and Mulde (Klemm et al., 2005).

Tab. 3.2: Amounts of trace elements as determined by aqua regia in the Ah horizon of a grassland Fluvisol from the Wupper river at Leichlingen, North Rhine-Westphalia, Germany [mg kg<sup>-1</sup>]

<b>Element</b>	<b>Amount</b>
Zinc	927 ± 40.7 <sup>†</sup>
Copper	567 ± 26.5
Chromium	488 ± 30.9
Lead	375 ± 25.6
Nickel	98.0 ± 7.14
Arsenic	35.9 ± 0.963
Cobalt	22.4 ± 0.630
Antimony	8.65 ± 0.261
Cadmium	8.54 ± 0.318
Molybdenum	5.82 ± 0.175

<sup>†</sup> standard deviation

### 3.3.2 Fractionation of trace elements

Table 3.3 shows the results of the sequential extraction procedure. The recovery of As, Cd, Cr, Ni, Sb, and Zn was excellent since the deviation of the totaled fractions was below 5 % compared with the single aqua regia extraction. The recovery was good for Co (-8 %) and sufficient for Cu (+12 %), Mo (-12 %) and Pb (+16 %).

Cadmium is a mobile element under the slightly acid conditions of the investigated soil. The high proportions of the mobile fraction (4.4 %) and the easily mobilized fraction (32.7 %) emphasize this matter of fact since the sum of both fractions was 37.1 %. Like Cd, Zn is quite mobile and the high proportion of the mobile fraction (2.2 %) and the easily mobilized fraction (17.3 %) underlines this. In contrast, both fractions are much lower for the other elements, especially for As (0.9 %) and Cr (0.5 %), but also for Pb when considering the mobile fraction (0.1 %).

Tab. 3.3: Sequential extraction of trace elements in the Ah horizon of a grassland Fluvisol from the Wupper river at Leichlingen, North Rhine-Westphalia, Germany [mg kg<sup>-1</sup>]

	F1§	F2	F3	F4	F5	F6	F7	Sum‡	Total aqua †	Sum/Total aqua rega
<b>Zn</b>	21.2# (2.2)¶	168 (17.3)	116 (12.0)	175 (18.1)	238 (24.6)	158 (16.4)	90.3 (9.3)	967	927	1.04
<b>Cu</b>	9.93 (1.6)	26.3 (4.1)	10.8 (1.7)	400 (62.8)	126 (19.7)	6.46 (1.1)	58.0 (9.1)	637	567	1.12
<b>Cr</b>	0.377 (0.1)	2.00 (0.4)	1.92 (0.4)	16.3 (3.4)	245 (51.5)	113 (23.6)	98.1 (20.6)	477	488	0.98
<b>Pb</b>	0.224 (0.1)	17.2 (4.0)	37.2 (8.6)	225 (52.0)	102 (23.5)	20.3 (4.4)	32.5 (7.5)	434	375	1.16
<b>Ni</b>	2.06 (2.1)	6.81 (6.9)	3.97 (4.0)	18.2 (18.4)	26.4 (26.7)	20.1 (20.4)	21.4 (21.6)	98.9	98.0	1.01
<b>As</b>	0.092 (0.3)	0.206 (0.6)	0.357 (1.0)	4.46 (12.9)	21.7 (62.6)	5.08 (14.5)	2.80 (8.1)	34.7	35.9	0.97
<b>Co</b>	0.430 (2.1)	1.56 (7.5)	1.85 (8.9)	3.92 (18.9)	3.85 (18.6)	4.88 (23.7)	4.21 (20.3)	20.7	22.4	0.92
<b>Sb</b>	0.203 (2.4)	0.185 (2.2)	0.222 (2.7)	0.577 (6.9)	4.38 (52.3)	0.833 (9.9)	1.98 (23.6)	8.38	8.65	0.97
<b>Cd</b>	0.375 (4.4)	2.81 (32.7)	1.18 (13.7)	1.25 (14.5)	1.73 (20.1)	0.342 (4.0)	0.910 (10.6)	8.60	8.54	1.01
<b>Mn</b>	0.283 (5.5)	0.145 (2.8)	0.326 (6.4)	0.513 (10.0)	1.49 (29.2)	0.946 (18.6)	1.47 (27.5)	5.17	5.82	0.88

§ Fraction 1 (F1): mobile fraction; F2: easily mobilizable fraction; F3: bound to Mn-oxides; F4: organic bound fraction; F5: bound to weakly crystalline Fe-oxides; F6: bound to crystalline Fe-oxide; F7: aqua regia; according to Zeien and Brümmner (1989)

# fraction in mg kg<sup>-1</sup>

¶ fraction in %

‡ sum F1 to F7

† separate aqua regia extraction [mg kg<sup>-1</sup>]

Copper was mostly related to the organic bound fraction (62.8 %), and just over half of the Pb was also found in this fraction (52.0 %). Organic matter-related Co, Ni, and Zn occurred at levels of nearly 20 %.

Arsenic, Cr, and Sb were strongly associated with Fe oxides because 77.1 %, 75.1 %, and 62.2 %, respectively, belonged to fraction F5 and F6. Of the Fe oxides, the poorly crystalline oxides were the more important ones, especially for As. Significant amounts of Mo, Ni, Co, and Zn were related to Fe oxides since the sum of F5 and F6 yielded between 41.0 % (Zn) and 47.8 % (Mo) for these elements.

It can be summarized that Cd and Zn are characterized by a high mobility in comparison to the other elements, that Cu and Pb are mostly bound to the organic components of the soil, that especially As, Cr, and Sb but also Co, Ni, Mo, and Zn showed a high affinity to Fe oxides. Overall, this observed element specific behavior is typical and is in agreement with those reported elsewhere (Adriano, 2001 and Hooda (2010) and literature cited therein).

### **3.3.3 Redox potential, temperature, and pH**

Figure 3.2 shows the development of the  $E_H$  (Fig. 3.2a) and pH (Fig. 3.2b) during the course of the experiments. The goal of our experiment was to achieve different redox conditions. The first range was oxidizing conditions that are characterized by an  $E_H$  greater than 400 mV. The second range was weakly reducing conditions with an  $E_H$  ranging from 200 to 400 mV. In the current experiment, the desired level of  $E_H$  was ~ 300 mV. The third range in this experiment was moderately reducing conditions with an  $E_H$  ranging from -100 to 200 mV. The goal was to achieve ~ 100 mV. Overall, with the experimental design and soil used, it was possible both to achieve well defined redox conditions in the soil suspension and to hold them for several days.

Obviously, the temperature had a significant effect on how fast the reducing soil conditions could be obtained. To achieve weakly reducing conditions it took 7 hours at 25 °C, 10 hours at 15 °C, and 160 hours at 7 °C. This time dependence was more pronounced during the change from weakly reducing to moderately reducing conditions since it took 21 hours at 25 °C, 55 hours at 15 °C, and 298 hours at 7 °C. Accordingly, the higher the temperature, the less time required for the onset of reducing conditions. Rabenhorst and Castenson (2005) showed that at soil temperatures < 2 °C essentially no ferrihydrite reduction occurred in a

field experiment with ferrihydrite painted tubes, even though the soil  $E_H$  was at  $Fe^{III}$  reducing range. As soil temperatures increased from 2 to 8 °C, the quantity of ferrihydrite reduction increased with time. When the soil temperature was between 8 and 20 °C, substantial reduction occurred within 7 days. In agreement with this observation, Vaughan et al. (2009) demonstrated in a two-year study that, at lower temperatures, longer periods of saturation were required to induce soil reduction with respect to ferrihydrite (Vaughan et al., 2009). Rabenhorst (2005) discussed soil temperatures below 5 °C to represent a ‘biological zero’ for redox processes. However, this was later clarified because a reducing soil environment is attainable at temperatures < 5 °C but requires a much longer time period (Vaughan et al., 2009). Consistent with this, decreasing the temperature from 23 to 14 and 5 °C strongly slowed down soil reduction and Fe in a laboratory incubation experiment with floodplain soil (Weber et al., 2010).

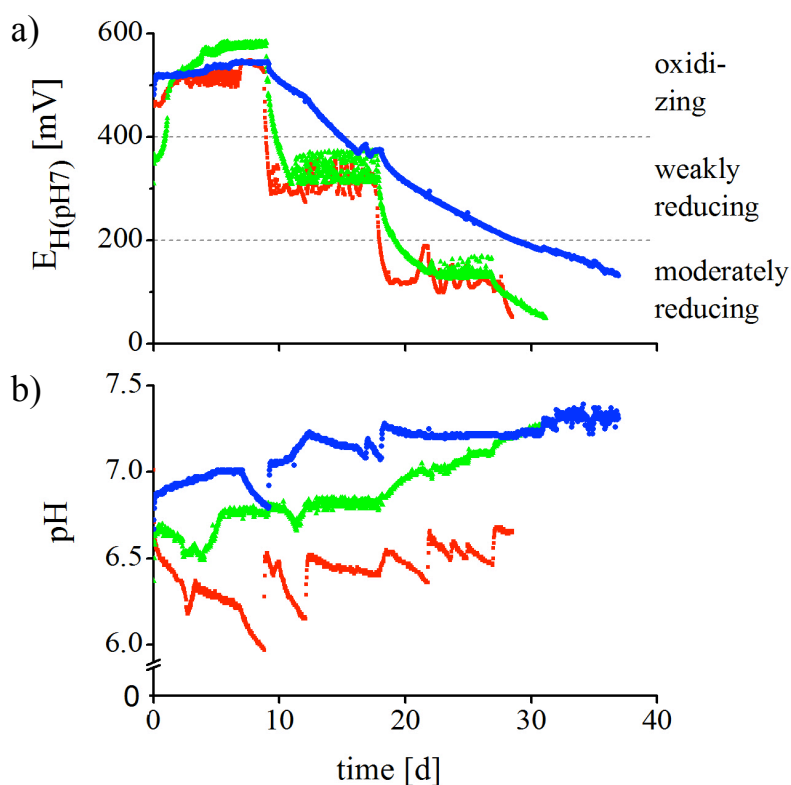


Fig. 3.2: Development of redox potential ( $E_H$ ) and pH during the microcosm experiments performed at 7, 15, and 25 °C (● 7 °C, ▲ 15 °C, ■ 25 °C)



The experiment performed at 7 °C showed a slight increase of the pH from 6.9 to 7.0 under oxidizing conditions at the beginning, as long as filtered air was pumped into the system; then, a decrease of the pH to 6.8 occurred. The conversion to weakly reducing conditions led to an increase of the pH up to 7.2. When the system was converted to moderately reducing conditions, the pH raised up to about 7.3. At 15 °C, the pH decreased from 6.7 to 6.5 when the  $E_H$  increased up to 550 mV under oxidizing conditions. When this level was achieved no filtered air was pumped into the system and the pH increased up to 6.8. The change to weakly reducing conditions led to a decrease of the pH to 6.7. When weakly reducing conditions with 300 mV were achieved, the pH increased up to 6.8. The pH increased again up to 7.2 when the system was adapted to reducing conditions. At 25 °C, the pH decreased strongly from 6.7 to 6.0 under oxidizing conditions, in contrast to the other variants during the beginning. We assume that there was a relatively intensive aerobic respiration at this high temperature resulting in the production of  $CO_2$  that lowered the pH of the suspension ( $C_6H_{12}O_6 + 6O_2 \rightarrow 6CO_2 + 6H_2O$  where glucose represents organic matter). The change from oxidizing to weakly reducing conditions led to an increase of pH to 6.5. When weakly reducing conditions were achieved, greater deviations of the pH between 6.2 and 6.5 were observed. It is presumed that these deviations happened because  $N_2$  or filtered air was pumped into the microcosms to hold the  $E_H$  level. When gas is bubbled through the microcosms,  $CO_2$  is removed from the system, thus lowering the  $CO_2$  partial pressure. The conversion to moderately reducing conditions resulted in a slight increase of the pH to 6.5. Overall, the pH varied during the course of the experiment from 6.8 and 7.2 at 7 °C, 6.5 and 7.2 at 15 °C, and 6.0 and 6.7 at 25 °C.

As a general trend, an increase of pH could be observed for all variants when the microcosms were adapted to reducing conditions. Reducing conditions are accompanied by proton-consuming processes (Bartlett and James, 1993) which is obvious by, e.g. the reduction of nitrate ( $5C_6H_{12}O_6 + 24NO_3^- \rightarrow 12N_2 + 30CO_2 + 24OH^- + 18H_2O$ ). On the other hand, oxidizing conditions are linked with proton-producing processes (Bartlett and James, 1993) which is obvious by, e.g.  $4Fe^{2+} + O_2 + 6H_2O \rightarrow 4FeOOH + 8H^+$ . Redox-induced changes of the pH can be important, because the pH is closely connected with the behavior of trace elements. This will be discussed later.

### **3.3.4 Further redox-sensitive and non-redox sensitive parameters**

The change of the  $E_H$  from oxidizing via weakly to moderately reducing conditions should have affected the behavior of the electron acceptors  $Mn^{III,IV}$  and  $Fe^{III}$ . In addition, the fate of the potential electron acceptor sulfate is presented. Dissolved organic matter, which may act as electron donor, and chloride, although not a redox active ion, will also be considered since they may affect the solubility of the trace elements under investigation. Figure 3.3 illustrates the development of these parameters.

#### **3.3.4.1 Manganese**

The change of the  $E_H$  from oxidizing to weakly reducing conditions resulted in a slight increase of the Mn concentrations in the soil suspension for the 15 and 25 °C variants (Fig. 3.3a). This is the range in the onset of the dissimilatory Mn reduction, and the subsequent release of  $Mn^{2+}$  from the dissolving oxides. Previous studies have demonstrated that the water-soluble Mn in flooded soils is largely manganous Mn, i.e.,  $Mn^{2+}$  (Gotoh and Patrick, 1972; Schwab and Lindsay, 1983). It can be assumed that this is also true in the present study. Manganese reduction can be expressed by  $CH_3COO^- + 4MnO_2 + 6H_2O \rightarrow 4Mn^{2+} + 2HCO_3^- + 7OH^-$ , where acetate represents the electron donor. In that  $E_H$  range, the reduction of nitrate also proceeds. Nitrate, however, was already not detectable from the beginning of the experiment (data not shown). Presumably, nitrate was only present in trace amounts in this soil and/or denitrification was completed within some hours. Surprisingly, at 7 °C, an increase of the Mn concentrations was observed from day eight. This high level was held until the  $E_H$  changed to reducing conditions. The reason for this strong increase is unknown. Changes in pH or  $E_H$  seem not to be the cause. When the  $E_H$  was lowered to moderately reducing conditions, a sharp increase of the Mn concentration was observed for all variants. Hence,  $Mn^{III,IV}$  acted also under moderately reducing conditions as an electron acceptor, and the pool of  $Mn^{III,IV}$  compounds was not exhausted during the course of the experiment.

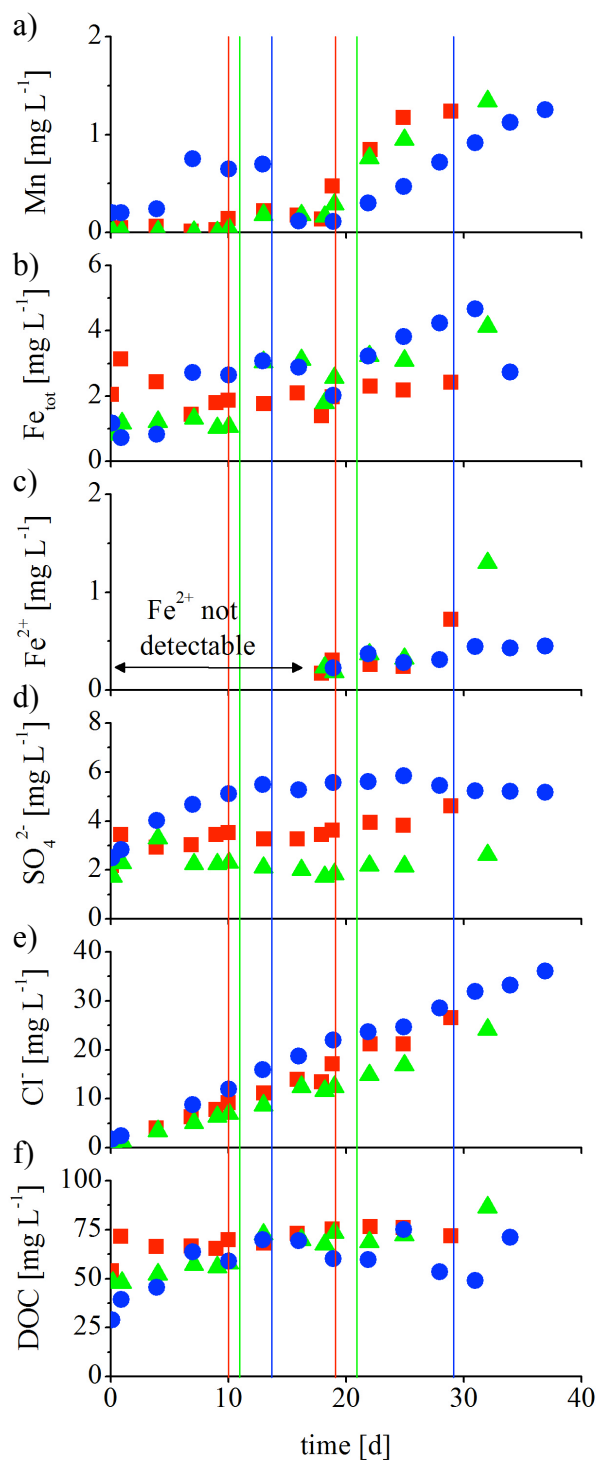


Fig. 3.3: Development of the concentrations of total Mn, total Fe ( $\text{Fe}_{\text{tot}}$ ), ferrous Fe ( $\text{Fe}^{2+}$ ), sulfate, chloride, and dissolved organic carbon (DOC) during the microcosm experiments performed at 7, 15, and 25 °C (● 7 °C, ▲ 15 °C, ■ 25 °C) with change of conditions from oxidising to weakly reducing und from weakly reducing to moderately reducing at 25 °C —, 15 °C —, and 7 °C —

### 3.3.4.2 Iron

Dissolved Fe was determined both as total Fe (Fig. 3.3b) and as Fe<sup>2+</sup> (Fig. 3.3c). The reduced Fe species was neither detectable at oxidizing nor at moderately reducing conditions, which is consistent with its thermodynamic stability. Nevertheless, we found Fe in all temperature variants at these redox conditions with a concentration around 2 mg L<sup>-1</sup>. Since Fe<sup>3+</sup> is quite insoluble at the moderately acid to circumneutral pH conditions of the experiment, we assume that this Fe was complexed with organic ligands. The highest concentration of total Fe appeared at the beginning of the experiment which could be caused by increasing solubility of salts or dispersion of Fe-containing DOC colloids (Favre et al., 1997; Li et al., 2010a). Dissimilatory Fe reduction starts at a E<sub>H</sub> of about 150 mV (Cogger et al., 1992; Patrick and Jugsujinda, 1992). Hence, under these moderately reducing conditions Fe<sup>2+</sup> should appear in the solution. This was true for all variants. The temperature variant at 7 °C showed only a small increase of Fe<sup>2+</sup> that was accompanied by a slow decrease of the E<sub>H</sub>. In contrast, the temperature levels at 15 and 25 °C showed a clear increase of Fe<sup>2+</sup> together with a stronger decrease in E<sub>H</sub>. The higher Fe<sup>2+</sup> concentration at 15 °C is explainable, because the E<sub>H</sub> was lower in comparison to the 25 °C variant. Overall, the Fe<sup>2+</sup> concentrations were closely related to the E<sub>H</sub> ( $r = 0.756^{***}$ ). Like Mn<sup>III,IV</sup>, Fe<sup>III</sup> acts at the appropriate E<sub>H</sub> as the electron acceptor according to the reaction  $\text{CH}_3\text{COO}^- + 8\text{Fe}(\text{OH})_3 + 6\text{H}_2\text{O} \rightarrow 8\text{Fe}^{2+} + 2\text{HCO}_3^- + 15\text{OH}^-$ . From the continuous increase of the Fe<sup>2+</sup> concentrations we conclude that the pool of bioavailable Fe<sup>III</sup> was not exhausted during the course of the experiment.

### 3.3.4.3 Sulfate

Sulfate concentrations were relatively stable and ranged at a quite low level from 2.5 to 5.9 mg L<sup>-1</sup> at 7 °C, 2.2 to 4.6 mg L<sup>-1</sup> at 15 °C, and 1.7 to 3.3 mg L<sup>-1</sup> at 25 °C (Fig. 3.3d). Dissimilatory sulfate reduction takes place when the E<sub>H</sub> level drops below -100 to -150 mV, i.e., at strongly reducing conditions (Connell and Patrick, 1968). This was not the case during our experiments, and we can exclude this process to be working here. Hence, we can also exclude that precipitation of chalcophile trace elements as sulfides occurred during the experiment.

#### **3.3.4.4 Dissolved Organic Carbon**

Figure 3.3e shows the development of the DOC concentrations. Dissolved organic matter is of importance because it acts as a ligand for trace elements, thus affecting their solubility. The temperature variant at 7 °C showed an increase from 28 up to 70 mg L<sup>-1</sup>. Then, the DOC concentrations alternated between 49 and 75 mg L<sup>-1</sup>. For 15 °C, an increase from 48 up to 86 mg L<sup>-1</sup> was also observed. For 25 °C the DOC concentrations varied on a high level between 54 and 88 mg L<sup>-1</sup> with a relatively high concentration of 71.4 mg L<sup>-1</sup> at the beginning of the experiment. At oxidizing conditions, some of the DOC was presumably consumed by oxidation of the organic C (especially at 25 °C) as presented before. At anaerobic conditions, this oxidation is much slower. The source of DOC in our experiment is released from the solid phase. This can be caused by the increase of the pH and/or the reductive dissolution of oxides (Fiedler and Kalbitz, 2003; Grybos et al., 2009). In the first case, adsorbed DOC is liberated, and in the second case, DOC bound to Mn or Fe oxides is released.

#### **3.3.4.5 Chloride**

For the chloride concentrations, a continuous, more or less linear increase during the course of the experiment was observed (Fig. 3.3f). Chloride is neither involved in redox processes nor is it adsorbed onto the solid phase in significant amounts. Instead, chloride was leached from the electrolyte of the pH electrode throughout the entire experiment. This is an experimental shortcoming that cannot be avoided; however, chloride has to be taken into account for the objective of the current study because it acts as a strong ligand for Cd (Garcia-Miragaya and Page, 1976).

### **3.3.5 Trace elements**

#### **3.3.5.1 Non-redox sensitive and cationic trace elements**

At first, the solubility of the trace elements that are exclusively occurring as divalent cations (dissolved as free ions and complexed with inorganic and organic ligands, respectively) under the redox conditions of soils, i.e., those of Cd, Ni, Pb, and Zn, will be presented and discussed. Since Cu might be reduced to  $\text{Cu}^{\text{I}}$  or even to  $\text{Cu}^0$  only under specific environmental circumstances (Simpson et al., 2000; Weber et al., 2009), dissolved Cu is assumed to be present in its divalent form. As a general rule, the solubility of divalent trace-metal cations in soils decreases with increasing pH which among other things is caused by strong inner-sphere surface complexation of the metal-hydroxido species on certain soil constituents. Differences in the first hydrolysis constant of the trace elements result in element-specific critical pH-values above which their solubility in soils is low. This critical pH is at 4.0 for Pb, 4.5 for Cu, 5.5 for Ni, 5.5 to 6.0 for Zn, and 6.5 for Cd. Considering the range and development of the pH in the soil suspensions (Fig. 3.2b), it can be inferred for the divalent metals that adsorption should be favored (increasing pH), that the pH-effect on adsorption should be low (for Cd) to negligible (for the other metals the pH is more or less well above the critical pH), and that other solubility-governing processes should be more important.

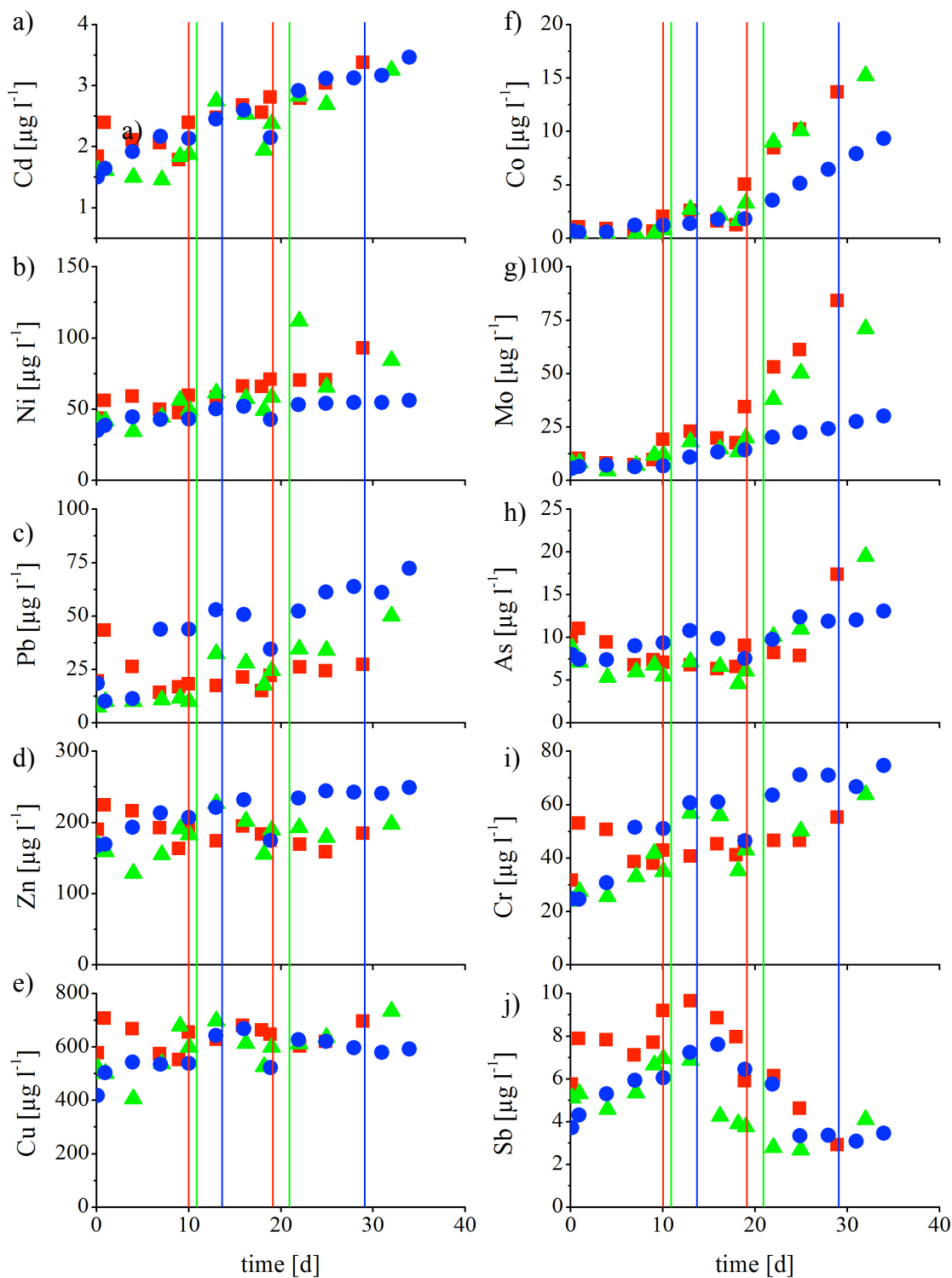


Fig. 3.4: Development of the concentration of ten trace elements during the microcosm experiments performed at 7, 15, and 25 °C (● 7 °C, ▲ 15 °C, ■ 25 °C) with change of conditions from oxidising to weakly reducing und from weakly reducing to moderately reducing at 25 °C —, 15 °C —, and 7 °C —

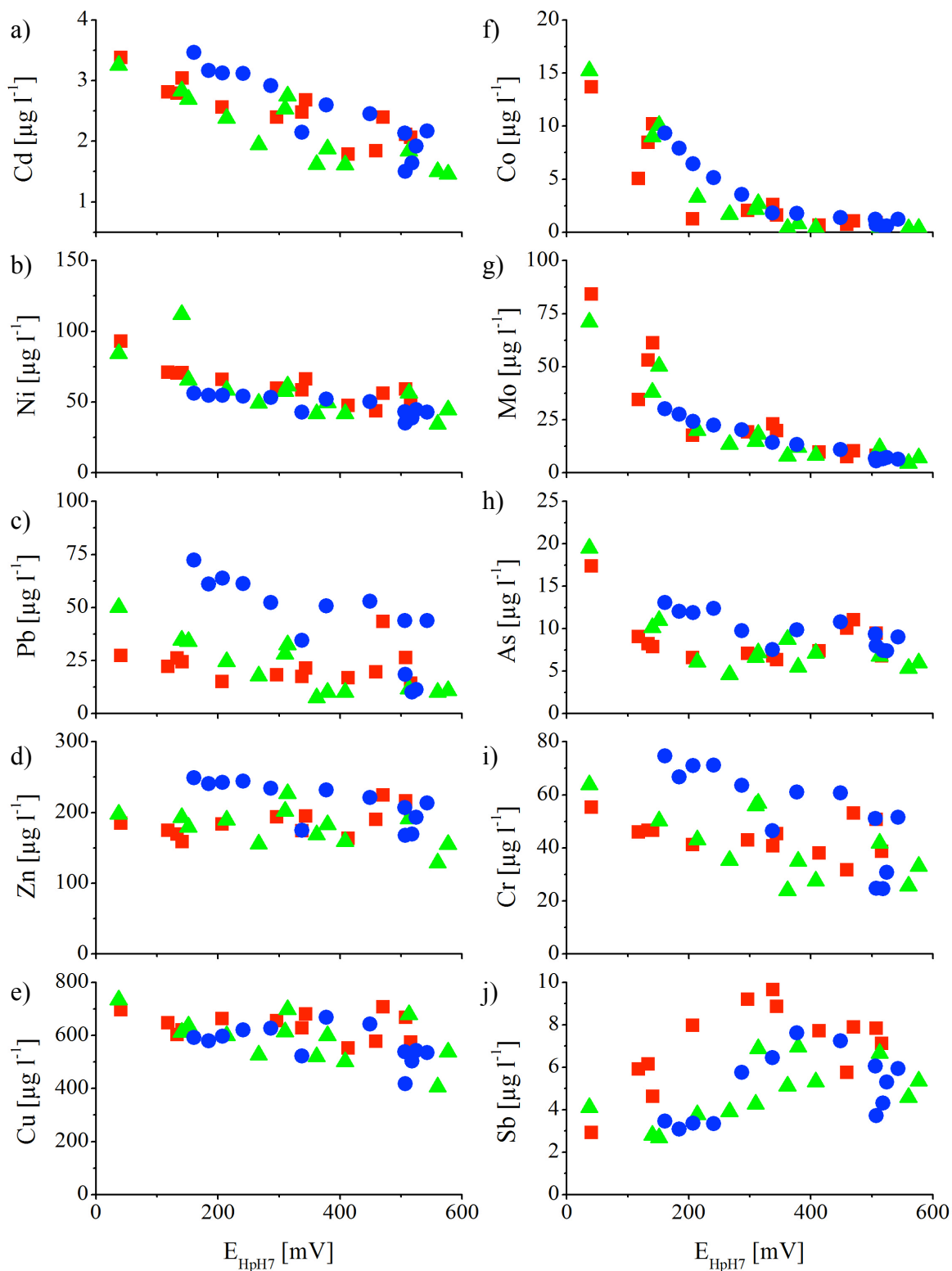


Fig. 3.5: Relationship between the concentrations of ten trace elements and the redox potential ( $E_{\text{HpH7}}$ ) performed at 7, 15, and 25 °C (● 7 °C, ▲ 15 °C, ■ 25 °C)



Tab. 3.4: Correlation between  $E_H$  and the trace element concentrations

	7 °C		15 °C		25 °C		Total	
	$r_s^{\ddagger}$	$p^{\ddagger}$	$r$	$p$	$r$	$p$	$r$	$p$
<b>Cd</b>	-0.914	< 0.001	-0.876	< 0.001	-0.881	< 0.001	-0.834	< 0.001
<b>Ni</b>	-0.839	< 0.001	-0.742	0.004	-0.864	< 0.001	-0.721	< 0.001
<b>Pb</b>	-0.800	0.001	-0.854	< 0.001	-0.015	0.961	-0.436	0.021
<b>Zn</b>	-0.735	0.004	-0.516	0.071	-0.567	0.043	-0.208	0.342
<b>Cu</b>	-0.513	0.073	-0.587	0.035	-0.273	0.366	-0.466	0.002
<b>Co<sup>#</sup></b>	-0.968	< 0.001	-0.947	< 0.001	0.907	0.001	-0.929	< 0.001
<b>Mo<sup>#</sup></b>	-0.995	< 0.001	-0.950	< 0.001	-0.934	< 0.001	-0.897	< 0.001
<b>As</b>	-0.802	0.001	-0.702	0.008	-0.313	0.299	-0.539	< 0.001
<b>Cr</b>	-0.811	0.001	-0.660	0.014	-0.378	0.203	-0.574	< 0.001
<b>Sb</b>	0.466	0.109	0.597	0.031	0.536	0.064	0.421	0.008

§ correlation coefficient  
 ‡ significance level  
 † number of samples  
 # exponential correlation

### **3.3.5.1.1 CADMIUM**

Cadmium is an ultra-trace metal even for this contaminated site which was reflected by the very low concentrations that did not exceed  $3.47 \mu\text{g L}^{-1}$  (at  $7^\circ\text{C}$ ) in the soil suspensions (Fig. 3.4a). For all temperature variants, an increase of the Cd concentrations with decreasing  $E_{\text{H}}$  could be observed (Fig. 3.5a). Interestingly, when the redox conditions changed from oxidizing to moderately reducing and from moderately to weakly reducing conditions, there was a low but distinct increase in the Cd concentrations. Whether Mn oxides play a significant role in the sequestration of Cd is unclear and should be studied in the future. Using a similar experimental design but not differentiating between weakly and moderately reducing conditions, an increase of the Cd solubility with decreasing  $E_{\text{H}}$  has been reported in the literature, and has been attributed to the reductive dissolution of Mn and Fe oxides and the subsequent release of adsorbed Cd (Charlatchka and Cambier, 2000; Chuan et al., 1996; Li et al., 2010a). A high correlation between the Cd concentrations and the  $E_{\text{H}}$  (Tab 3.4), as well as with total Fe ( $r = 0.752^{***}$ ) and Mn ( $r = 0.754^{***}$ ), underlines this. Indeed, the sequential extraction showed that significant proportions of Cd were associated with Mn (13.7 %) and Fe oxides (24.1 %) (Tab. 3.3).

Another important factor for the solubility of Cd is the concentration of chloride, since this anion acts as a strong ligand for  $\text{Cd}^{2+}$  (Garcia-Miragaya and Page, 1976). In this study, the chloride concentrations increased in a relatively constant manner because of the bleeding of the electrolyte (Fig. 3.3e). As a consequence, a strong relationship between the concentrations of chloride and Cd was found ( $r = 0.875^{***}$ ). Modeling of the species distribution revealed, however, that the proportions of the Cd-chlorido species, e.g.  $\text{CdCl}^+$ , increased only slightly from 0.04 % to 1.8 % of total dissolved Cd during the course of the experiment. Hence, the formation of such inorganic complexes cannot explain the increasing solubility of Cd. Although the influence of organic ligands on the Cd solubility is less important in comparison to other trace elements (Adriano, 2001), most of the dissolved Cd was organically complexed (63.9 to 86.7 %). Free  $\text{Cd}^{2+}$  concentrations ranged from 12.3 to 36.0 % of total dissolved Cd.

### **3.3.5.1.2 NICKEL**

Figure 3.4b displays the development of the Ni concentrations and Fig. 3.5b shows the relationship between the  $E_{\text{H}}$  and the dissolved phase. The solubility of Ni increased with decreas-

ing  $E_H$ , although this pattern was not so pronounced as for Cd. Initially, under oxidizing conditions, the concentrations were relatively constant (7 and 15 °C) or decreased slightly (25 °C). When the redox conditions changed to weakly reducing and moderately reducing, a slight increase of the Ni concentration occurred for all temperature variants. Overall, the Ni concentrations increased from 35.1 to 56.1  $\mu\text{g L}^{-1}$  at 7 °C, from 34.4 to 84.2  $\mu\text{g L}^{-1}$  at 15 °C, and from 43.3 to 93.1  $\mu\text{g L}^{-1}$  at 25 °C. The Ni concentrations were significantly correlated to the  $E_H$  (Tab. 3.4) and to a lesser extent to total Fe ( $r = 0.491^{***}$ ) and Mn ( $r = 0.567^{***}$ ).

Nickel release after the reductive dissolution of Mn and Fe oxides was also reported by Antić-Mladenović et al. (2011), Grybos et al. (2007) and Weber et al. (2009). Moreover, the solubility of Ni is promoted by an increasing solubility of organic matter since Ni forms relatively stable complexes with organic ligands (Adriano, 2001). This relationship is shown in the experiment by a stronger correlation between dissolved Ni and DOC ( $r = 0.694^{***}$ ). Indeed, the sequential extraction confirmed that large amounts of Ni were bound to Fe oxides (nearly the half) as well as to organic matter (nearly one-fifth) (Tab. 3.3). Furthermore, between 83.0 and 93.9 % of the dissolved Ni was coordinated with organic ligands, as revealed by modeling.

#### **3.3.5.1.3 LEAD**

With the exception of the 25 °C temperature variant, the concentrations of Pb increased during the course of the experiment (Fig. 3.4c) and showed a stronger relationship to the  $E_H$  for the 7 and 15 °C variants (Fig. 3.5c; Tab. 3.4). However, the overall relationship between both parameters was poor (Tab. 3.4). The reason for the initial increase of the Pb concentrations at 25 °C could be the rewetting of the dry soil sample and subsequent release of Pb-loaded DOC or inorganic colloids, e.g. Fe oxides. However, during the entire experiment, Pb-containing colloids could have been released. This is supported by the very high correlation between Pb and total Fe ( $r = 0.898^{***}$ ). With the real dissolved and reduced Fe fraction, i.e.  $\text{Fe}^{2+}$  the correlation was considerably lower and not significant ( $r = 0.285$ ). Increasing Pb concentrations in the range of  $\text{Fe}^{\text{III}}$  reduction were reported by Charlatchka and Cambier (2000), Grybos et al. (2007) and Weber et al. (2009). It is well known that Pb forms very strong complexes with the functional groups of the soil organic matter pool (Adriano, 2001). As a result, about half of the Pb was associated with the organic extractable fraction (Tab. 3.3), and high correlations between dissolved Pb and DOC were found for the individual temperature variants

(7 °C:  $r = 0.719^{**}$ ; 15 °C:  $r = 0.913^{***}$ ). Also, almost all of the dissolved Pb was organically complexed (99.4 to 99.9 %).

#### **3.3.5.1.4 ZINC**

The concentrations of Zn showed an inconsistent development between the three temperature variants (Fig. 3.4d). While the Zn concentrations slightly increased during the course of the experiment for the 7 °C (from 168 up to 249  $\mu\text{g L}^{-1}$ ) and 15 °C (from 129 up to 227  $\mu\text{g L}^{-1}$ ) variant, the Zn concentrations of the 25 °C variant decreased at the beginning of the experiment and then tended to remain constant. As a result, the correlation between the Zn concentrations and the  $E_H$  was positive but not significant for the 25 °C variant (Tab. 3.4). Both other variants revealed a negative relationship between the Zn concentrations and the  $E_H$ .

Using similar equipment, Chuan et al. (1996) found a Zn release and related this to the reductive dissolution of Mn and Fe oxides. Although we observed a stronger correlation between total Fe and Zn ( $r = 0.668^{***}$ ), the low correlation between  $\text{Fe}^{2+}$  and Zn ( $r = 0.134$ ) allowed us to assume that some Zn occurred in a colloidal form. Like Cd, the influence of organic ligands on the Zn solubility is not so pronounced in comparison to other trace elements (Adriano, 2001). However, most of the dissolved Zn was organically complexed (61.7 to 89.2 %), and a significant proportion (10.5 to 37.9 %) occurred in the free form as  $\text{Zn}^{2+}$ .

#### **3.3.5.1.5 COPPER**

Copper concentrations were at a high level and ranged from 406 to 734  $\mu\text{g L}^{-1}$  (Fig. 3.4e). Independent from temperature, the concentrations scattered more or less strongly and showed no clear relationship to the  $E_H$  (Fig. 3.5e). The overall correlation between the Cu concentrations and the  $E_H$  was low, which was also the case for the individual variants (Tab. 3.4). Of all divalent trace elements investigated, Cu together with Zn showed the poorest relation to the  $E_H$ . Such high variability of dissolved Cu concentrations was also demonstrated in other experiments (Olivie-Lauquet et al., 2001; van der Geest and León Paumen, 2008; Wang and Staunton, 2006).

The most important adsorbent for Cu in soil is the organic matter. Consistent, the sequential extraction showed that about two-thirds of the Cu was bound to the organic fraction (Tab. 3.3). Copper forms very strong complexes with DOC (Adriano, 2001); accordingly,

more than 99.9 % of total dissolved Cu was coordinated with organic ligands as revealed by modeling, and there was a high correlation between Cu and DOC ( $r = 0.755^{***}$ ).

### **3.3.5.2 Redox sensitive and/or anionic trace elements**

The elements As, Cr, Mo, and Sb are known to occur in aqueous solutions exclusively as oxoanions with the exception of the trivalent Cr cation ( $\text{Cr}^{3+}$ ). Cobalt occurs in a cationic form with the oxidized species  $\text{Co}^{3+}$  and the reduced species  $\text{Co}^{2+}$ . All of these elements participate in electron exchange reactions and hence change their valence state. Because many redox reactions are not in equilibrium and kinetically not favored, we did not model the distribution of the redox species.

#### **3.3.5.2.1 COBALT**

Figure 3.4f presents the development of the Co concentrations. Overall, a clear increase of the concentration with decreasing  $E_H$  is recognizable for all temperature variants. More accurately, two individual increases appeared during the experiment. A first slight increase occurred when the  $E_H$  was converted from oxidizing to weakly reducing conditions. Then the Co concentrations increased up to  $6.47 \mu\text{g L}^{-1}$  (at  $7^\circ\text{C}$ ). When the  $E_H$  was switched from weakly reducing to moderately reducing conditions, the second increase of Co concentrations happened which was much stronger and nearly linear indicating a continuous release of Co (up to  $15.2 \mu\text{g L}^{-1}$  at  $15^\circ\text{C}$ ). Under these redox conditions, the Co release of the  $7^\circ\text{C}$  variant was lower than those of both other variants, which were nearly identical.

The Co concentrations showed high correlations to  $E_H$  (Tab. 3.4),  $\text{Fe}^{2+}$  ( $r = 0.744^{***}$ ) and Mn ( $r = 0.901^{***}$ ). Cobalt is featured by a high affinity to Fe oxides and, in contrast to many other elements, a very high affinity to Mn oxides. On the surface of Mn oxides, dissolved Co is oxidized from  $\text{Co}^{2+}$  to  $\text{Co}^{3+}$  (Burns, 1976; Murray and Dillard, 1979). Trivalent  $\text{Co}^{3+}$ , in turn, can be embedded into the crystal lattice of Mn oxides (Kay et al., 2001; Manceau et al., 1997), thus minimizing its mobility. When the oxides of Fe, and especially Mn, are reductively dissolved, the Co associated with these oxides is released into the solution. The outstanding role of Mn oxides for the behavior of Co is reflected by the appearance of Co in the soil solution already under weakly reducing conditions and the very strong correlation between Co dissolved Mn. Since the bioavailable pool of Mn oxides was not exhausted during this

experiment (Fig. 3.3b), the main source of the released Co even under moderately reducing conditions should be Mn oxides. A similar strong correlation between dissolved Co and Mn ( $r = 0.952^{***}$ ) was found by Pelfrêne et al. (2009) in pore waters of an unpolluted soil. Cornu et al. (2009) showed that Co was released at the same rate as Mn when the  $E_H$  in columns filled with soil nodules was lowered to about 100 mV, i.e., in the  $Mn^{III,IV}$  reduction range. However, Fe oxides as a source of Co cannot be excluded for the current study since the sequential extraction indicated that Fe oxides seemed to be the main binding partners of Co (Tab. 3.3).

Divalent Co should be the dominant species in this experiment according to the literature (Collins and Kinsela, 2010, and references cited therein). In contrast to  $Co^{2+}$ , trivalent Co reveals an extremely low solubility in the absence of strong organic ligands due to the formation of sparingly soluble hydroxides ( $K_{sp}$  of  $Co(OH)_3$  is at  $10^{-44.5}$ ) (Smith and Martell, 1976) and oxyhydroxides ( $K_{sp}$  of  $CoOOH$  is at  $10^{-50.0}$ ) (Hem et al., 1985). It was previously assumed that the impact of organic complexes is not important, because Co does not have the tendency to form stronger complexes with soil organic matter (McLaren et al., 1986). However, Collins and Kinsela (2010) stated that due to the kinetics of the  $Co^{II}$  complexation and dissociation to and from natural organic ligands the speciation of Co is likely to diverge from modeling based on thermodynamics equilibrium calculations. This renders the speciation of Co quite questionable.

### **3.3.5.2.2 MOLYBDENUM**

Like Co, the Mo concentrations increased not only with decreasing  $E_H$  (Fig. 3.4g) but also two jumps appeared during the experiment. Under oxidizing conditions, only small amounts of Mo were present in the solution ( $<12.1 \mu g L^{-1}$ ). When the  $E_H$  achieved weakly reducing conditions, the solubility of Mo increased up to  $24.3 \mu g L^{-1}$ . The largest increase appeared under moderately reducing conditions with concentrations of  $30.2 \mu g L^{-1}$  at  $7^\circ C$ ,  $71.0 \mu g L^{-1}$  at  $15^\circ C$ , and  $84.2 \mu g L^{-1}$  at  $25^\circ C$  at the end of the experiment. Under moderately reducing conditions, the release of Mo was nearly linear, like that of Co, indicating a continuous release of Mo. In contrast to Co, however, the temperature dependence was more evident since the release of Mo increased in the order  $7^\circ C > 15^\circ C > 25^\circ C$ .

Like Co, Mo showed a very high correlation to  $E_H$  (Tab. 3.4). Strong adsorption of this oxoanion onto the surfaces of Fe oxides is well established (Goldberg et al., 1996; Xu et al.,

2006). Results of the sequential fractionation matched this, because about half of the Mo was bound to Fe and Mn oxides (Tab. 3.3), and reductive dissolution of these oxides seemed to be the major source of the released Mo. The high correlation between Mo and  $\text{Fe}^{2+}$  ( $r = 0.614^{**}$ ) and especially Mn ( $r = 0.812^{***}$ ) confirm this behavior. Bennett and Dudas (2003) found in a soil incubation experiment under reducing conditions that aqueous phase concentrations of Mo were largely controlled by dissolution and desorption from the Fe oxide host. However, the pH could also have contributed to the release of Mo. At pH 4, the maximum adsorption of Mo is achieved and with increasing pH the solubility of Mo rises due to lowered adsorption (Goldberg et al., 1996). This behavior is in contrast to that of the cationic trace elements. Furthermore, increasing DOM concentrations promote the solubility of Mo because Mo can be bound to the soil organic matter (Wichard et al., 2009).

#### **3.3.5.2.3 ARSENIC**

Arsenic concentrations scattered under oxidizing and weakly reducing conditions with concentrations that ranged from 7.37 to 12.4  $\mu\text{g L}^{-1}$  at 7 °C, from 4.59 to 8.73  $\mu\text{g L}^{-1}$  at 15 °C, and from 6.34 to 11.0  $\mu\text{g L}^{-1}$  at 25 °C (Fig. 3.4h). However, for all temperature variants, the concentrations increased when the  $E_H$  achieved the range of moderately reducing conditions. Under these redox conditions, the As concentrations increased up to 13.1  $\mu\text{g L}^{-1}$  at 7 °C, up to 19.5  $\mu\text{g L}^{-1}$  at 15 °C, and up to 17.4  $\mu\text{g L}^{-1}$  at 25 °C. The release of As showed a temperature dependence, because the increase was much larger at 15 °C and 25 °C than at 7 °C, which was in contrast to both previous redox ranges where no clear relationship existed.

Arsenic in the soil suspensions was strongly correlated to  $\text{Fe}^{2+}$  ( $r = 0.864^{***}$ ) and weaker to total Fe ( $r = 0.624^{***}$ ), Mn ( $r = 0.731^{***}$ ) and  $E_H$  (Tab. 3.4). Sequential fractionation revealed that by far the largest portion, i.e. three quarters of As belonged to Fe oxides (Tab. 3.3). The release of As into the aqueous phase of soils after water saturation has been previously reported by many studies (Deuel and Swoboda, 1972; Hess and Blanchar, 1977; Masscheleyn et al., 1991; Weigand et al., 2010) and has been related to the reductive dissolution of As-hosting Fe oxides. The strong correlation between dissolved As and  $\text{Fe}^{2+}$  in the current study underlines the importance of this process. However, the release of sorbed As after the dissolution of Fe oxides is not the only method of As mobilization under reducing conditions. As a second process, dissimilatory arsenate-reducing prokaryotes are able to reduce sorbed arsenate to arsenite without dissolution of the oxide (Oremland and Stolz, 2005).

Because the surface complexes of arsenite are far more labile than its oxidized counterpart at acidic to near-neutral pH, arsenite is therefore preferentially released into solution (Fendorf and Kocar, 2009). It cannot be excluded that the second process also occurred in the current study. The importance of Mn oxides in sequestering As is not yet clarified. Smedley and Kinniburgh (2002) suggested that Mn oxides might be important carriers for As, and it is indeed known that Mn oxides are strong adsorbents for As (Deschamps et al., 2003; Oscarson et al., 1983). On the other hand, Mn oxides are relatively unstable minerals, especially in soils with reducing conditions, which weakened their role in As sequestration (Mitsunobu et al., 2006; Takahashi et al., 2003). Also, in the floodplain soils of the German river Mulde, Mn oxides did not contribute significantly to As sequestration, which was in contrast to Fe oxides (Ackermann et al., 2010). Using the same equipment as this study, Mansfeldt and Overesch (2013) did not observe any As mobilization under weakly reducing conditions but a significant mobilization under moderately reducing conditions in a soil with naturally elevated levels of As. Additionally, the DOM may have enhanced the solubility of As since As can be coordinated by organic ligands (Bauer and Blodau, 2006).

#### **3.3.5.2.4 CHROMIUM**

Figure 3.4i illustrates the development of the Cr concentrations and figure 3.5i shows the relationship between the Cr concentrations and the  $E_H$ . For Cr no clear temperature dependence could be observed. Whereas the 7 °C and the 15 °C variants revealed an increase of the Cr concentrations during the course of the experiment and were strongly correlated with the  $E_H$ , the 25 °C variant scattered strongly and was only loosely correlated to the  $E_H$  (Tab. 3.4).

In nature, the oxidation states of +III and +VI are prevalent for Cr. The two species show contrasting geochemical behavior. Aqueous dissolved  $Cr^{VI}$  is exclusively present in anionic form as  $HCrO_4^-$  predominant at pH <6.5, and as  $CrO_4^{2-}$  predominant at pH >6.5 (Fendorf, 1995) which is the pH-range in this experiment. Like other oxoanions,  $Cr^{VI}$  tend to bind strongly onto Fe oxides (Abdel-Samad and Watson, 1997; Fendorf et al., 1997). These oxides even play an outstanding role in the sequestration of Cr in this soil because about three quarters of the total Cr was bound to Fe oxides, especially to the none-crystalline Fe fraction (Tab. 3.3). Hence, a strong correlation between the Cr concentrations and total dissolved Fe was found ( $r = 0.842^{***}$ ) and dissolution of Fe oxide can be regarded as important for the Cr solubility. For  $Cr^{VI}$  an adsorption maximum is expected at pH values close to the  $pK_{a1}$  of the



conjugate acid, chromic acid, which is very low ( $pK_{a1} = -0.2$ ; (Martell et al., 2004). Therefore, experimental data typically show a decrease in  $Cr^{VI}$  adsorption with increasing pH (Jiang et al., 2008). Overall,  $Cr^{VI}$  tends to have a high solubility in soils, particularly under slightly acid to alkaline conditions which was the case in this study.

Trivalent Cr is strongly retained by minerals and, at  $pH > 5.5$   $Cr^{III}$  precipitates as a sparingly soluble amorphous Cr(III)-hydroxide, which is highly reactive with soil mineral surfaces such as Fe oxides (Rai et al., 1987). Only if complexed with organic acids  $Cr^{III}$  can remain soluble at pH values up to 6.7 or higher depending on  $pK_a$  and concentrations of complexing ligands (James and Bartlett, 1983). The low solubility of  $Cr^{III}$ -hydroxide and the strong adsorption onto soil constituents at  $pH > 5.0$  result in a low mobility of  $Cr^{III}$  in soils (Hooda, 2010). Considering this, it can be assumed that most of the dissolved Cr occurred as the oxidized species. If  $Cr^{III}$  was adsorbed onto Fe oxides and released by their reductive dissolution, it should be rapidly removed by precipitation and adsorption unless it was not organically complexed.

### **3.3.5.2.5 ANTIMONY**

At the beginning, the Sb concentrations increased under oxidizing to weakly reducing conditions from 3.71 up to 7.62  $\mu g L^{-1}$  at 7 °C, from 4.59 up to 6.95  $\mu g L^{-1}$  at 15 °C, and from 5.77 up to 9.67  $\mu g L^{-1}$  at 25 °C (Fig. 3.4j). Remarkably, when the  $E_H$  dropped below 345 mV (7 °C), 315 mV (15 °C), and 285 mV (25 °C), the Sb concentrations more or less continuously decreased to 3.08  $\mu g L^{-1}$  at 7 °C, to 2.68  $\mu g L^{-1}$  at 15 °C, and to 2.93  $\mu g L^{-1}$  at 25 °C (Fig. 3.5j). At the end of the experiment, Sb concentrations tended to slightly increase. The Sb concentrations were positively but not significantly correlated to  $E_H$  (Tab. 3.4),  $Fe^{2+}$  ( $r = -0.271$ ) and total Mn ( $r = -0.524^{**}$ ). Overall, Sb showed a unique behavior of all elements under investigation because its concentration decreased soon after the onset of weakly reducing conditions that was the case for all variants.

Antimony exists in the environment as antimonate ( $Sb^V$ ) at oxidizing conditions and as antimonicite ( $Sb^{III}$ ) at reducing conditions. The corresponding main species for antimonate in acid to neutral environments is  $Sb(OH)_6^-$  as indicated by the  $pK_a$ -value of 2.47. Antimonate is very soluble in oxic environments. Assuming that at the beginning of the experiment  $Sb(OH)_6^-$  was the main species, the high solubility is reflected in the current study because Sb concentrations were at oxidizing conditions in a similar order of magnitude like the As

concentrations, although the total Sb content was substantially lower (Tab. 3.2). The main trivalent Sb species in natural environments is  $\text{Sb}(\text{OH})_3^0$  because the  $\text{pK}_a$ -value of the antimonous acid is 11.82. As reviewed by Filella and Williams (2012) and Wilson et al. (2010), Fe oxides are the main adsorbents for Sb in soil, which is confirmed for this site because about two-thirds of Sb belonged to Fraction 5 and 6 (Tab. 3.3). However, binding on Fe oxides is significant at acidic pH values both for  $\text{Sb}^{\text{III}}$  and  $\text{Sb}^{\text{V}}$ , but decreases abruptly above pH 6 to 8 in the case of  $\text{Sb}^{\text{V}}$ . Hence, the species distribution could have greatly influenced the solubility of Sb in the current study because the experiments' pH was in the sensitive range and the following is taken into account: according to the  $E_{\text{H}}$ /pH diagram of Fe, Mn and Sb solubility, the reduction of  $\text{Sb}^{\text{V}}$  to  $\text{Sb}^{\text{III}}$  occurs after reduction of  $\text{Mn}^{\text{III,IV}}$  but before or at the same time as  $\text{Fe}^{\text{III}}$ -reduction in the pH range from 7 to 8 (Cornelis et al., 2012). In this study, Sb concentrations decreased soon after weakly reducing conditions were achieved. Hence, the reduction of  $\text{Sb}^{\text{V}}$  to  $\text{Sb}^{\text{III}}$  and the subsequent preferential adsorption of the reduced species might have resulted in the decrease of Sb concentrations. At the end of the experiment, the rate of the dissolutions of Fe oxides was presumably greater than the rate of the  $\text{Sb}^{\text{III}}$  adsorption resulting in an increase of the Sb concentration. Reduction of  $\text{Sb}^{\text{V}}$  and subsequent sorption of  $\text{Sb}^{\text{III}}$  was also postulated by Wan et al. (2013), who performed a pot experiment under different water regimes with accompanying Sb species analyses and  $E_{\text{H}}$  measurements; this mechanism was also postulated by Mitsunobu et al. (2010). However, this behavior is in contradiction to that seen by Mitsunobu et al. (2006); they found that Sb was present exclusively as  $\text{Sb}^{\text{V}}$  over a wide  $E_{\text{H}}$  range (from 360 to  $-140$  mV, pH 8) and stated that  $\text{Sb}^{\text{V}}$  is a very stable form in the environment. More studies dealing with the mechanisms and kinetics of redox processes at which Sb is involved are needed.

### **3.4 Conclusion**

This laboratory experiment investigated the release of ten trace elements in soil suspensions of a multiple-contaminated floodplain soil which were held at fixed  $E_{\text{H}}$  representing different redox conditions, namely oxidizing ( $\text{O}_2$  is predominant), weakly reducing (onset of  $\text{Mn}^{\text{III,IV}}$  reduction) and moderately reducing (onset of  $\text{Fe}^{\text{III}}$  reduction). Furthermore, the effects of temperature were studied. The following findings should be highlighted. First, the temperature exerts a significant effect on how fast reducing soil conditions could be obtained. Obviously, a higher temperature accelerates the biological activity which, in turn, resulted in a faster  $\text{O}_2$ -consumption and subsequent reductive dissolution of Mn and Fe oxide. Risk assessment and nutrient management for periodically water saturated soils should consider soil

temperature. Second, weakly reducing conditions should be distinguished from moderately reducing conditions because Co but also Mo are already mobilized when  $\text{Mn}^{\text{III,IV}}$  acts as the terminal electron acceptor. Third, Cd, Ni, Pb, As and Cr were more sensitive to the reductive dissolution of Fe oxides than Zn and especially Cu. Finally, Sb revealed a contrasting behavior because its concentration decreased soon after weakly reducing conditions were obtained indicating rather immobilization than mobilization at such redox conditions. Reduction of the more soluble  $\text{Sb}^{\text{V}}$  and subsequent sorption of  $\text{Sb}^{\text{III}}$  might have caused this, which underlines the need for Sb speciation analysis.

## **4 MERCURY VOLATILIZATION FROM A FLOODPLAIN SOIL DURING A SIMULATED FLOODING EVENT**

### **4.1 Introduction**

Mercury is a toxic element and may cause serious environmental and health problems (Counter and Buchanan 2004). Especially the methylated species  $\text{CH}_3\text{Hg}^+$ , monomethylmercury (MMHg), is responsible for major diseases. Monomethylmercury is a neurotoxin that is largely present in fish and seafood products and accumulates in the food chain (Morel et al. 1998). Another species of concern is  $(\text{CH}_3)_2\text{Hg}$ , dimethylmercury (DMHg). Because of their different behaviors, mobilities, and bioavailabilities, it is important to distinguish between the Hg species.

Floodplains are found worldwide. Their soils feature frequent flooding and thus induced permanent delivery of new sediments. With the supply of new sediments through the flooding, high amounts of trace elements including Hg can be deposited (Du Laing et al. 2009; Overesch et al. 2007). The main sources of Hg in floodplains are industrial and mining activities but also agricultural uses, atmospheric deposition, the disposal of municipal wastewaters, and runoff (Du Laing et al. 2009). The increased deposition of Hg in floodplains started during industrialization. Nowadays only small amounts of Hg enter the floodplain soils. However, the amounts of Hg are often still high and deposited Hg has the potential to be remobilized.

One example of highly Hg-contaminated areas is the floodplains of the Elbe River in Germany. As stated by Rinklebe et al. (2010), these floodplain soils contain ten times more Hg compared to floodplain soils in the USA. Unlike other toxic elements, Hg can easily volatilize. The main degassing species is elemental Hg ( $\text{Hg}^0$ ), which represents more than 95 % of atmospheric Hg and is thus the major Hg species in the atmosphere (Cobos et al. 2002). However, methylated Hg species can also be produced in environments with anoxic conditions (Hintelmann 2010; Jonsson et al. 2010). Floodplains function as important links between terrestrial and aquatic systems. Floodplain soils are considered to be semi-terrestrial soils because they are temporally flooded. Then even their topsoils are water-saturated and redox conditions change from aerobic to anaerobic. These redox conditions are potentially suitable for the generation of methylated Hg species. While there are certain studies which

investigated the degassing of total gaseous mercury (TGM) from floodplain soils of the Elbe River (Böhme et al. 2005; During et al. 2009; Rinklebe et al. 2010), only Wallschläger et al. (1995) considered the volatilization of different Hg species. Whether methylated Hg is degassed in floodplain soils during and/or after a lasting flooding event is unclear.

The influence of a lasting flooding event and redox conditions on the Hg volatilization and Hg species formation from contaminated floodplain soils of the Elbe River was investigated in the current study. Redox conditions were assessed by measuring the  $E_H$ . A flooding event was simulated by working under water-saturated conditions for two weeks; falling water tables were simulated by two dewatering events after two and three weeks. Changes of these parameters occur naturally at the site under investigation. For example, longer flooding periods happened in August 2002 and, quite recently, in June 2013. To minimize other factors important for the Hg volatilization, for example wind speed or solar radiation, the experiments were performed in the laboratory. For these experiments, columns filled with undisturbed soil taken from a contaminated floodplain site were used. Undisturbed sampling means that the soil physical parameters like pore volume and pore size distribution were preserved so that natural physical soil conditions were realized in the experiments. Overall, the aims of this study were (i) to determine the Hg volatilization from a contaminated floodplain soil affected by water content and redox conditions, and (ii) to identify the degassing Hg species.

## **4.2 Material and Methods**

### **4.2.1 Study site, sampling, and sample preparation**

Soil samples were taken from the grassland of the biosphere reserve “Niedersächsische Elbaue” at Hohnstorf in Lower Saxony, Germany (53°21′25.05″ N; 10°34′42.22″ E). The sampling site was close to the Fiver Elbe and is characterized by periodic flooding events, which are associated with the sedimentation of new soil material. The soil at this site is contaminated by former mining activities, industrial use, and inputs of agriculture and municipal sewage. For the column experiments 12 undisturbed soil samples were collected using polyvinylchloride (PVC) columns (115 mm inner diameter, 100 mm high, 0.935 L volume). First the sod was removed. The PVC columns were equipped with a stainless steel ring and pounded into the soil. Subsequently the columns were excavated, transported to the laboratory, and stored at  $-30\text{ }^{\circ}\text{C}$ . In addition to the column experiments, one kilogram of soil (0 to

100 mm, aAh horizon) was taken from the same place for the soil characterization. This soil sample was manually homogenized, air-dried, and sieved (2 mm). A subsample was ground manually for analysis of total Hg content. Undisturbed soil samples used for the determination of the bulk density were taken from the topsoil with 100 cm<sup>3</sup> steel cylinders (n = 10).

#### **4.2.2 Soil characteristics**

The soil pH was measured potentiometrically in both 0.01 mol L<sup>-1</sup> CaCl<sub>2</sub> solution and water [mixed 5:1 with soil (vol/vol)] by a glass electrode. The particle size distribution was determined by wet sieving and sedimentation using the pipette sampling technique. The organic matter was destroyed by H<sub>2</sub>O<sub>2</sub> before the analyses. The bulk density was measured by drying the cylinders at 105 °C and subsequent weighing. The soil pore space (total porosity) was calculated according the equation: total porosity (%) = 100 % - (d<sub>b</sub>/d<sub>p</sub> × 100), with bulk density (d<sub>b</sub>, kg L<sup>-1</sup>) and particle density (d<sub>p</sub>, kg L<sup>-1</sup>) assuming a particle density of 2.65 kg L<sup>-1</sup> for inorganic particles and 1.30 kg L<sup>-1</sup> for organic matter. The contents of total Fe and Mn were determined after aqua regia extraction. For the extraction, 200 mg of sample was weighed and 6 mL of concentrated HNO<sub>3</sub> (Suprapur, Merck, Germany) and 2 mL of concentrated HCl (Suprapur, Merck, Germany) were added. After microwave digestion (Multiwave, Anton Paar, Austria), the samples were filtered through 2 µm blue ribbon filter (589/3, Whatman, USA) and filled up to 50 mL with demineralized water (Nanopure Diamond, Barnstead, USA). Three replications of each sample were performed. To analyze the binding forms of Fe, oxalate extraction (Fe<sub>o</sub>) according to Schwertmann (1964) and dithionite extraction according to Mehra and Jackson (1960) were performed. Total C and N were quantified with an elemental analyzer (Vario EL, Elementar, Germany). Total C was equal to organic C since the soil was free of carbonates. The total Hg content was determined by a mercury analyzer (DMA-80, MLS, Germany) using the air-dried and manually ground samples in five replicates.

The soil was sequentially extracted according to the extraction scheme of Bloom et al. (2003) with one modification: instead of a 12 M HNO<sub>3</sub> solution, a 6.4 M solution was used to obtain Fraction 4. Briefly, 0.4 g of soil was weighed into 50 mL centrifuge tubes. The tubes were extracted using a bench top shaker (3006, GFL, Germany). After each step the samples were centrifuged (Rotina 46, Hettich, Germany) for 20 minutes and the supernatant was removed. The extracts of steps 1 to 3 were filtered through a cellulose acetate syringe filter (0.22 µm)

and those of steps 4 and 5 were filtered through 2  $\mu\text{m}$  blue ribbon filters (598/3 Whatman, USA). Then, 1.25 mL of 0.2 M BrCl was added to extracts from steps 1, 2, and 4 and 10.0 mL was added to the filtered supernatant of extraction step 3. Bromine chloride was used to oxidize the samples for the measurement of total Hg. Total Hg was measured with a direct mercury analyzer (DMA-80). Four replications were run for each step. The extraction steps included the following: Fraction 1 (F1): water soluble fraction with deionized water (extraction time 18 h); Fraction 2 (F2): human stomach acid soluble fraction with 0.1 M  $\text{CH}_3\text{COOH}$  and 0.01 M HCl, (pH 2) (extraction time 18 h); Fraction 3 (F3): organic-bound fraction with 1 M KOH (extraction time 18 h); Fraction 4 (F4): elemental Hg fraction with 6.4 M  $\text{HNO}_3$  (extraction time 18 h); Fraction 5 (F5): mercuric sulfide fraction with aqua regia.

#### **4.2.3 Soil column experiments**

To study the gaseous release of Hg under different water contents and redox conditions, column experiments were performed. The columns containing the undisturbed soil samples were thawed. A nylon fleece was fixed at the bottom of the columns before the columns were watered for 24 hours until a water film was detected on the soil surface. Figure 4.1 shows the design of the column experiment. The columns filled with the water-saturated soil were set into the column base, including a porous plate (0.2  $\mu\text{m}$ ) and a connection for extracting water from the column (UIT, Germany). To determine the  $E_{\text{H}}$  an Ag-AgCl reference electrode (SE 23, Meinsberg, Germany) and an  $E_{\text{H}}$  electrode, as described by Mansfeldt (2003), were added. Both electrodes were connected to a data logger (LogTrans 16 GPRS, UIT, Germany) to store the data points. The measured  $E_{\text{H}}$  was related to the standard hydrogen electrode by adding 207 mV to the measured value, referred to the Ag-AgCl reference electrode. Flux chambers according to Rinklebe et al. (2008) were fixed on the upper side of the column. The columns were tightly sealed so that the released gaseous Hg could accumulate in the head-space. Columns were placed in an incubator (KB 400, Binder, Germany) and stored for 28 days at 20 °C.

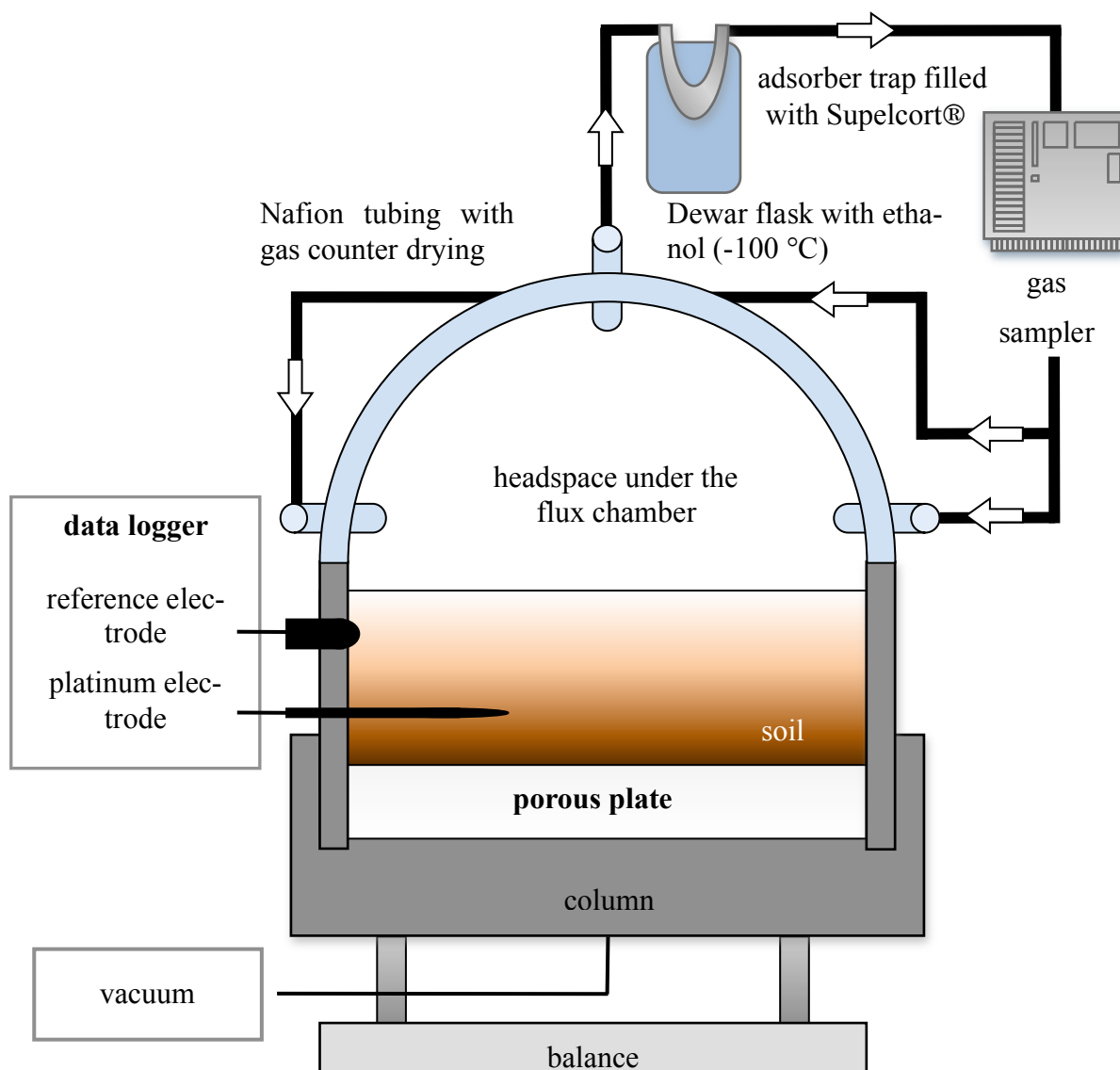


Fig. 4.1: Scheme of the experimental design for sampling of gaseous Hg including a column with a flux chamber and a gas sampler equipped with an ethanol-filled Dewar flask cooled to  $-100\text{ °C}$

To determine the accumulated gaseous Hg in the column headspace, the gas phase was pumped over cooled traps filled with Supelcort (80/100, 10 % SP, Supelco, USA) as adsorbents. The U-shaped traps (quartz, diameter 6 mm) were wrapped with a heating wire for later desorption of the Hg. For storage and transport the traps were hermetically sealed with Swagelok® plugs. For sampling, the traps needed to be cooled. Therefore ethanol (Merck, Germany) was put into a Dewar flask (3C, Isoterm KGW, Germany) and cooled with liquid



nitrogen ( $-178\text{ }^{\circ}\text{C}$ ) to a temperature of  $-100\text{ }^{\circ}\text{C}$ . The traps were clipped into the Dewar flask. Tygon tubes were used to connect the headspace of the flux chamber to the cooled traps and a gas sampler (GS 212, Desaga, Germany). The cleaned air was retransferred to the flux chamber, so that the air was pumped in circulation and to ensure that all of the Hg could be trapped. For each sampling the headspace was pumped through the columns for 15 minutes with a flow rate of  $0.3\text{ mL min}^{-1}$ , which resulted in a gas volume of about 5.5 L of air. After sampling the traps were stored at  $-178\text{ }^{\circ}\text{C}$  in a transport Dewar (CX500, Taylor Wharton, USA) and brought to the laboratory for measurement and speciation analysis of Hg (University of Duisburg-Essen, Germany). The gaseous probes were sampled on days 1, 3, 7, 10, 14, 17, 21, and 28.

After two weeks of water saturation, we lowered the water content by removing water from the columns using a membrane vacuum pump (M2, Vacubrand, Germany). Five percent of the water content was removed; after a further week, another 5 % of the water was sucked off. The removed soil solutions of the columns were filtered ( $0.45\text{ }\mu\text{m}$  cellulose-nitrate filter, Sartorius, Germany) and stabilized by adding 2 %  $\text{HNO}_3$  for the subsequent total Hg measurement. At the end of the experiment, some water was removed for the determination of total dissolved Hg.

At the end of the experiment the soils of the columns were analyzed for their Hg contents. Therefore, the remaining water of the columns was removed with the membrane vacuum pump. Afterwards the PVC columns were removed and the soil was air-dried and ground manually before the measurement of the total Hg content.

#### **4.2.4 Analyses of soil solution and extractants**

Both Fe and Mn were determined by flame atomic absorption (iCE 3500, Thermo scientific, USA); Hg was measured as described above. The reference material “Metals on Soil/Sediment” (CRM008-050, RTC, USA) was used for quality control. The recovery rates were between 99 and 108 %. Sequential extractions and total Hg content were also quantified by the elemental Hg analyzer. Recovery for the measurement of the sequential extraction procedure was between 105 and 111 % and for the measurement of total Hg content, between 99 and 109 %.

#### **4.2.5 Species analyses of gaseous mercury**

The gaseous samples were measured using a GC/ICP-MS system. This system was composed of a gas chromatograph 6890 N (Agilent Technologies, Waldbronn, Germany) equipped with a UNIS 2000 Inlet-System (Joint Analytical Systems, Moers, Germany) and connected to a 7500a ICP-MS (both instruments from Agilent Technologies, Waldbronn, Germany). The ion traces of  $m/z$  200 ( $^{200}\text{Hg}$ ) and 202 ( $^{202}\text{Hg}$ ) were used for detection and quantification of the gaseous Hg species.

### **4.3 Results and discussion**

#### **4.3.1 Soil properties and sequential extraction of mercury**

Table 4.1 summarizes the main properties of the topsoil, which, according to WRB and IUSS Working Group (2006), is a Eutric Fluvisol. The pH is in a moderately acid range, which is typical for floodplain soils of the temperate zone. The texture is dominated by silt and clay. The high content of organic C ( $66 \text{ g kg}^{-1}$ ) and the relatively low ratio of C/N are characteristic for grassland floodplains. About one-half of the Fe is bound in Fe oxides. The ratio of  $\text{Fe}_o/\text{Fe}_d$  is 0.92 and indicates a high proportion of less stable, poorly crystalline Fe oxides. The total Hg content was  $9.2 \pm 0.2 \text{ mg kg}^{-1}$ . In comparison, the median of background values of Hg in floodplain soils in environs of agglomerations used as grassland in the state of Lower Saxony is only  $0.12 \text{ mg kg}^{-1}$  (LABO, 2003). Such strong contamination of the floodplains of the Elbe River with Hg was also reported by Devai et al. (2005), Overesch et al. (2007), and Wallschläger et al. (1996).

Tab. 4.1: Chemical and physical characteristics of the Ah horizon of a Fluvisol from the Elbe River at the biosphere reserve "Niedersächsische Elbaue" at Hohnstorf, Lower Saxony, Germany

<b>Property</b>	
pH (in H <sub>2</sub> O), [-]	6.7
pH (in CaCl <sub>2</sub> ), [-]	6.3
Particle size distribution	
Sand [g kg <sup>-1</sup> ]	160
Silt [g kg <sup>-1</sup> ]	565
Clay [g kg <sup>-1</sup> ]	275
Texture	silty clay loam <sup>†</sup>
Bulk density [kg L <sup>-1</sup> ]	1.00
Total Fe [g kg <sup>-1</sup> ]	41.9
Fe <sub>o</sub> [g kg <sup>-1</sup> ]	18.0
Fe <sub>d</sub> [g kg <sup>-1</sup> ]	19.6
Fe <sub>o</sub> /Fe <sub>d</sub>	0.92
Total Mn [g kg <sup>-1</sup> ]	1.40
Total C [g kg <sup>-1</sup> ]	68.5
Total N [g kg <sup>-1</sup> ]	5.70
C/N	12
Hg [mg kg <sup>-1</sup> ]	9.20

<sup>†</sup> According to FAO

Table 4.2 summarizes the results of the sequential extraction procedure. The total amount removed by each extractant was in good agreement with the amount determined by thermal combustion. The extraction revealed that about one third of the Hg occurred in the organic-bound fraction (F3) and another third in the elemental fraction (F4) followed by the mercuric sulfide fraction (F5) with about one-fifth. Residual Hg amounted to 7.6 % whereas the water soluble (F1) and especially the acid soluble fraction (F2) yielded only very low amounts. Using Bloom's extraction protocol, other soil and sediment studies have consistently shown that Hg mainly occurs in F3, F4, and F5 and that the F1- and F2-Hg pool, although important in view of environmental concern, is negligible to low (Kocman et al. 2004; Liu et al. 2006; Shi et al. 2005; Yu et al. 2012).

Tab. 4.2: Sequential extraction of Hg in the Ah horizon of a grassland Fluvisol from the Elbe River in the biosphere reserve "Niedersächsische Elbaue" at Hohnstorf, Lower Saxony, Germany [mg kg<sup>-1</sup>]

	Fraction (mg kg <sup>-1</sup> )	Fraction (%)
F1 <sup>a</sup>	0.025	0.302
F2	0.004	0.044
F3	2.99	36.7
F4	2.92	35.8
F5	1.60	19.6
Soil residual	0.623	7.63
Sum <sup>b</sup>	8.16	100
Total Hg <sup>c</sup>	9.20	
Sum/total Hg	0.89	

<sup>a</sup> Fraction 1 (F1): water soluble fraction; F2: human stomach acid soluble fraction; F3: organic-bound fraction; F4: elemental Hg fraction; F5: mercuric sulfide fraction; according to Bloom et al. (2003)

<sup>b</sup> Sum F1 to F5 and soil residual

<sup>c</sup> Separate measure of Hg

### 4.3.2 Redox potential and water content

Initially the soil was saturated with water from the bottom of the columns. After 14 days about 5 % and after 21 days an additional 4 % of the soil water was removed. Figure 4.2 shows the effects of the water content on the E<sub>H</sub>.

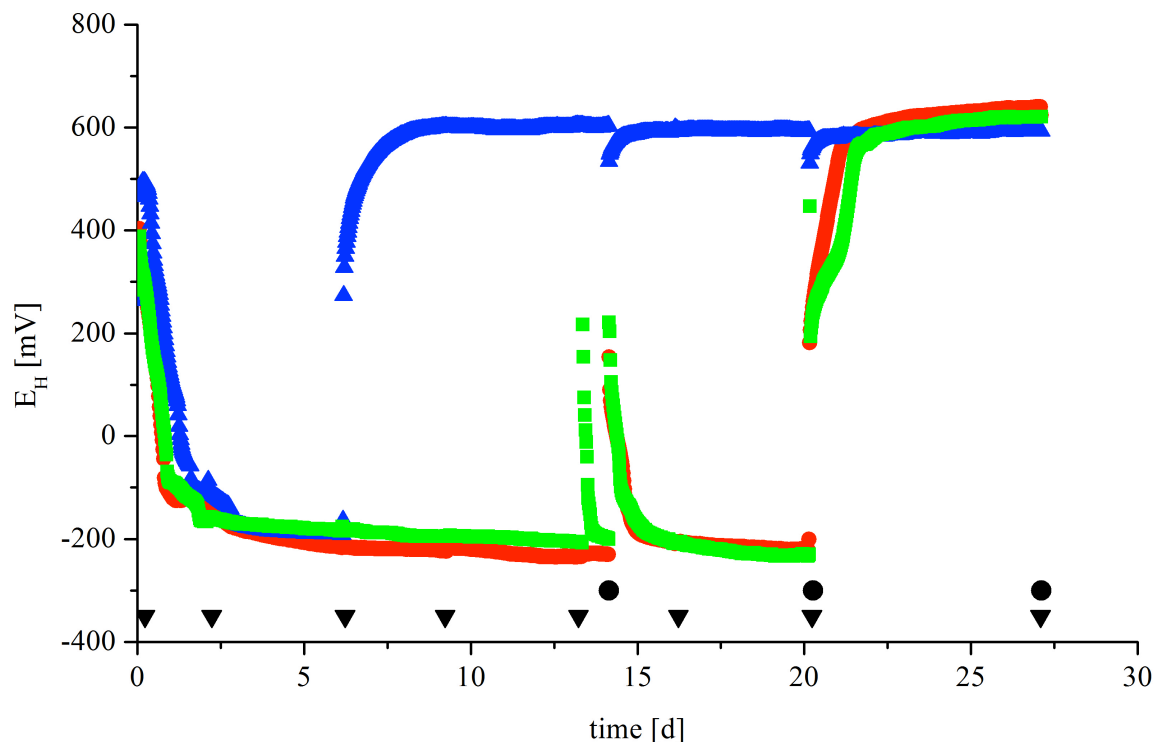


Fig. 4.2: Development of redox potential ( $E_H$ ) during the column experiments (● column A; ▲ column B; ■ column C; ▼ sampling gas probe of the headspace under the flux chambers; ● removal of water)

In column A the  $E_H$  was at 408 mV at the beginning of the experiment. This  $E_H$  corresponds to oxidizing conditions ( $E_H > 400$  mV; Zhi-Guang 1985). Under such conditions,  $O_2$  is present and acts as the terminal electron acceptor during the microbial oxidation of soil organic matter. Within 20 hours, the  $E_H$  decreased and reached  $E_H < -100$  mV. This  $E_H$  corresponds to strongly reducing conditions (Zhi-Guang 1985). Under such conditions, the  $O_2$  pool is completely exhausted by microbial respiration and hexavalent S; that is, sulfate, acts as the main electron acceptor. Furthermore, the  $E_H$  decreased continuously to  $-220$  mV. Strongly reducing conditions were maintained for 14 days. The water removal at day 14 led to an increase of the  $E_H$  up to 200 mV, but within the next 11 hours the previous redox conditions were achieved again. The second water removal on day 21 resulted in an increase in the  $E_H$  up to oxidizing conditions within 12 hours. This level was maintained until the end of the experiment.

Column B showed a different behavior. It started under oxidizing conditions with 494 mV, and strongly reducing conditions were achieved within 40.5 hours. The  $E_H$  decreased continuously to  $-190$  mV  $E_H$  and strongly reducing conditions were maintained for the next four

days. The sampling on day 7 resulted in an increase in the  $E_H$ . Within 4.5 hours oxidizing conditions were achieved and then this level was maintained until the end of the experiment. The water removal on days 14 and 21 resulted in a decrease in the  $E_H$  of 70 mV, but the  $E_H$  remained under oxidizing conditions.

Column C showed a behavior very similar to column A, as proven by a strong correlation between the  $E_H$  of both columns ( $r = -0.991$ ,  $p < 0.001$ ,  $n = 1,349$ ).

The development of the  $E_H$  indicates an association with the water content of the soil. Water-saturation of the columns resulted in a quick decrease in the  $E_H$ . The zones of weakly reducing conditions, that is, pentavalent N (nitrate) and tri- and tetravalent Mn (Mn oxides), which act as the electron acceptor, and moderately reducing conditions, that is, trivalent Fe (Fe oxides), which act as the electron acceptor, were rapidly passed through, and an overlap of the anaerobic redox zones can be expected, not the classical sequential reduction (Bartlett and James 1993). In columns A and C the alteration of the water content is the key for the development of the  $E_H$ , as proven by the strong correlation between the water content and the  $E_H$  (column A:  $r = -0.791$ ,  $p < 0.001$ ,  $n = 1,349$ ; column C:  $r = -0.821$ ,  $p < 0.001$ ,  $n = 1,349$ ). However, in column B, diffusion of  $O_2$  during the third sampling presumably caused the increasing  $E_H$  and lasting oxidizing conditions. One reason for this behavior might have been differences in soil physical properties between the columns. The bulk density of the topsoil was relatively low (Tab. 4.1) and total porosity was calculated to be 61 % (see Section 4.2.2.), which is very high. Typically, there is a wide variety of sizes and shapes of pores in soils. Especially a stronger development of macropores may have resulted in enhanced aeration of column B.

### **4.3.3 Total mercury in the soil columns**

Because determination of the initial Hg content in the intact soil cores was not possible, the total Hg was analyzed after the experiment. The Hg contents of the samples were  $12.1 \pm 1.10$  mg kg<sup>-1</sup> in column A,  $12.8 \pm 0.10$  mg kg<sup>-1</sup> in column B, and  $11.3 \pm 1.10$  mg kg<sup>-1</sup> in column C. Overall, the Hg content showed only a low variation. By considering the soil bulk density (Tab. 4.1), the volume of the soil columns, and the Hg content, the total amount of Hg in each column was calculated. This was necessary in order to compare the columns with each other. Total Hg amounted to 7.72 mg in column A, 6.91 mg in column B, and 7.65 mg in column C. Bahlmann et al. (2006), Choi and Holsen (2009), and Gustin et al.

(2006) have shown that Hg volatilization is positively correlated with the total Hg concentration.

#### 4.3.4 Dissolved mercury in the soil columns

When small parts of water were removed to regulate the soil moisture and the  $E_H$ , the soil solution was analyzed for its Hg concentration (Tab. 4.3). The highest Hg concentration was found in column A after day 14 ( $68.3 \mu\text{g L}^{-1}$ ); then the concentration decreased until the end of the experiment ( $23.4 \mu\text{g L}^{-1}$ ). Columns B and C showed lower Hg concentration ( $17.2 \mu\text{g L}^{-1}$  and  $23.9 \mu\text{g L}^{-1}$ ) after day 14. The concentration in these columns also decreased at the end of the experiment to  $5.78 \mu\text{g L}^{-1}$  and  $10.0 \mu\text{g L}^{-1}$ . In summary, all columns showed a similar trend; namely, during the course of the experiment the Hg concentrations decreased. The presence of dissolved Hg is a precursor to the volatilization of Hg from soils.

Tab. 4.3: Concentration of Hg in the soil solution measured after days 14, 21, and 28

Column	Day	Hg ( $\mu\text{g L}^{-1}$ )
A	14	68.3
	21	47.2
	28	23.4
B	14	17.2
	21	10.4
	28	5.78
C	14	23.9
	21	21.7
	28	10.0

#### 4.3.5 Gaseous mercury in the headspace of the soil columns

##### 4.3.5.1 Mercury species

Figure 4.3 shows a typical chromatogram for Hg speciation using the GC/ICP-MS system. With a retention time of 173 seconds only  $\text{Hg}^0$  was detected. Further peaks in the chromatogram can be explained by matrix and plasma interferences of the ICP-MS. Only in very high-

ly concentrated samples (column A on day 3 or column B on day 17) was a slight, unquantifiable signal detected for DMHg ( $< 20 \text{ ng/m}^3$ ; data not shown). Hence, TGM is equal to  $\text{Hg}^0$  in the current study.

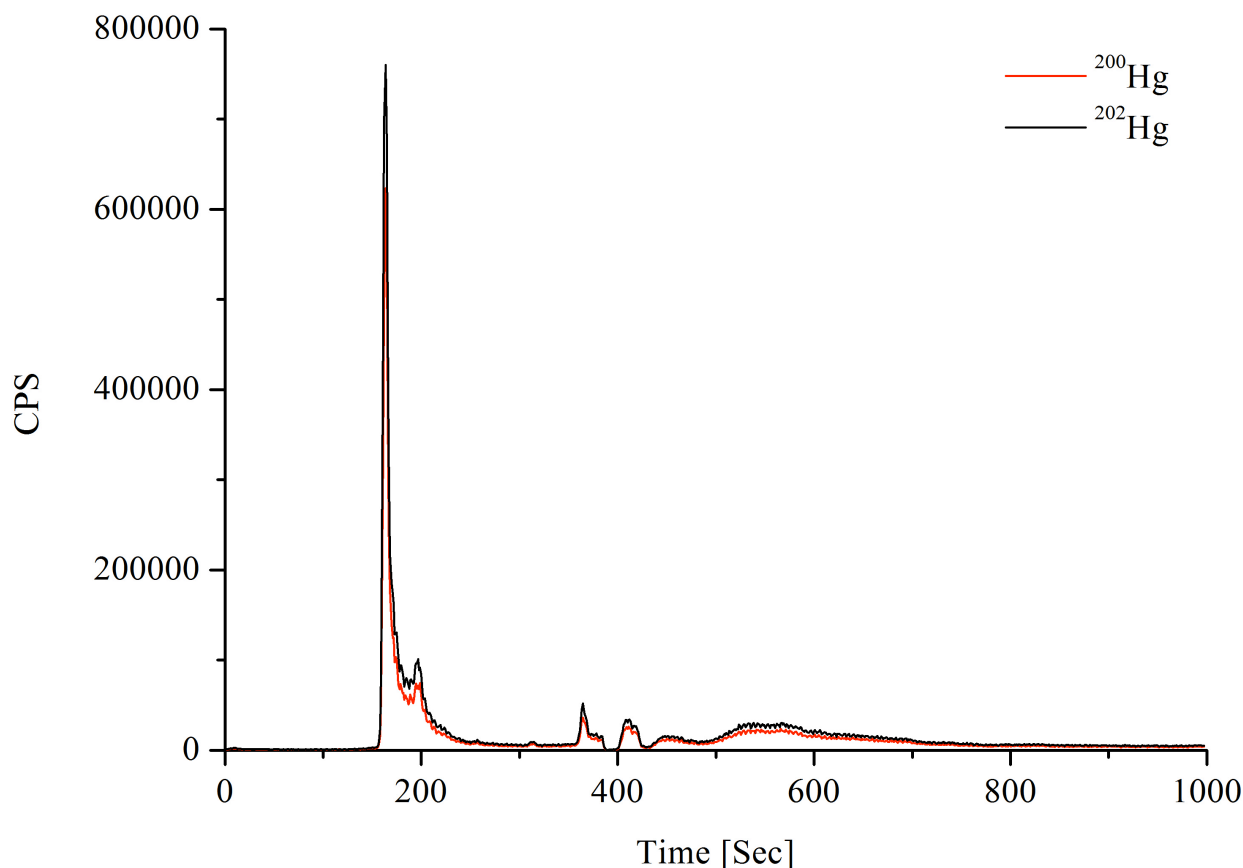


Fig. 4.3: Measurement of sampling 3 of column A by GC-ICP-MS ( $^{200}\text{Hg}$ ; and  $^{202}\text{Hg}$ )

Exclusively natural processes generate methylated Hg species. The main pathway of MMHg generation is the bacterial methylation of  $\text{Hg}^{2+}$  in anoxic environments, whereas the pathway of DMHg production is still unknown (Hintelmann 2010), although further methylation of MMHg seems to be plausible as it is shown for e.g. waste landfills (Li et al. 2010) or coastal sediments (Wasserman et al. 2004). Sulfate-reducing bacteria play a dominant role in the production of MMHg (Fitzgerald et al. 2007; Gilmour et al. 1992; Harmon et al. 2004). In freshwater systems containing limited amounts of sulfate, other anaerobic bacteria, including iron-reducing bacteria, may be involved in Hg methylation (Kerin et al. 2006; Fleming et al. 2006). Organic matter-bound Hg was shown to be strongly correlated to the methylation potential (Bloom et al. 2003; Kocman et al. 2004). This fraction (F3) was present in the soil in



significant amounts (Tab. 4.2). In addition, columns A and C ran under strongly reducing conditions for about three weeks and at a temperature (20 °C) suitable for high microbial activity. The results of some studies led to the conclusion that such high temperatures promote the methylation rates (Canário et al. 2007; Hintelmann and Wilken 1995). Nevertheless, methylated Hg was not volatilized in detectable amounts in this study. It should be taken into account that, in contrast to DMHg, MMHg is only a semi-volatile Hg species. Hence, we cannot exclude the possibility that some MMHg was produced and remained in the soil solution, probably associated with the organic fraction (F3). However, the main reason should be the limitation of sulfate in the floodplain system. Methylation rates are strongly dependent upon the activity of sulfate reducing bacteria and they are the main producers of methylated Hg (King et al. 2000; Warner et al. 2003). Finally, the amount of soluble Hg in this study may be too toxic for microorganisms (see halo hypothesis, Hirner and Hippler 2011). Overall, even when flooded, floodplain soils are more similar to terrestrial than to anoxic environments.

#### **4.3.5.2 Mercury volatilization during the course of the experiment**

Figure 4.4 illustrates the volatilization of Hg during the course of the experiment. Unfortunately, no samples were obtained for column A on day 17, column B on day 14, or column C on days 7 and 17, because of either broken traps (columns B and C, day 17) or analytical shortcomings (columns A and C, day 7). However, it can be estimated that for column A at least 150 ng of Hg and for column C (day 7) at least 5 ng of Hg evaporated. Column A showed two clear peaks of the Hg concentration on day 3 (411 ng) and day 14 (146 ng). After the first increase, the emission decreased for the next days. At the end of the experiment, a third, less intensive increase in Hg emission appeared. In contrast to column A, column B revealed only one clear peak in Hg volatilization on day 17 (229 ng). A minor emission of Hg<sup>0</sup> (about 60 to 70 ng) occurred during the first days of the experiment. Column C also showed two peaks in Hg emission. The first, lower increase in Hg appeared on day 3 (75 ng) and was followed by a decrease down to 12 ng. A second, major increase in Hg<sup>0</sup> emission appeared between days 14 and 21 with a maximal emission of approximately 170 ng Hg<sup>0</sup>. At the end of the experiment, the emission decreased to 22 ng. Generally, the columns showed similar development with a more or less intensive increase in Hg emission within the first

three days. Subsequently, Hg was detected only in small amounts. Furthermore, all columns revealed a second increase in volatilization between days 14 and 28.

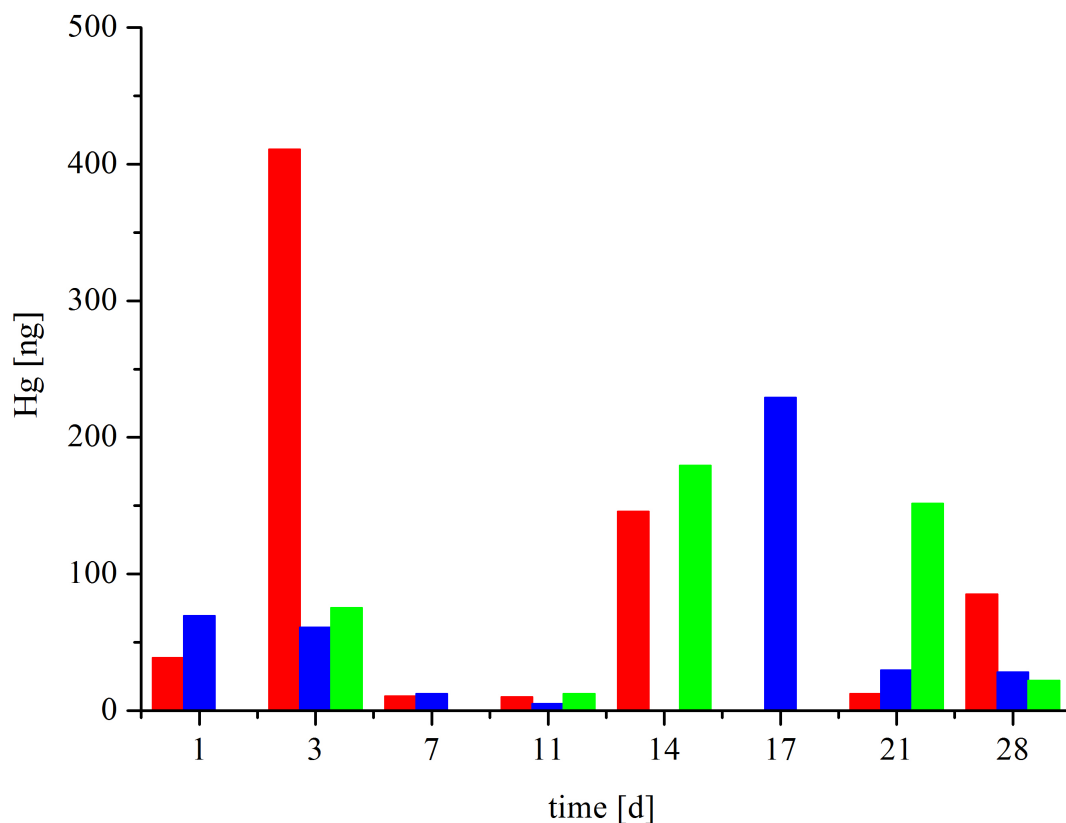


Fig. 4.4: Development of the amounts of gaseous Hg (■ column A; ■ column B; and ■ column C). On day 1, an amount of 0.4 ng Hg was detected for column C. All other missing values are due to sampling or analytical shortcomings. Removal of water was done on days 14 and 21.

In the current study, we have (i) minimized the effect of wind speed, air movement, and turbulences because we used a low pump speed ( $0.3 \text{ L min}^{-1}$ ), (ii) standardized the effect of temperature because the experiment was kept at  $20 \text{ }^\circ\text{C}$ , and (iii) eliminated the effect of UV radiation because we worked in the dark. Hence, the soil water content and soil redox condition were the master variables in this experiment, with the soil having a natural bulk density, porosity, and pore size distribution.

As outlined in Section 4.3.5.1, the only detectable degassing species was  $\text{Hg}^0$ . It seems that in our experiment two processes were important for the volatilization of  $\text{Hg}^0$ . At the beginning

of the experiment, the  $\text{Hg}^0$  already present in the soil air took part in the volatilization. By filling the soil pores with water, this  $\text{Hg}^0$  could be physically displaced, as proposed by Lindberg et al. (1999), and left the soil surface. Furthermore,  $\text{Hg}^0$  adsorbed to the soil could be replaced by water molecules (Gustin and Stamenkovic 2005; Lindberg et al. 1999; Song and van Heyst 2005). This behavior was very pronounced in column A, because a strong increase in the volatilization was detected. Indeed, the presence of  $\text{Hg}^0$  was confirmed by F4 in our sequential fractionation (Tab. 4.3). For degassing of Hg, it is necessary for the Hg to be able to pass through the soil by diffusion or mass transport and enter the soil surface (Wallschläger et al. 2000; Zhang and Lindberg 1999). In our column experiment, the transport of the gaseous species was initially inhibited because the pores were completely filled with water. However, the water removal, which simulated a falling water table on day 14, promoted the transport of water and air in the soil. By means of this process, the air enriched with gaseous Hg could have passed through the soil and diffused to the surface. The entrance of air during the sampling of gaseous probes also promotes the transport of Hg-enriched soil air (Wallschläger et al. 2000; Zhang and Lindberg 1999).

Another important process should have been the production of  $\text{Hg}^0$  and the following volatilization of this species. In order for the Hg to be released it must be reduced from dissolved  $\text{Hg}^{2+}$  to  $\text{Hg}^0$ . This reduction can be mediated by biotic processes (Barkay et al. 2003; Rogers 1979; Rogers and McFarlane 1979; Schlüter, 2000) and abiotic processes including photolysis and redox reactions with fulvic or humic acids (Alberts et al. 1974; Allard and Arsenie 1991; Costa and Liss 2000, 1999; Schlüter 2000). Mercury emission from soil containing less than  $1 \text{ mg Hg kg}^{-1}$  and low in organic matter (e.g.  $< 1 \%$  organic carbon) is dominated by biological processes, whereas soils with higher organic matter content favor abiotic mediated volatilization (Rogers 1979; Rogers and McFarlane 1979; Schlüter 2000). Considering the properties of the soil under investigation, we conclude that in our experiment abiotic processes prevailed. Limitation of these processes is not expected in the near future.

#### **4.3.5.3 Rates of mercury volatilization**

For floodplain soils of the Elbe River with total Hg contents of  $3.45$  to  $16.7 \text{ mg kg}^{-1}$ , Rinklebe et al. (2010) determined Hg volatilization rates of  $10$  to  $849 \text{ ng m}^{-2} \text{ h}^{-1}$  as measured with flux chambers. Measurements made by Wallschläger et al. (1996) for floodplain soils of the same river with about  $10 \text{ mg kg}^{-1}$  total Hg content resulted in volatilization rates of  $20$  to  $500 \text{ ng m}^{-2} \text{ h}^{-1}$ . For these measurements, different methods were used. New measurements by

Wallschläger et al. (2002) for sites comparable to the river Elbe with flux chambers showed Hg volatilization rates of 38 to 48 ng m<sup>-2</sup> h<sup>-1</sup>. The conversion of our data indicated volatilization rates of 1.73 to 824 ng m<sup>-2</sup> h<sup>-1</sup> Hg, which coincide with the above-mentioned data. As summarized by Rinklebe et al. (2010), rates of Hg volatilization of unpolluted soils rarely exceed 0.7 to 1.1 ng m<sup>-2</sup> h<sup>-1</sup>. This highlights the strong Hg volatilization of anthropogenically affected areas like the Elbe River. Mobilization by biomethylation may be problematic in sediments with high total Hg loads (e.g. Kocman et al. 2004), because of reduced microbial activity (Hirner and Hippler, 2011). Only one case was reported with a marginal methylation rate of 1‰: Sample S9 containing 9 mg kg<sup>-1</sup> (Shi et al. 2005).

#### **4.4 Conclusion**

In this study, Hg volatilization was investigated using undisturbed soil samples taken from a contaminated floodplain soil and simulating a flooding event. Even under a worst-case scenario, that is, at high temperature, water saturation for a longer period of time and strongly reducing conditions, exclusively Hg<sup>0</sup> and not methylated Hg species volatilized from the soil. Apparently the conditions were not favorable for Hg biomethylation, possibly (i) the reducing conditions did not last long enough to establish an environment suitable for methylating microorganisms, and/or (ii) the system was sulfate limited, and/or the high Hg concentrations were too toxic to the microbiota to survive. Volatilization of elemental Hg, in turn, was not exceptionally high or low during or after the flooding event in comparison to other studies. Hence, flooding events have the same effect on Hg volatilization as other factors which influence soil water content, that is, precipitation or water table levels.

## **5 PHASE DISTRIBUTION OF MERCURY UNDER DEFINED REDOX CONDITIONS OF A FLOODPLAIN SOIL OF THE ELBE RIVER**

### **5.1 Introduction**

Floodplain soils are formed by the periodical deposition of sediments during flood events. Such sedimentation takes place over a long period (Du Laing et al., 2009). Anthropogenic affected floodplain soils are characterized by high trace element content (Du Laing et al., 2009; Schulz-Zunkel and Krueger, 2009). Since the 18th/19th century, trace elements concentration has increased due to intensive mining and industrial activities. Other sources of contamination include sewage discharge, agricultural non-point sources, and run off, but also atmospheric deposition and natural geogenic processes (Du Laing et al., 2009; Schulz-Zunkel and Krueger, 2009). Currently, only low quantities of trace elements are deposited, but the concentration of trace elements in floodplain soils remains high.

Floodplain soils are characterized by various redox states caused by flooding events and various soil moisture contents induced by changing water table levels. During the water saturation of floodplain soils a change from aerobic to anaerobic conditions appears. Catalyzed by microorganisms a series of sequential redox reactions take place including denitrification, manganic manganese reduction, ferric iron reduction, sulfate reduction, and methanogenesis (Alewell et al., 2008; Du Laing et al., 2009). The change in the redox states can be measured by the  $E_H$ ; this shows the tendency of the soil to become dominated by oxidizing or reducing processes (Fiedler and Sommer, 2004). The change in  $E_H$  affects the solubility of trace elements due to the redox-induced change of the metal-binding capacity of organic material, the formation of insoluble metal sulfides, or the reductive dissolution of Fe and Mn oxides (Du Laing et al., 2009). Another possibility for influencing the solubility of trace elements is the  $E_H$ -induced change in pH. During reduction, protons are consumed and the pH increases. Through this, the negative charge on the surface of the organic matter, clay particles and the Fe and Al oxides increases (Du Laing et al., 2009).

The pollution of floodplains with Hg is a worldwide problem, especially because Hg is a persistent pollutant and it accumulates in soils (Devai et al., 2005; Rinklebe et al., 2010). The chemistry of Hg in the environment has been reviewed intensively (Gabriel and Williamson, 2004; Schuster, 1991; Zhang et al., 2003). Regarding our paper, special attention should be given to the following; (1) the reduction of  $Hg^{II}$  to gaseous  $Hg^0$  is enhanced when the  $E_H$  is

low; (2) organometallic forms like methylated and dimethylated Hg can exist at low  $E_H$ ; and (3)  $Hg^0$  and dimethylated Hg can volatilize.

The pollution of the Elbe River with Hg is well documented (Devai et al., 2005; Overesch et al., 2007; Wallschläger et al., 1996). Up until 1996,  $1500 \pm 500$  tons of Hg had been deposited in the floodplains of the river (During et al., 2009; Wallschläger et al., 1996). The pollution originates from various sources, but particularly industrial point sources (Hamburg Port Authority, 2005; Wallschläger et al., 1996).

In our experiments, we aimed to document the influence of the  $E_H$  on the distribution of Hg in soils. We performed microcosm experiments by which the  $E_H$  could be maintained at fixed levels. For this study, the naturally contaminated floodplain soil of the Elbe River was taken. The objectives of this study were; (1) to determine the influence of  $E_H$  on the Mn, Fe, sulfate, chloride, and DOC concentrations; (2) to trap and measure gaseous Hg in the microcosm experiment; (3) to determine the distribution of Hg on the solid, liquid, and gaseous phases; and (4) to examine the influence of  $E_H$  on the phase distribution of Hg.

## **5.2 Material and Methods**

### **5.2.1 Study site, sampling, and sample preparation**

Soil samples were taken from the grassland of the biosphere reserve “Niedersächsische Elbaue” in Hohnstorf, Lower Saxony, Germany ( $53^{\circ}21'25.05''$  N;  $10^{\circ}34'42.22''$  E). The sampling site was near to the Elbe River and is characterized by flooding events which are associated with continuous sedimentation. The soil at this site is contaminated by former mining activities, industrial use and inputs of agriculture and municipal sewage. Currently, significant amounts of pollutants are released by industrial and municipal direct injection (Hamburg Port Authority, 2005). For the microcosm experiments we collected approximately 12 kg of disturbed soil. For the soil sampling we removed the sod. For the sampling we only use the aAh horizon (0 to 10 cm). The samples were manually homogenized, air-dried, and sieved below 2 mm. Subsamples were ground manually for chemical analysis.

### **5.2.2 Soil characteristics**

The soil pH was measured potentiometrically both in 0.01 mol L<sup>-1</sup> CaCl<sub>2</sub> solution and water (mixed 5:1 with soil (vol/vol)) by a glass electrode. Particle size distribution was determined by wet sieving and sedimentation using the pipette sampling technique. The organic matter was destroyed by H<sub>2</sub>O<sub>2</sub> before the analyses. The content of total Fe and Mn were determined after aqua regia extraction. For the aqua regia extraction 200 mg of sample was weighted in and 6 mL concentrated HNO<sub>3</sub> (supra pure, Merck) and 2 mL concentrated HCl (supra pure, Merck) was added. After digestion the samples were filtered (2 µm, Whatman 589/3, blue ribbon filter) and fulfilled up to 50 mL with demineralized water (Nanopure Diamond, Barnstead). We performed three replications of each sample. To analyze the binding forms of Fe we used oxalate extraction according to Schwertmann (1964) and dithionite extraction according to Mehra and Jackson (1960). Total C and N were quantified with an elemental analyzer (Vario EL, Elementar). Total C equals organic C since the soil was free of carbonates. The total content of Hg was determined directly by a direct mercury analyzer (DMA-80, MLS) using the air-dried and manually ground samples. We performed five replicates.

The soil was sequentially extracted according to the extraction scheme of Bloom et al. (2003) with one modification: Instead of a 12 M HNO<sub>3</sub>, a 6.4 M solution was used to obtain Fraction 4. Briefly, 0.4 g soil was weighted into 50 mL centrifuge tubes. The tubes were extracted using a bench top shaker (3006, GFL, Germany). After each step the samples were centrifuged (Rotina 46, Hettich, Germany) for 20 minutes and the supernatant was removed. The extracts of steps 1 to 3 were filtered through a cellulose acetate syringe filter (0.22 µm), and those of steps 4 and 5 were filtered through 2 µm blue ribbon filters (598/3 Whatman, USA). 1.25 mL of 0.2 M BrCl was added to extraction steps 1, 2 and 4, and 10.0 mL to the filtered supernatant of extraction step 3. Bromine chloride was used to oxidize the samples for the measurement of total Hg. Total Hg was measured with a direct mercury analyzer (DMA-80). Four replications were run for each step. The extraction steps were: Fraction 1 (F1): water soluble fraction with deionized water (extraction time 18 h); Fraction 2 (F2): human stomach acid soluble fraction with 0.1 M CH<sub>3</sub>COOH and 0.01 M HCl (pH 2) (extraction time 18 h); Fraction 3 (F3): organic-bound fraction with 1 M KOH (extraction time 18 h); Fraction 4 (F4): elemental Hg fraction with 6.4 M HNO<sub>3</sub> (extraction time 18 h); and Fraction 5 (F5): mercuric sulfide fraction with aqua regia.

### 5.2.3 Soil incubation in microcosms

To study the behavior and distribution of Hg under different redox regimes we performed microcosm experiments at controlled redox potentials. Microcosms were filled with 1.25 kg air-dried soil (< 2 mm) and 6 L deionized water and were continuously stirred (Fig. 5.1).

Forty g cellulose powder (Fluka) was added as an additional source of organic matter, i.e., as an electron donor. Soil suspensions were incubated at moderately reducing ( $\sim 100$  mV) or strongly reducing conditions ( $\sim -100$  mV) in the microcosms system. Regulation of  $E_H$  was possible by flushing  $N_2$  or filtered ambient air through the microcosm (Rennert and Mansfeldt, 2005). Redox potentials in the first microcosms were adjusted to moderately reducing conditions and in the second to strongly reducing conditions. The experiment was held at 20 °C. Temperature, pH, and  $E_H$  were recorded every 30 minutes with a data logger. Temperature was determined by temperature probe (PT 100, Meinsberg) and  $E_H$  as well as pH with combination electrodes (EMC 33, Ag-AgCl, and EGA 153, Meinsberg). The measured  $E_H$  was related to the standard hydrogen electrode by adding 207 mV, which refers to the Ag-AgCl reference electrode. Redox measurements were converted into values corresponding to pH 7 using the pH of soil suspensions by the equation  $E_H(\text{pH}7) = E_H + (\text{pH} - 7) \cdot 59$  where  $E_H$  is expressed in mV. Although the value of  $-59$  mV per pH unit is reasonable for most measurements (Bohn et al., 2001), we reported both the measured  $E_H$  and the pH.

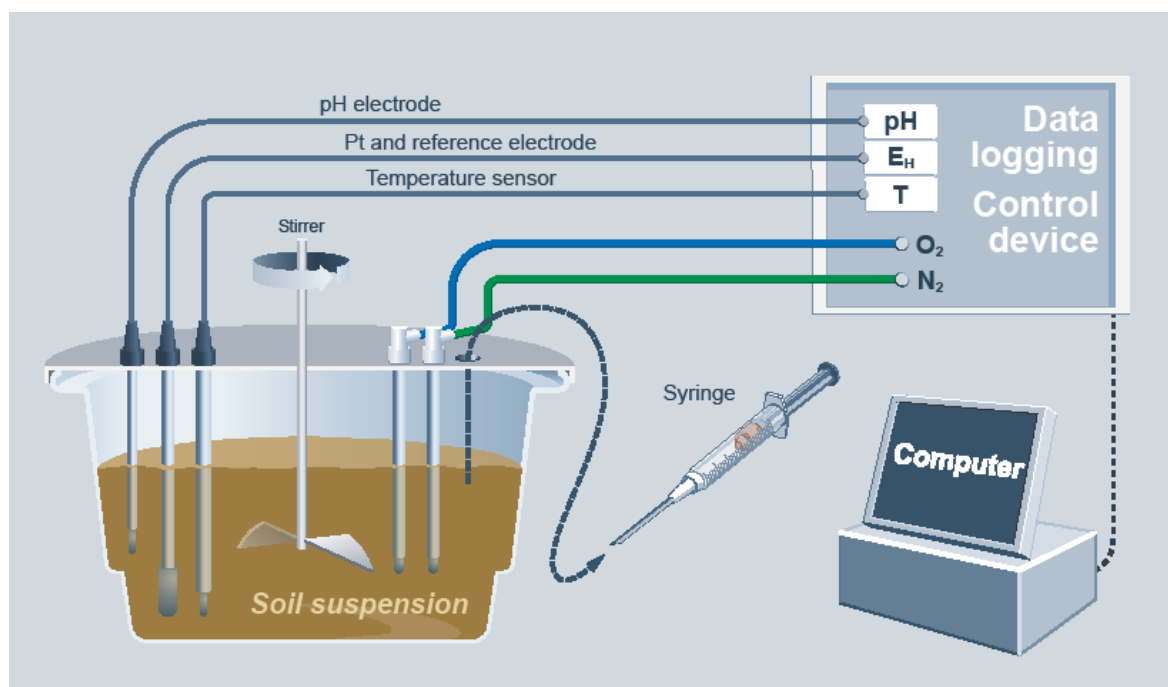


Fig. 5.1: Scheme of a microcosm and control device



Every third day, 50 mL of the soil suspension was taken from the microcosms with a 60 mL sterile syringe (Exelmed, I.M.I.) and a 15 cm tygon tube on top of the syringe. Soil suspensions were filtered with 0.45  $\mu\text{m}$  cellulose-nitrate filter (Satorious) and after day 43 with 0.45  $\mu\text{m}$  (VacuCap 90 filter unit, Pall Corporation, USA), and aqueous subsamples were stabilized by adding  $\text{HNO}_3$ . The adding of  $\text{N}_2$  or filtered ambient air leads to an overpressure in the microcosm system. This overpressure was conducted out of the system. To filter the gaseous Hg in this outgassing air we used absorber traps filled with activated carbon (MLS). This allowed the binding of the total amount of Hg. At day 23 we added to the microcosm maintained at strongly reducing, sulfate in the form of  $\text{Na}_2\text{SO}_4$  (4.44 g resulting in 250  $\text{mg L}^{-1}$  sulfate) and acetate in the form of  $\text{CH}_3\text{COONH}_4$  (0.530 g resulting in 0.01 M) because we wanted to simulate the influence of sulfate reduction on the distribution of Hg. To strengthen the effect of sulfate reduction, at day 37 we added an inoculum consisting of sulfate reducing bacteria (a few drops of wet sediments from the German Wadden Sea).

#### **5.2.4 Analyses of soil suspensions, extractants, filter residual and gaseous Hg phase**

Ferrous Fe ( $\text{Fe}^{2+}$ ) concentrations of the aqueous phase of the soil suspensions were analyzed spectrophotometrically (Lambda 25, Perkin Elmer) according to Viollier et al. (2000) immediately after sampling. Sulfate and chloride was determined by ion chromatography (ICS-1000, Dionex). Total dissolved organic C was determined by high temperature catalytic oxidation. Using this procedure, dissolved C was oxidized to  $\text{CO}_2$  and quantified by a non-dispersive, infrared analyzer. A Shimadzu TOC-5050 analyzer operating at 680  $^\circ\text{C}$  was used. Dissolved inorganic carbon was measured by quantifying the  $\text{CO}_2$  generated following phosphoric acid addition and was subtracted from the total dissolved C to give DOC. The stabilized subsamples were used to measure the total concentrations of Fe, Mn, and Hg. Iron (248.3 nm) and Mn (279.5 nm) were determined by flame atomic absorption (iCE 3500, Thermo scientific). The Hg was measured with a direct mercury analyzer (DMA-80, MLS). In the DMA-80 the sample is dried and then thermally decomposed by controlled heating. Decomposition products are carried to a catalyst by an oxygen flow. When the sample oxidation is completed and halogens and nitrogen/sulfur oxides are trapped, the final decomposition products can pass through a Hg amalgamator. Elemental Hg is trapped on the amalgamator, then heated up to 700  $^\circ\text{C}$  and the  $\text{Hg}^0$  concentration is quantified (Maggie et al., 2009). To control all measurements with the DMA-80 system, the reference material “metals on soil/sediments” (CRM-050-008) was analyzed. Recovery of this measurement was 97 %.

Sequential extraction and aqua regia extractions were also quantified by DMA-80. Recovery for the measurement of the reference material for the sequential extraction was 105 and 111 %. The filter residual was also measured with the DMA-80. This measurement was also controlled by the use of the reference material “metals on soil/sediments” (CRM-050-008). The recovery ranged from 96 to 106 %. The gaseous Hg adsorbed on the traps with activated carbon was also measured by the DMA-80 system. The recovery for the reference material during the determination of gaseous Hg was 99 to 105 %.

### **5.2.5 Modeling and statistical calculations**

All statistical calculations were performed with the program IBM SPSS Statistics 20. We modeled the species distribution in our experiments with the software Visual Minteq 3.0. Complexation by dissolved organic ligands was considered with the Stockholm Humic Model (Gustafsson, 2001). The model calculation was carried out with the following assumptions as to the composition of DOM: 65 % of DOM is fulvic acid and 35 % is inert. The DOM concentration was calculated as 1.65 times that of dissolved organic carbon (DOC).

## **5.3 Results and Discussion**

### **5.3.1 Soil properties**

Table 5.1 summarizes the main properties of the floodplain soil located 20 m from the Elbe River. The soil is, according to the WRB and IUSS Working Group (2006) a Eutric Fluvisol. The pH of the soil is in a moderate acid range. The particle size distribution reveals that a large proportion of silt ( $560 \text{ g}^{-1} \text{ kg}$ ) occurs in this soil. According to the FAO the soil texture is a silty clay loam. The high content of C ( $60.2 \text{ g}^{-1} \text{ kg}$ ) and the low ratio of C/N are characteristic for a soil covered with grass. The half of Fe in the soil is bound to Fe oxides. The main Fe oxides in this soil are poorly crystalline Fe oxides, this is documented in the ratio of  $\text{Fe}_d/\text{Fe}_o$  with 0.89. The Hg content of  $9.33 \text{ mg}^{-1} \text{ kg}$  exceeds the German threshold value for precautionary soil protection for loamy soil with  $0.5 \text{ mg}^{-1} \text{ kg}$  (BBodSchV, 1999). The median for background values of floodplain soils in the environs of agglomerations used as grassland in the state of lower Saxony is  $0.12 \text{ mg}^{-1} \text{ kg}$  for Hg (LABO, 2003). The contamination of the floodplains of the Elbe River with Hg has also been reported by Devai et al. (2005), Overesch et al. (2007), and Wallschläger et al. (1996). The causes of this contamination, especially in the past, were the anthropogenic inputs from industrial point sources (Hamburg

Port Authority, 2005; Wallschläger et al., 1996). Currently, pollution with Hg and other trace elements is lower, but still detectable. The sources of pollution today are more diverse, including groundwater, historical mining, atmospheric deposition, drainage, municipal waste water and industrial discharge.

Tab. 5.1: Chemical and physical characteristics of the Ah horizon of a Fluvisol from the Elbe river at the biosphere reserve "Niedersächsische Elbaue" at Hohnstorf, Lower Saxony, Germany

<b>Property</b>	
pH (in H <sub>2</sub> O), [-]	6.6
pH (in CaCl <sub>2</sub> ), [-]	6.1
Particle size distribution	
Sand [g kg <sup>-1</sup> ]	150
Silt [g kg <sup>-1</sup> ]	560
Clay [g kg <sup>-1</sup> ]	290
Texture	silty clay loam <sup>†</sup>
Total Fe [g kg <sup>-1</sup> ]	43.4
Fe <sub>o</sub> [g kg <sup>-1</sup> ]	18.0
Fe <sub>d</sub> [g kg <sup>-1</sup> ]	20.4
Fe <sub>o</sub> /Fe <sub>d</sub>	0.89
Total Mn [g kg <sup>-1</sup> ]	1.33
Total C [g kg <sup>-1</sup> ]	60.2
Total N [g kg <sup>-1</sup> ]	5.04
C/N	12
Hg [mg kg <sup>-1</sup> ]	9.33

<sup>†</sup>according to FAO

### 5.3.2 Sequential extraction

It is well known that Hg shows strong bindings both to inorganic and organic soil components (Schuster, 1991). The sequential extraction (Tab. 5.2) of the soil revealed that 36.7 % of the Hg was bound to the organic matter. Dmytriw et al. (1995) showed that the main part of Hg in soil is bound to the organic matter, whereas Hg is mostly bound to S-functional groups of the organic matter (Gabriel and Williamson, 2004; Johansson and Iverfeldt, 1994; Schuster, 1991). The main binding partners in soils, in addition to the organic matter, are oxides and clay minerals (Gabriel and Williamson, 2004; Schuster, 1991). The sequential extraction showed that 35.8 % of the Hg occurred in the elemental Hg fraction and 19.6 % in the mercuric sulfide fraction. The strong binding of Hg to soils commonly entails a small

solubility of Hg. This is documented in our sequential extraction, because less than 1 % of the total Hg was bound to the water soluble and human stomach acid fraction.

Tab. 5.2: Sequential extraction of Hg in the Ah horizon of a grassland Fluvisol from the Elbe river at the biosphere reserve "Niedersächsische Elbaue" at Hohnstorf, Lower Saxony, Germany [mg kg<sup>-1</sup>]

	fraction in mg kg <sup>-1</sup>	fraction in %
F1 <sup>a</sup>	0.025	0.302
F2	0.004	0.044
F3	2.99	36.7
F4	2.92	35.8
F5	1.60	19.6
soil residual	0.623	7.63
sum <sup>b</sup>	8.16	100
total Hg <sup>c</sup>	9.20	
sum/ total Hg	0.89	

<sup>a</sup> Fraction 1 (F1): water soluble fraction; F2: human stomach acid soluble fraction; F3: organic-bound fraction; F4: elemental Hg fraction; F5: mercuric sulfide fraction; F6: soil residual; according to Bloom et al. (2003)

<sup>b</sup> sum F1 to F5 and soil residual

<sup>c</sup> separate measure of Hg

### 5.3.3 Redox potential and pH

Floodplain soils are characterized by temporary or permanent water saturation in their topsoils or subsoils, respectively. These water saturations influence the processes and developments in the soil. One factor that is strongly controlled by the water regime is the  $E_H$ . Water saturation leads to a decrease of the oxygen partial pressure of the soil and with that, a decrease of the  $E_H$ ; this is the development we wanted to show within our experiments. The aim was to achieve  $E_H$  in soils where in the first experiment the reduction of Fe starts (moderately reducing,  $\sim 100$  mV), and in the second experiment, the reduction of sulfate (strongly reducing,  $\sim -100$  mV) occurs. Figure 5.2 shows the development of the  $E_H$  and the connected pH.

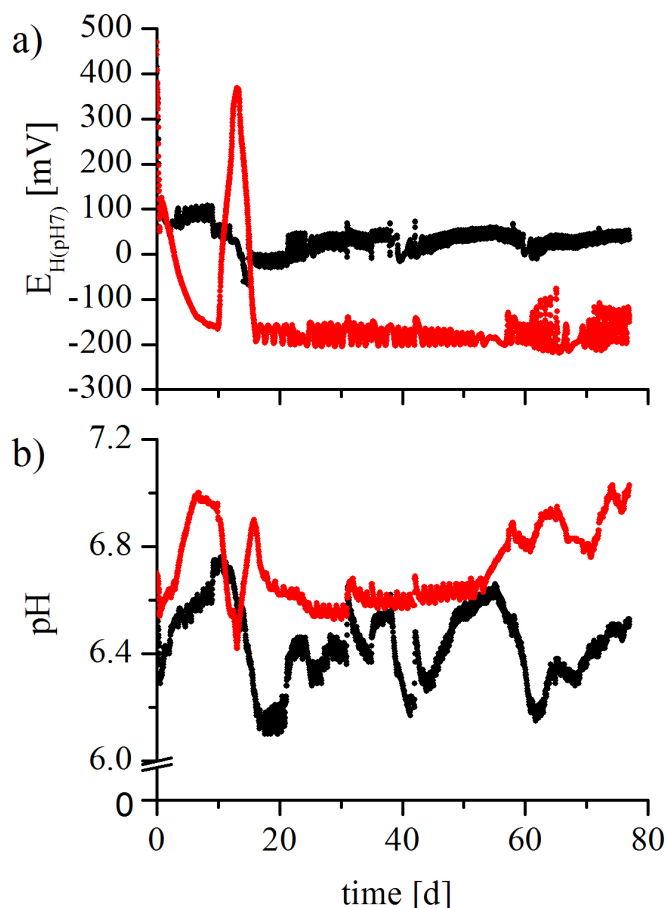


Fig. 5.2: Development of redox potential ( $E_H$ ) and pH during the microcosm experiments (● moderately reducing, ● strongly reducing)

The  $E_H$  of the first experiment showed with 443 mV oxidizing conditions at the beginning of the experiment. Within nine hours the range of moderately reducing conditions was achieved. To reinforce the effect of the reduction of Fe oxides, we lowered the  $E_H$  to 50 mV. This adjustment was made at day 10. Then the  $E_H$  decreased within six hours to 50 mV and at day 15 to -70 mV. This development was caused by an incorrect inlet of  $N_2$  due to a wrong adjustment at the control unit. Within three hours the previous level of 50 mV was achieved again. After day 16 the  $E_H$  fluctuated between -10 and 70 mV. This development was caused by the inlet of filtered air or  $N_2$  to stabilize the desired  $E_H$ .

The second experiment also started at oxidizing conditions (442 mV) and within 122 hours the range of strongly reducing conditions was achieved ( $< -100$  mV). The  $E_H$  increased at day 11 up to 370 mV within 70.5 hours, caused by the inlet of filtered air. This development was caused by a wrong adjustment at the control unit. After correction of the adjustment the

$E_H$  achieved the range of strongly reducing conditions within 58.5 hours. From day 16 to the end of the experiment the  $E_H$  fluctuated between  $-100$  and  $-200$  mV.

The decrease of  $E_H$  in both experiments was caused by the consumption of oxygen in the soil. When no oxygen is available, specialized microorganisms can act as a substitute. Specialized microorganisms use nitrate, Mn oxides, Fe oxides, or sulfate as their electron acceptor (Reddy and Delaune, 2008).

The development of the pH is associated with the  $E_H$  because reduction is accompanied by proton-consuming processes (Bartlett and James, 1993). During reduction in soils, the soil pH should increase. In our experiment, the pH fluctuated between 6.10 and 6.76. At the beginning of the first experiment, the pH decreased from 6.54 to 6.29 within 14.5 hours. Then the pH increased up to 6.70 at day 13. After that, the pH decreased from 6.70 to 6.10. After day 20, the pH decreased to 6.65 with strong fluctuations until day 38. After day 38 the pH decreased again to 6.17 at day 41 and increased again until day 56 (pH 6.66). After day 56 the pH decreased to 6.15 at day 62 and finally a last increase to 6.53 occurred at the end of the experiment.

In the second experiment, the pH decreased from 6.65 to 6.54 within 12.5 hours. Then the pH increased up to 7.00 at day 7. The reaction of the pH to the strong increase of the  $E_H$  to oxidizing conditions at day 11 was a decrease to 6.43. After that, the pH increased again to 6.89 at day 16. Then the pH decreased again and varied from 6.70 to 6.55. From day 53 to the end of the experiment the pH increased to 7.03. The correlation between the pH and  $E_H$  in this experiment was not strong ( $r = 0.268$ ,  $p > 0,001$ ,  $n = 3,695$ ). Overall, for the second experiment the development of the pH fits to the development of the  $E_H$ . When the  $E_H$  decreased strongly an increase of the pH was obvious. The first experiment showed stronger fluctuations. The development of the pH did not show an opposite trend to the  $E_H$ . The correlation between the pH and  $E_H$  for this experiment was not strong ( $r = -0.251$ ,  $p > 0.001$ ,  $n = 3,695$ ).

#### **5.3.4 Manganese, iron, sulfate, chloride, and dissolved organic carbon**

An objective of this study was to assess the influence of the  $E_H$  on the solubility of Mn, Fe, Fe(II), sulfate, chloride, and DOC. All of these parameters can influence the solubility and outgassing of Hg. Figure 5.3 illustrates the development of these parameters.

The development of the parameter Mn is shown in Fig 5.3a and 5.3g. In the experiment with moderately reducing conditions the concentration of Mn was very low with  $0.042 \text{ mg L}^{-1}$  at

the beginning. During the first 10 days the Mn concentration increased to  $2.49 \text{ mg L}^{-1}$  and after day 11 the Mn concentrations increased to  $9.72 \text{ mg L}^{-1}$ . The strong decrease of Mn after day 11 is the result of the lowering of the  $E_H$  to about 50 mV. After this increase Mn fluctuates between  $9.72$  and  $5.46 \text{ mg L}^{-1}$ . These fluctuations are caused by dissolution (at lower  $E_H$ ) and precipitation (at higher  $E_H$ ) processes of Mn oxides. The high correlation between Mn and  $E_H$  in this experiment ( $r = -0.644$ ,  $p = 0.003$ ,  $n = 19$ ) underlines the overall importance of redox processes for the solubility of Mn. In the second experiment with strongly reducing conditions the Mn concentrations revealed at the start were very similar to those of the first experiment. However, after day 20 there was a strong increase of the Mn concentrations to about  $26.0 \text{ mg L}^{-1}$ . Obviously, this corresponds to the lowering of the  $E_H$  and the reaching of strongly reducing conditions. A very intensive reductive dissolution of Mn oxides can be expected and this explains the significantly higher Mn concentrations in comparison to the other microcosm. At day 59, Mn concentrations sharply decreased to  $16.0 \text{ mg L}^{-1}$  and remained more or less constant for the rest of the experiment. The possible reason for this decrease will be outlined later. The correlation between Mn and  $E_H$  in this experiment was also high ( $r = -0.697$ ,  $p = 0.001$ ,  $n = 19$ ).

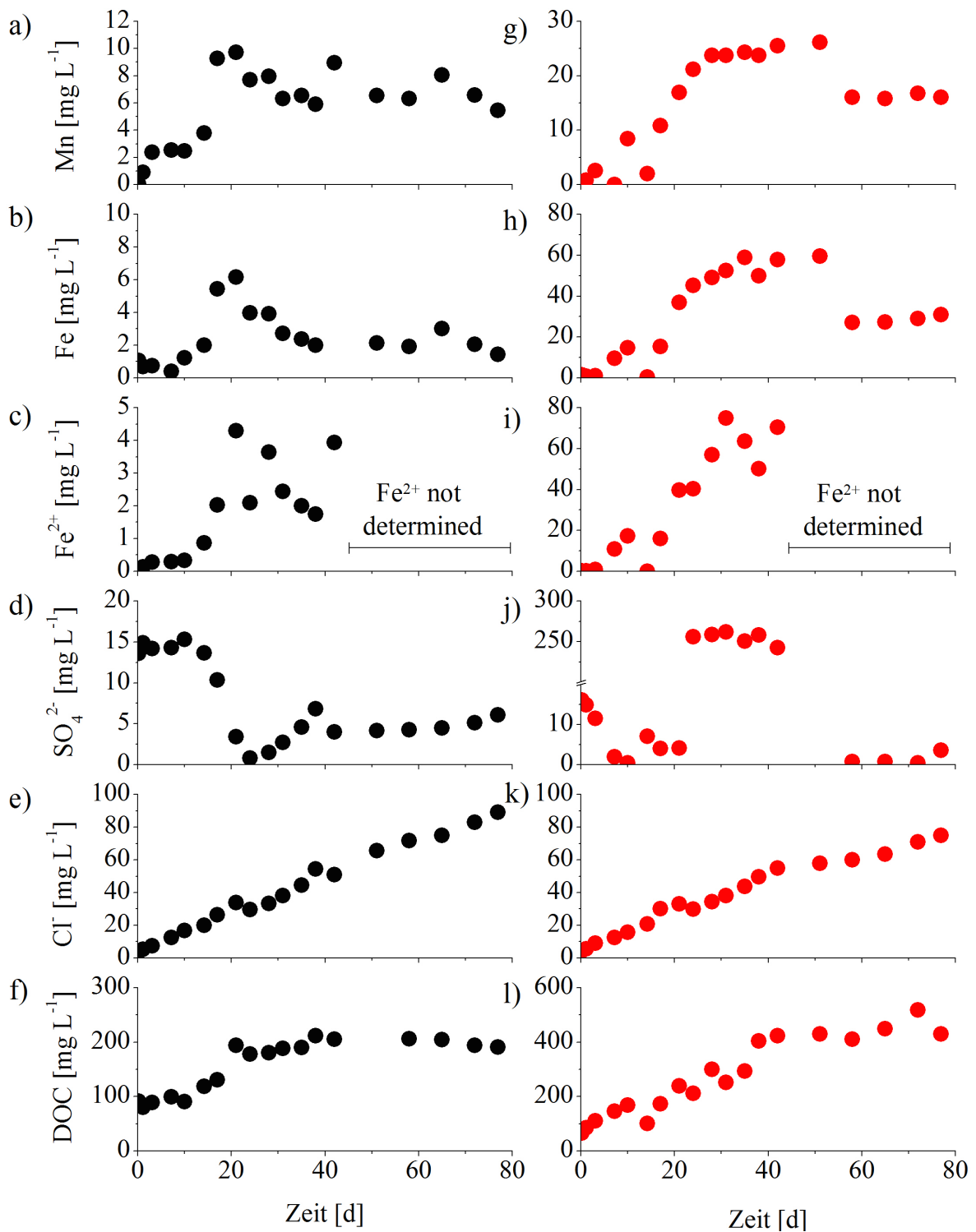


Fig. 5.3: Development of the concentrations of total Mn, total Fe ( $\text{Fe}_{\text{tot}}$ ), ferrous Fe ( $\text{Fe}^{2+}$ ), sulfate, chloride, and dissolved organic carbon (DOC) during the microcosm experiments

(● moderately reducing, ● strongly reducing)



The second element with a solubility strongly influenced by the  $E_H$  is Fe. Like Mn, Fe can be used as an electron acceptor by specialized microorganisms (Reddy and Delaune, 2008). The dissolved Fe was determined as total Fe (Fig. 5.3b and 5.3h) and also as  $Fe^{2+}$  (Fig. 5.3c and 5.3i) until day 43. The difference between total Fe and  $Fe^{2+}$  corresponds to organically complexed Fe (either  $Fe^{III}$  or  $Fe^{II}$ ) or colloidal Fe (e.g. Fe in silicate or Fe oxide particles). The experiment under moderately reducing conditions showed an increase of the total Fe concentration to  $6.16 \text{ mg L}^{-1}$  at day 22. This development was caused by the decrease of the  $E_H$  to 0 mV. Under this  $E_H$ , the reduction of Fe by microorganisms was in progress. The  $Fe^{2+}$  concentration showed a similar behavior with increasing concentration to a maximum of  $4.30 \text{ mg L}^{-1}$  at day 22. The Fe concentration then decreased until the end of the experiment to  $1.43 \text{ mg L}^{-1}$ . The decrease of the Fe concentration was caused by the increase of the  $E_H$  to about 50 to 100 mV. One exception is the Fe concentration at day 43 with  $11.8 \text{ mg L}^{-1}$ . The  $Fe^{2+}$  concentrations showed variations between  $1.75$  and  $3.94 \text{ mg L}^{-1}$  until day 43. In the second experiment with strongly reducing conditions, an increase of the Fe concentration to  $14.7 \text{ mg L}^{-1}$  until day 11 was obvious. The  $Fe^{2+}$  concentration increased also to  $17.2 \text{ mg L}^{-1}$  day 11. At this point of the experiment, total dissolved Fe in the solution equaled  $Fe^{2+}$ . At day 15 total Fe and the  $Fe^{2+}$  concentration decreased to  $0.286$  and  $0.024 \text{ mg L}^{-1}$ , respectively, because of the increase of the  $E_H$  to oxidizing conditions. At this  $E_H$ , oxygen is available and the microorganisms do not require Fe oxides. When the  $E_H$  decreased to strongly reducing conditions again the Fe concentration increased to a maximum of  $59.6 \text{ mg L}^{-1}$  at day 52. The  $Fe^{2+}$  concentration also increased so that all the dissolved Fe in the solution was  $Fe^{2+}$ . A maximum  $75.0 \text{ mg L}^{-1}$  of  $Fe^{2+}$  could be detected in this experiment. At day 59 total Fe decreased to  $27.1 \text{ mg L}^{-1}$ . The possible reason for this decrease will be discussed later.

Fig. 5.3d and 5.3j show the concentration of sulfate during the course of the experiment. The dissimilatory sulfate reduction started at an  $E_H$  of  $-50 \text{ mV}$  (Brümmer, 1974) and was very intensive when the  $E_H$  level dropped below  $-100$  to  $-150 \text{ mV}$ , i.e., at strongly reducing conditions (Du Laing et al., 2009; Gambrell et al., 1991; Mansfeldt, 2004). The sulfate concentration in the moderately reducing experiment started with  $13.4 \text{ mg L}^{-1}$  and decreased at day 25 to  $0.764 \text{ mg L}^{-1}$ . This could have been caused by the lowering of the  $E_H$  to  $-30 \text{ mV}$  at day 15 indicating the onset of sulfate reducing conditions. Then the  $E_H$  and the concentration of sulfate increased again and fluctuated between  $4.01$  and  $6.84 \text{ mg L}^{-1}$ . In the experiment with strongly reducing conditions, the sulfate concentration started with a comparable level of

16.1 mg L<sup>-1</sup> which indicates the homogeneity of both soil samples. However, the sulfate concentration immediately decreased and only 0.46 mg L<sup>-1</sup> sulfate were detectable at day 8. Then with increasing E<sub>H</sub> to oxidizing conditions sulfate increased again to 7.01 mg L<sup>-1</sup>. At day 23 we added sulfate and ammonium acetate, so that the sulfate concentration increased to 250 mg L<sup>-1</sup>. The sulfate was added because we wanted to simulate the influence of sulfate reduction on the distribution of Hg. Because sulfate reducing bacteria require low-molecular organic acids as an electron donator we added acetate to our system. To intensify the effect of the sulfate reduction we also added an inoculum at day 37. As a result, the sulfate concentrations decreased drastically between days 43 (242 mg L<sup>-1</sup>) and 59 (0.786 mg L<sup>-1</sup>). The reduction of sulfate led to the formation of the reduced sulfur species sulfide. This species should be present in our experiment as hydrogen sulfide (HS<sup>-</sup>) and sulfide (S<sup>2-</sup>). Sulfide, in turn, forms sparingly soluble compounds with many metals including Mn and Fe. Examples are alabanite (MnS) for Mn and mackinawite for Fe (Fe<sub>x</sub>S). Their corresponding solubility products are pK<sub>s</sub> = -0.2 for alabanite and pK<sub>s</sub> = 3.6 for mackinawite (Allison et al., 1990). The decrease in the concentrations of Fe (Fe<sup>2+</sup>) and Mn (Mn<sup>2+</sup>) in the soil solution of the strongly reducing microcosms was presumably caused by the precipitation of the corresponding metal sulfides.

For the chloride concentrations, a continuous and more or less linear increase during the course of the experiment was observed (Fig. 5.3e and 5.3k). Chloride is not involved in redox processes and no significant amounts are adsorbed into the solid phase. Instead, chloride was leached from the electrolyte of the pH electrode throughout the whole experiment. This is an experimental shortcoming that cannot be avoided. However, chloride has to be taken into account for the objective of the current study because it may act as a ligand for Hg (Schuster, 1991). By this complexation, the solubility of Hg is increased.

Fig. 5.3f and 5.3k show the development of the DOC concentrations. This parameter represents the dissolved organic matter (DOM) in the soil suspension. Dissolved organic matter is of importance because DOM acts as a ligand for Hg, thus affecting its solubility. The experiment with moderately reducing conditions showed a continuous increase of the DOC concentrations from 91 up to 194 mg L<sup>-1</sup> at day 22. Then the DOC concentrations varied between 178 and 212 mg L<sup>-1</sup>. For the strongly reducing experiment, an increase from 66 up to 519 mg L<sup>-1</sup> was also observed. The source of DOC in our experiment was the release of DOC from the solid phase since cellulose is insoluble. This can be caused by the increase of pH

and the subsequent release of adsorbed DOM and/or the reductive dissolution of DOM-hosting oxides (Fiedler and Kalbitz, 2003; Grybos et al., 2009).

### **5.3.5 Hg in different phases**

The main objective of the present study was to study the behavior of Hg. Therefore, the concentration and amounts of Hg in the solid phase (soil), dissolved phase (soil solution) and gaseous phase were investigated.

#### **5.3.5.1 Hg in filter residual**

When the soil suspension was withdrawn from the microcosms, it was filtered by a vacuum filter unit. The soil residual remaining on the filter was then analyzed to determine the Hg concentration during the different samplings. Figure 5.4a shows the development of the Hg content during the first 43 days of the experiment. After day 43, the concentration of the Hg in the filter residuals could not be determined because we used another filter system for more simple and accurate sampling.

In the moderately reducing microcosm, the concentration of Hg in the filter residuals varied between 11.3 and 16.7 mg kg<sup>-1</sup> (mean 14.7 ± 1.75 mg kg<sup>-1</sup>) without any trend. In the strongly reducing microcosm, the Hg concentration fluctuated between 11.8 and 18.8 mg kg<sup>-1</sup> with a mean of 15.2 ± 1.79 mg kg<sup>-1</sup>. Also in this experiment, no clear tendency could be observed.

The total concentration of Hg in the soil was 9.33 mg kg<sup>-1</sup> (Tab. 5.1). However, the total concentration in the residuals was significantly higher as outlined above. At first glance this result is inconsistent because only a loss of Hg (by volatilization) could have happened and not an enrichment. We assume that our experimental design led to the observed discrepancy. Although the soil suspension was continuously stirred, a fractionation of the soil particles presumably occurred. This fractionation depends on the particle size and particle density. The smaller and lighter soil particles were more “available” for sampling in the microcosms than the greater and heavier particles, because the latter have a tendency to accumulate in the bottom of the microcosm system. At the bottom, no sampling was possible. Furthermore, the sampling of the soil solution with a syringe and tygon tube took place at a different depth (±2 cm) of the microcosm. As a result, soil suspensions with different particle size were sampled. Mercury, in turn, seemed to have accumulated on the smaller and lighter fractions of soil particles, for example on DOC-containing particles.

The initial idea was to monitor the Hg amount of the filter residual and to link this data with the volatilization rates of Hg (see below). Unfortunately, due to the shortcomings associated with the experimental setup this was not possible.

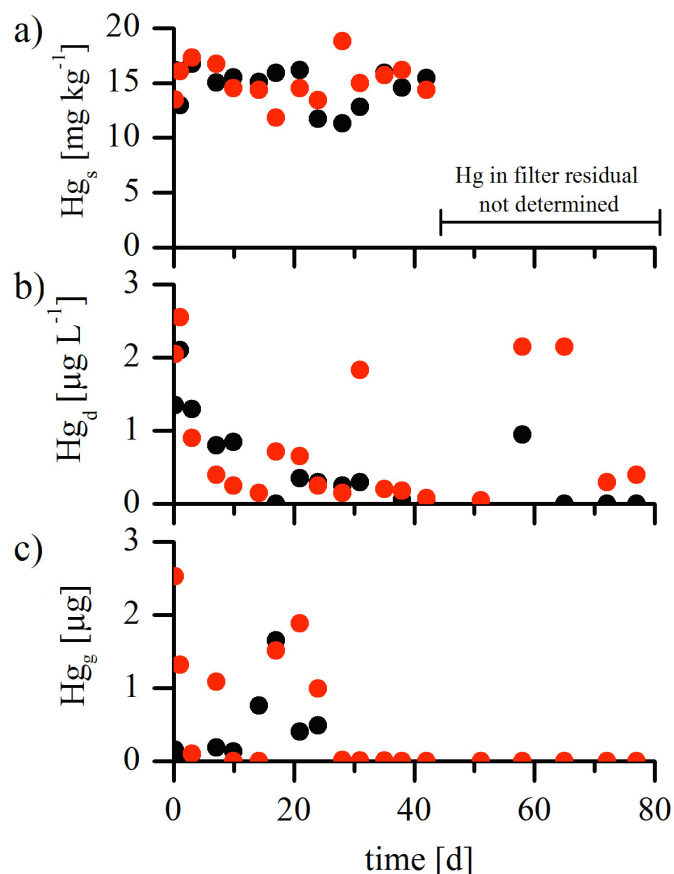


Fig. 5.4: Development of the concentrations of Hg in the filter residual (solid) ( $Hg_s$ ), dissolved Hg ( $Hg_d$ ), and gaseous Hg ( $Hg_g$ ) (● moderately reducing, ● strongly reducing)

### 5.3.5.2 Hg in soil solution

Figure 5.4b illustrates the development of the Hg concentrations in both microcosms.

In the moderately reducing microcosm, the concentrations increased up to  $2.10 \mu\text{g L}^{-1}$  within two days. Then the concentrations decreased, and after day 16 Hg was not detectable. The concentrations then increased again up to  $0.350 \mu\text{g L}^{-1}$  at day 22. From day 22 to 36 the concentrations varied between  $0.200$  and  $0.350 \mu\text{g L}^{-1}$ . Then until the end of the experiment no Hg was detectable with one exception (day 59). This value ( $0.950 \mu\text{g L}^{-1}$ ) seemed to be an outlier.

The microcosm maintained under strongly reducing conditions showed similar behavior compared to the moderately reducing microcosm. Within two days, the concentrations increased up to  $2.55 \mu\text{g L}^{-1}$ , and then the concentrations decreased. The concentration varied between  $0.050$  and  $0.75 \mu\text{g L}^{-1}$  until the end of the experiment. At this experiment two peaks of the concentration at days 32 ( $1.8 \mu\text{g L}^{-1}$ ) and 59 ( $2.15 \mu\text{g L}^{-1}$ ) were noticeable.

Both experiments showed an increase of Hg concentrations at the beginning of the experiment. This can be explained by the dissolution of the weakly bound Hg, which represents a kind of labile Hg. Also Favre et al. (1997) and Li et al. (2010a) described the effect of increasing trace element concentrations during the rewetting of a dry soil. The reason for this could be the expansion of clay minerals, increasing solubility of salts, dispersion of colloids, or increasing competition to reactive surfaces with other dissolved components like DOC. After this first increase, the concentration of Hg in the soil solution decreased in both experiments. The reasons for this development could be the re-adsorption of dissolved Hg into the soil, the reduction of Hg to its elemental species and subsequent volatilization, and the formation of insoluble Hg minerals. In our experiments, the binding partners of Hg, like organic matter or Mn and Fe oxides, were transferred into the dissolved phase. Hence, we conclude that Hg was liberated and entered the solution. However, because of the fact that there were many adsorption partners in the soil, Hg can be continuously re-adsorbed. This hypothesis is supported by the fact that Hg concentration increased only for one sampling event. An example is shown in the strongly reducing microcosm at day 32 with  $1.80 \mu\text{g L}^{-1}$ . This event can be explained by the reductive dissolution of Fe or Mn oxides, which liberate adsorbed Hg (Belzile et al., 2008).

In soil solution, Hg is mostly bound to the DOM (Akerblom et al., 2008; Gabriel and Williamson, 2004; Skyllberg et al., 2003). These findings are confirmed by our geochemical modeling because in both experiments most of the Hg (> 99 %) was bound to organic ligands. Only very small parts of the Hg were bound to chlorides, i.e. as Hg-chlorido complexes.

To the strongly reducing microcosm, sulfate was added at day 23. The aim was the formation of sulfide ions during the reduction of sulfate under strongly reducing conditions ( $E_{\text{H}} < -100 \text{ mV}$ ). These sulfides can decrease the solubility of Hg, because Hg reacts with sulfide to Hg sulfides. These minerals have extremely low solubility products, e.g.  $\text{p}K_{\text{s}} = 45.7$  for cinnabar (Allison et al., 1990). However, in our experiment the concentration of Hg in the

soil solution was so low, that we could not observe this process. Only for Mn and Fe could we observe a decreasing solubility after adding sulfate.

Based on the Hg concentrations of the microcosms and the amount of water, we calculated a maximum of 12.6  $\mu\text{g}$  Hg dissolved in the moderately reducing microcosm and 15.3  $\mu\text{g}$  Hg dissolved in the strongly reducing microcosm, respectively. This means that only 0.11 % and 0.13 % of the total Hg in soil was dissolved during the course of the study. These values are low and very similar for both samples. The data emphasizes the strong binding of Hg in soils and its low solubility (Schuster, 1991).

### **5.3.5.3 Volatilization of Hg**

The Hg concentrations in the soil solution decreased in our experiments after the third day. The reasons for this could be the re-adsorption of dissolved Hg into the different soil constituents, but also the volatilization of Hg. Figure 5.4c illustrates the amounts of the gaseous Hg during the course of the experiment.

After a first increase of gaseous Hg at the beginning of the moderately reducing experiment, only low amounts of gaseous Hg were shown until day 11. The maximum Hg amount at this stage of the experiment was 184 ng at day 8. The amount then increased to 1650 ng at day 18, but then decreased again. From day 29 until the end of the experiment, the gaseous Hg amounts were lower than 10 ng.

The experiment with strongly reducing conditions revealed very high gaseous Hg amounts at the beginning of the experiment with 2527 ng Hg. This might have been caused because the supply of  $\text{N}_2$  was very strong at the beginning of the experiment resulting in large flow rates. The supply was regulated to a lower level at day 3. Then only small parts of  $\text{N}_2$  entered the system. The gaseous Hg amounts then decreased and two strong peaks occurred at day 8 with 1085 ng and at day 22 with 1885 ng Hg. Then the gaseous Hg amounts decreased and from day 32 until the end of the experiment, the amounts were lower than 10 ng.

In the moderately reducing experiment, a total amount of 3.94  $\mu\text{g}$  Hg was volatilized which represents only 0.033 % of the total Hg. Correspondingly, in the strongly reducing experiment 9.46  $\mu\text{g}$  Hg evaporated which is 0.081 % of the total Hg.

Both experiments showed a similar behavior. After a first increase at the beginning of the experiments, the Hg amount decreased. It seems that after the rewetting of the dry soil and

the supply of N<sub>2</sub>, gaseous Hg, which already exists in the soil suspension, left the system. With the lowering of the E<sub>H</sub> the amount of gaseous Hg increased. In the moderately reducing experiment the Hg concentration increased when the E<sub>H</sub> fell below 0 mV. In the experiment with strongly reducing conditions the concentration increased when the E<sub>H</sub> decreased below -100 mV. Then the E<sub>H</sub> increased up to 230 mV and the amount of gaseous Hg increased. With decreasing E<sub>H</sub>, the amount of gaseous Hg increased again. The increase of the gaseous Hg amounts could be caused by the reduction of dissolved Hg (Hg<sup>2+</sup>) in the soil solution. During the lowering of the E<sub>H</sub> the reduction of dissolved Hg to elemental Hg is strengthened.

#### **5.4 Conclusions**

In this study, the distribution of Hg between the solid, dissolved, and gaseous phase under defined redox conditions was investigated. The experiment showed that even under strongly reducing conditions only small amounts of Hg were dissolved. The dissolution of Hg is one important factor for the volatilization of Hg and as a result, less Hg evaporated. The behavior of Hg in soils is characterized by strong binding to soil constituents and this influences the distribution of dissolved and gaseous Hg in soils.

## 6 CONCLUSIONS

The aim of this work was to answer the question: "Does redox potential and temperature influence the solubility of trace elements and volatilization of Hg, respectively?" To answer this question soil from the floodplains of the Elbe and Wupper Rivers in Germany were used for the experiments. Both sites are characterized by high trace element contents and fluctuations in the  $E_H$  that are caused by flooding events.

### *Solubility of trace elements*

Trace elements showed different behaviors with regard to variations in the  $E_H$ . One group included elements that reacted very sensitively to variations in the  $E_H$ . The elements Mo and Co belong to this group, because they already showed increased solubility when the  $E_H$  reached weakly reducing conditions. These effects could be attributed to the strong binding of these elements to Mn oxides. Under weakly reducing conditions Mn oxides could already be reductively dissolved and Mo and Co that were adsorbed by these oxides were liberated. The second group included elements that showed increased solubility under moderately reducing conditions. The elements As and Cr could be included in this group. These elements showed strong binding to Fe oxides, could be dissolved under moderately reducing conditions. When Fe oxides were dissolved under moderately reducing conditions, trace elements adsorbed by these oxides were also dissolved. The third group included trace elements that did not show strong reactions to variations in the  $E_H$ . The trace elements Zn, Pb, Ni, Cd, and Cu belong to this group. Instead, the solubility of these trace elements was influenced by parameters such as pH. The strong binding of Pb and Cu to organic matter is documented in literature. The solubility of Pb and Cu increased with increasing solubility of organic matter. Solubility of the organic matter was determined by measuring the DOC. The DOC concentration increased during the experiment and with that the concentration of Pb and Zn increased. The solubility of other elements such as Zn depend on pH; the solubility of Zn decreased with increasing pH. With a decrease in the  $E_H$ , the pH increased. This phenomenon can be explained because reducing conditions are accompanied by proton consuming processes.

The trace element Sb showed a special behavior. After an increase in its concentration under weakly reducing conditions, its solubility decreased under moderately reducing conditions.



This behavior was caused by a modification of the species. Under oxidizing and weakly reducing conditions the antimonate  $\text{Sb(OH)}_6^-$  was the dominant species, but under moderately reducing conditions antimonite  $\text{Sb(OH)}_3^0$  became the dominant species. These species differed in their strength of binding to soil constituents. Antimonite bound strongly, whereas antimonate bound less strongly. Hence, the reduction of antimonate to antimonite induced a decreasing solubility by preferential sorption of the reduced species.

### *Influence of temperature on the solubility of trace elements*

The influence of temperature on the behavior of trace elements has been documented. With increasing temperature the solubility of trace elements increases. These effects have been well documented for the  $E_H$ -sensitive elements such as Co, Mo, As, and Cr. The main binding parameters for these elements are Fe and Mn oxides. These oxides participate in redox processes. Redox processes are catalyzed by microbes. Variations in temperature influence microbial activity and this was reflected in the concentration of the redox sensitive parameters Fe and Mn. The solubility of trace elements is linked to seasons, because in the warmer summer months a higher solubility can be expected when the soils are flooded.

### *Influence of $E_H$ variations on the solubility and volatilization of Hg*

A decreasing  $E_H$  due to reducing conditions (especially to strongly reducing conditions) led to an increased solubility of Hg. Under reducing conditions Mn and Fe oxides could be reductively dissolved and the Hg adsorbed by these binding partners could also be dissolved. Hg was mostly bound to the organic matter, although Fe and Mn oxides also acted as binding partners of Hg. Mercury showed less solubility under strongly reducing conditions; a maximum of 0.13% of the total Hg could be found in the soil solution. A reason for this was that Hg showed strong binding to the soil matrix.

The solubility of Hg was important for the later volatilization of Hg, because the dissolved Hg in the soil solution could be reduced to gaseous Hg. This process was mainly controlled by sulfate reducing bacteria. The volatilization of elemental Hg was also very low, because only low amounts of dissolved Hg could be found in the soil solution.

### *Distribution of Hg in soil, soil solution, and gaseous phase from the Elbe River floodplains*

The distribution of Hg in the floodplain soil of the Elbe River showed that most of the Hg was bound to soil particles. Even strongly reducing conditions led only to low solubility of Hg. Only 0.13% of Hg was found in soil solutions under strongly reducing conditions. The dissolution of Hg is one important factor for the volatilization of Hg and as a result less Hg evaporated. The behavior of Hg in soils was characterized by strong binding to soil constituents, which influenced the distribution of dissolved and gaseous Hg in soils.

### *Hg species in the soil solution and gaseous phase*

In our experiments only elemental Hg was identified. Even under a worst-case scenario, such as high temperatures with water saturation for a longer period of time and strongly reducing conditions, only elemental Hg and not methylated Hg species volatilized from the soil. Apparently the conditions were not favorable for Hg biomethylation. Possible reasons for this might be that the reducing conditions did not last long enough to establish an environment suitable for methylating microorganisms, and/or the system was sulfate limited, and/or the high Hg concentrations were too toxic for the microbiota to survive.

Determination of the methylated species is important, because methylated species are responsible for major diseases. Methyl-Hg is a neurotoxin that is largely present in fish and seafood products and can accumulate in the food chain. However, the proportion of methylated Hg in the total degassed Hg was very small, with less than 1% of total Hg. This complicated the detection of methylated species.

In the soil solution most of the Hg was bound to the DOC. These findings were confirmed by our geochemical modeling, because in both experiments most of the Hg (> 99%) was bound to organic ligands. Only a very small portion of Hg was bound to chlorides (i. e., as Hg-chlorido complexes).

### *General conclusions*

The  $E_H$  has an influence on the solubility of trace elements. This influence is element specific. For example, the elements Mo, As, and Co, showed increasing solubility under decreasing  $E_H$ . The reasons for the increased solubility were the dissolution of Mn and Fe oxides and with that the dissolution of the adsorbed trace element. The element Pb, for example, showed

strong binding to organic matter and the dissolution of DOC was not redox sensitive. Mercury showed increasing solubility under reducing conditions and the dissolved Hg could be reduced to a gaseous species.

The increasing solubility of trace elements has an influence on the environment. Repeated flooding can lead to increased solubility of trace elements. These elements can be incorporated into surrounding soils. This can be problematic if these soils are used as grassland, farmland, building land, or playground for children. Trace elements can enter the food chain or they can be adsorbed directly.

The volatilization of Hg has to be analyzed in other soils. Experiments for the volatilization of Hg in floodplain soils of the Oker River (Vienenburg, Lower Saxony) showed stronger degassing rates than the experiments presented in this work. To better understand the behavior of Hg, more experiments are necessary. The procedure for analyzing gaseous Hg has to be improved, because only total Hg can be measured with the tubes filled with activated carbon. The trapping of the cooled traps filled with Hg adsorber is very complicated. For the determination of the methylation process the addition of methyl-Hg can be considered. With this addition the proportion of degassed methylated species would increase and could, therefore, be detected more easily.

## 7 LITERATURE

- Abdel-Samad H, Watson PR (1997) An XPS study of the adsorption of chromate on goethite ( $\alpha$ -FeOOH). *Appl Surf Sci* 108:371-377.
- Ackermann J, Vetterlein D, Kuehn T, Kaiser K, Jahn R (2010) Minerals controlling arsenic distribution in floodplain soils. *Eur J Soil Sci* 61:588-598.
- Adriano, DC (2001) Trace elements in terrestrial environments: biogeochemistry, bioavailability, and risks of metals, 2nd edn. Springer, New York.
- Akerblom S, Meili M, Bringmark L, Johansson K, Kleja DB, Bergkvist B (2008) Partitioning of Hg between solid and dissolved organic matter in the humus layer of boreal forests. *Water Air Soil Poll* 189:239-252.
- Alberts JJ, Schindler JE, Miller RW, Nutter DE (1974) Elemental mercury evolution mediated by humic acid. *Science* 184:895–897.
- Alewell C, Paul S, Lischeid G, Storck FR (2008) Co-regulation of redox processes in freshwater wetlands as a function of organic matter availability?. *Sci Total Environ* 404:335-342.
- Allard B, Arsenie I (1991) Abiotic reduction of mercury by humic substances in aquatic system - an important process for the mercury cycle. *Water Air Soil Poll* 56:457-464.
- Allison JD, Brown DS, Novo-Gradac KJ (1990) MINTEQA2/PRODEFA2 - A geochemical assessment model for environmental systems. Environmental Research Laboratory, Office of Research and Development. U.S. Environmental Protection Agency, Athens, Georgia.
- Antić-Mladenović S, Rinklebe J, Frohne T, Stärk H-J, Wennrich R, Tomić Z, Ličina V (2011) Impact of controlled redox conditions on nickel in a serpentine soil. *J Soil Sediment* 11:406-415
- Atlas RM, Bartha R (1987) *Microbial ecology: Fundamentals and applications*. 2nd edn. The Benjamin/Cummings Publishing Co, San Francisco.

- Bahlmann E, Ebinghaus R, Ruck W (2006) Development and application of a laboratory flux measurement system (LFMS) for the investigation of the kinetics of mercury emissions from soils. *J Environ Manage* 81:114-125.
- Barkay T, Miller SM, Summers AO (2003) Bacterial mercury resistance from atoms to ecosystems. *FEMS Microbiol Rev* 23:355–384.
- Bartlett RJ, James BR (1993) Redox chemistry of soils. *Adv Agronomy* 50:151-208.
- Bauer M, Blodau C (2006) Mobilization of arsenic by dissolved organic matter from iron oxides, soils and sediments. *Sci Total Environ* 354:179-190.
- BBodSchV (1999) Directive of the execution of the federal soil protection act (Federal soil protection and hazardous waste directive BBodSchV) (in German). *Bundesgesetzblatt I*, 1554e1582, 1999.
- Belzile N, Lang CY, Chen YW, Wang M (2008) The competitive role of organic carbon and dissolved sulfide in controlling the distribution of mercury in freshwater lake sediments. *Sci Total Environ* 405:226-238.
- Bennett B, Dudas MJ (2003) Release of arsenic and molybdenum by reductive dissolution of iron oxides in a soil with enriched levels of native arsenic. *J Environ Eng Sci* 2:265-272.
- BGR (2008) Flächenrepräsentative Hintergrundwerte für As, Sb, Be, Mo, Co, Se, Tl, U und V in Böden Deutschlands aus länderübergreifender Sicht, [http://www.lfu.bayern.de/boden/hintergrundwerte/doc/bgr\\_hintergrundwerte\\_2008.pdf](http://www.lfu.bayern.de/boden/hintergrundwerte/doc/bgr_hintergrundwerte_2008.pdf). Last accessed Oktober 01, 2013.
- Bloom NS, Preus E, Katon J, Hiltner M (2003) Selective extractions to assess the biogeochemically relevant fractionation of inorganic mercury in sediments and soils. *Anal Chim Acta* 479:233-248.
- Böhme F, Rinklebe J, Stark HJ, Mothes S, Neue HU (2005) A simple field method to determine mercury volatilization from soils. *Environ Sci Poll Res* 12:133-135.
- Bohn HL, Myer RA, O'Connor GA (2001) *Soil chemistry*. 3rd edn. John Wiley & Sons, New York.

- Brümmer G (1974) Redox potentials and redox processes of manganese, iron and sulfur-compounds in hydromorphic soils and sediments. *Geoderma* 12:207-222.
- Burns RG (1976) The uptake of cobalt into ferromanganese nodules, soils, and synthetic manganese (IV) oxides. *Geochim Cosmochim Acta* 40:95-102.
- Canario J, Branco V, Vale C (2007) Seasonal variation of monomethylmercury concentrations in surface sediments of the Tagus Estuary (Portugal). *Environ Poll* 148:380-383.
- Carbonell A, Porthouse JD, Mulbah CK, Delaune RD, Patrick WH (1999) Metal solubility in phosphogypsum-amended sediment under controlled pH and redox conditions. *J Environ Qual* 28:232-242.
- Carrera J, Vicent T, Lafuente FJ (2001) Influence of temperature on denitrification of an industrial high-strength nitrogen wastewater in a two-sludge system. *Water SA* 29:11-16.
- Charlatchka R, Cambier P (2000) Influence of reducing conditions on solubility of trace metals in contaminated soils. *Water Air Soil Poll* 118:143-168.
- Chen H, Yang X, Perkins C (2003) Trend and variability of total gaseous mercury (TGM) in the state of connecticut, U.S.A. during 1997-1999. *Water Air Soil Poll* 151:103-116.
- Choi H-D, Holsen TM (2009) Gaseous mercury emissions from unsterilized and sterilized soils: The effect of temperature and UV radiation. *Environ Poll* 157:1673-1678.
- Chuan MC, Shu GY, Liu JC (1996) Solubility of heavy metals in a contaminated soil: Effects of redox potential and pH. *Water Air Soil Poll* 90:543-556.
- Cobos DR, Baker JM, Nater EA (2002) Conditional sampling for measuring mercury vapor fluxes. *Atmos Environ* 36:4309-4321.
- Cogger CG, Kennedy PE, Carlson D (1992) Seasonally saturated soils in the Puget Lowland: 2. Measuring and interpreting redox potentials. *Soil Sci* 154:50-58.
- Collins RN, Kinsela AS (2010) The aqueous phase speciation and chemistry of cobalt in terrestrial environments. *Chemosphere* 79:763-771.
- Connell WE, Patrick WH (1968) Sulfate reduction in soil - effects of redox potential and pH. *Science* 159:86-87.

- Cornelis G, Van Gerven T, Vandecasteele C (2012) Antimony leaching from MSWI bottom ash: Modelling of the effect of pH and carbonation. *Waste Manage* 32:278-286.
- Cornu S, Cattle JA, Samouelian A, Laveuf C, Guilherme LRG, Alberic P (2009) Impact of redox cycles on manganese, iron, cobalt, and lead in nodules. *Soil Sci Soc Am J* 73:1231-1241.
- Costa M, Liss PS (1999) Photoreduction of mercury in sea water and its possible implications for Hg<sup>0</sup> air-sea fluxes. *Mar Chem* 68:87-95.
- Costa M, Liss PS (2000) Photoreduction and evolution of mercury from seawater. *Sci Total Environ* 261:125-135.
- Counter SA, Buchanan LH (2004) Mercury exposure in children: a review. *Toxicol Appl Pharm* 198:209-230.
- David MB, Gentry LE, Smith KM, Kovacic DA (1997) Carbon, plant and temperature control of nitrate removal from wetland mesocosms. *Trans Ill Acad Sci* 90:103-112.
- Deschamps E, Ciminelli VST, Weidler PG, Ramos AY (2003) Arsenic sorption onto soils enriched in Mn and Fe minerals. *Clays Clay Min.* 51:197-204.
- Deuel LE, Swoboda AR (1972) Arsenic solubility in a reduced environment. *Soil Sci Soc Am Proc* 36:276-278.
- Devai I, Patrick Jr WH, Neue H-U, DeLaune RD, Kongchum M, Rinklebe J (2005) Methyl mercury and heavy metal content in soils of rivers Saale and Elbe (Germany). *Anal Lett* 38:1037-1048.
- Dmytriw R, Mucci A, Lucotte M, Pichet P (1995) The partitioning of mercury in the solid components of dry and flooded forest soils and sediments from a hydroelectric reservoir, Quebec (Canada). *Water Air Soil Poll* 80:1099-1103.
- Du Laing G, Rinklebe J, Vandecasteele B, Meers E, Tack FMG (2009) Trace metal behaviour in estuarine and riverine floodplain soils and sediments: A review. *Sci Total Environ* 407:3972-3985.

- During A, Rinklebe J, Bohme F, Wennrich R, Stark HJ, Mothes S, Du Laing G, Schulz E, Neue H-U (2009) Mercury volatilization from three floodplain soils at the central Elbe River, Germany. *Soil Sed Contamin* 18:429-444.
- Farmer JG, Paterson E, Bewley RJF, Geelhoed JS, Hillier S, Meeussen JCL, Lumsdon DG, Thomas RP, Graham MC (2006) The implications of integrated assessment and modeling studies for the future remediation of chromite ore processing residue disposal sites. *Sci Total Environ* 360:90-97.
- Favre F, Boivin P, Wopereis MCS (1997) Water movement and soil swelling in a dry, cracked Vertisol. *Geoderma* 78:113-123.
- Fendorf SE (1995) Surface-reactions of chromium in soils and waters. *Geoderma* 67:55-71.
- Fendorf S, Eick MJ, Grossl P, Sparks DL (1997) Arsenate and chromate retention mechanism on goethite. 1. Surface structure. *Environ Sci Technol* 31:315-320.
- Fendorf S, Kocar BD (2009) Biogeochemical processes controlling the fate and transport of arsenic: Implications for south and southeast Asia. *Adv Agron* 104:137-164.
- Fiedler S, Kalbitz K (2003) Concentrations and properties of dissolved organic matter in forest soils as affected by the redox regime. *Soil Sci* 168:793-801.
- Fiedler S, Sommer M (2004) Water and redox conditions in wetland soils - Their influence on pedogenic oxides and morphology. *Soil Sci Soc Am J* 68:326-335.
- Filella M, Williams PA (2012) Antimony interactions with heterogeneous complexants in waters, sediments and soils: A review of binding data for homologous compounds. *Chemie Erde - Geochem* 72:49-65.
- Fitzgerald WF, Lamborg CH, Hammerschmidt CR (2007) Marine biogeochemical cycling of mercury. *Chem Rev* 107:641-662.
- Fleming EJ, Mack EE, Green PG, Nelson DC (2006) Mercury methylation from unexpected sources: Molybdate-inhibited freshwater sediments and an iron-reducing bacterium. *Appl Environ Microbiol* 72:457-464.



- Gabriel MC, Williamson DG (2004) Principal biogeochemical factors affecting the speciation and transport of mercury through the terrestrial environment. *Environ Geochem Heal* 26:421-434.
- Gambrell RP, Delaune RD, Patrick Jr. WH (1991) Redox processes in soils following oxygen depletion. In: Jackson MB, Davies DD, Lambers H (ed) *Plant life under oxygen deprivation*, 1st edn. SPB Academic Publishing, USA, pp 101-117.
- Garcia-Miragaya J, Page AL (1976) Influence of ionic-strength and inorganic complex-formation on sorption of trace amounts of Cd by montmorillonite. *Soil Sci Soc Am J* 40:658-633.
- Gilmour CC, Henry EA, Mitchell R (1992) Sulfate stimulation of mercury methylation in freshwater sediments. *Environ Sci Technol* 26:2281-2287.
- Goldberg S, Forster HS, Godfrey CL (1996) Molybdenum adsorption on oxides, clay minerals, and soils. *Soil Sci Soc Am J* 60:425-432.
- Google Earth (2013a) Northern Germany. <http://www.earth.google.de>. Last accessed Oktober 19, 2013.
- Google Earth (2013b) Sampling sites (a) Wupper in Leichlingen and (b) Elbe in Hohnstorf. <http://www.earth.google.de>. Last accessed Oktober 19, 2013.
- Gotoh S, Patrick WH (1972) Transformation of manganese in a waterlogged soil as affected by redox potential and pH. *Soil Sci Soc Am Proc* 36:738-742.
- Grybos M, Davranche M, Gruau G, Petitjean P (2007) Is trace metal release in wetland soils controlled by organic matter mobility or Fe-oxyhydroxides reduction?. *J Coll Interface Sci* 314:490-501.
- Grybos M, Davranche M, Gruau G, Petitjean P, Pedrot M (2009) Increasing pH drives organic matter solubilization from wetland soils under reducing conditions. *Geoderma* 154:13-19.
- Gustafsson JP (2001) Modeling the acid-base properties and metal complexation of humic substances with the Stockholm Humic Model. *J Colloid Interf Sci* 244:102-112.

- Gustin MS, Stamenkovic J (2005) Effect of watering and soil moisture on mercury emissions from soils. *Biogeochemistry* 76:215-232.
- Gustin MS, Engle M, Ericksen J, Lyman S, Stamenkovic J, Xin M (2006) Mercury exchange between the atmosphere and low mercury containing substrates. *Appl Geochem* 21:1913-1923.
- Hamburg Port Authority (2005) Studie zur Schadstoffbelastung der Sedimente im Elbeeinzugsgebiet. [http://bis.tutech.de/B/Content/download/Elbe\\_finale\\_250106\\_mit\\_Kraemer\\_und\\_HPA-Groessenreduziert\\_mit\\_Kennwort.pdf](http://bis.tutech.de/B/Content/download/Elbe_finale_250106_mit_Kraemer_und_HPA-Groessenreduziert_mit_Kennwort.pdf). Last accessed 20 August 2013.
- Harmon SM, King JK, Gladden JB, Chandler GT, Newman LA (2004) Methylmercury formation in a wetland mesocosm amended with sulfate. *Environ Sci Technol* 38:650-656.
- Hem JD, Roberson CE, Lind CJ (1985) Thermodynamic stability of CoOOH and its coprecipitation with manganese. *Geochim Cosmochim Acta* 49:801-810.
- Hess RE, Blanchar RW (1977) Dissolution of arsenic from waterlogged and aerated soil. *Soil Sci Soc Am J* 41:861-865.
- Hintelmann H, Wilken RD (1995) Levels of total mercury and methylmercury compounds in sediments of the polluted Elbe river - Influence of seasonally and spatially varying environmental-factor. *Sci Total Environ* 166:1-10.
- Hintelmann H (2010) Organomercurials. Their formation and pathways in the environment. In: Sigel A, Sigel H, Sigel RKO (eds) *Metal ions in life sciences*, 7th edn. RSC Publishing, London.
- Hirner AV, Hippler J (2011) Trace Metal(loid)s (As, Cd, Cu, Hg, Pb, PGE, Sb, and Zn) and their Species. In: Wilderer P (ed) *Treatise on Water Science* (3), Elsevier Academic Press, Oxford, pp 31-57.
- Hooda PS (2010) *Trace elements in soils*. John Wiley & Sons, New York.
- James BR, Bartlett RJ (1983) Behavior of chromium in soils. 5. Fate of organically complexed Cr(III) added to soil. *J Environ Qual* 12:169-172.

- Jiang J, Xu R, Wang Y, Zhao A (2008) The mechanism of chromate sorption by three variable charge soils. *Chemosphere* 71:1469-1475.
- Johansson K, Iverfeldt A (1994) The relation between mercury content in soil and the transport of mercury from small catchments in Sweden. In: Watras CJ, Huckabee JW (ed) *Mercury pollution Integration and Synthesis*, 1st edn. Lewis, Boca Raton, Ann Arbor, London, Tokyo, pp 323-328.
- Jonsson S, Skyllberg U, Björn E (2010) Substantial Emission of Gaseous Monomethylmercury from Contaminated Water-Sediment Microcosms. *Environ Sci Technol* 44:278-283.
- Kabata-Pendias A, Mukherjee AB (2007) *Trace elements from soil to human*. 1st edn. Springer, Berlin, Heidelberg, New York.
- Kay JT, Conklin MH, Fuller CC, O'Day PA (2001) Processes of nickel and cobalt uptake by a manganese oxide forming sediment in Pinal Creek, globe mining district, Arizona. *Environ Sci Technol* 35:4719-4725.
- Kerin EJ, Gilmour CC, Roden E, Suzuki MT, Coates JD, Mason RP (2006) Mercury methylation by dissimilatory ironreducing bacteria. *Appl Environ Microbiol* 72:7919-7921.
- King JK, Kostka JE, Frischer ME, Saunders FM (2000) Sulfate-reducing bacteria methylate mercury at variable rates in pure culture and in marine sediments. *Appl Environ Microbiol* 66:2430-2437.
- Klemm W, Greif A, Broekaert JAC, Siemens V, Junge FW, van der Veen A, Schultze M, Duffek A (2005) A study on arsenic and the heavy metals in the Mulde river system. *Acta Hydrochim Hydrobiol* 33:475-491.
- Knechtenhofer LA, Xifra IO, Scheinost AC, Fluhler H, Kretzschmar R (2003) Fate of heavy metals in a strongly acidic shooting-range soil: small-scale metal distribution and its relation to preferential water flow. *J Plant Nutr Soil Sci* 166:84-92.
- Kocman D, Horvat M, Kotnik J (2004) Mercury formation in contaminated soils from the Idrija mercury mine region. *J Environ Monit* 6:696-703.

- LABO (2003) Hintergrundwerte für anorganische und organische Stoffe in Böden. [https://www.labo-deutschland.de/documents/LABO-HGW-Text\\_4e3.pdf](https://www.labo-deutschland.de/documents/LABO-HGW-Text_4e3.pdf). Last accessed 22 July, 2013.
- LANUV (2003) Hintergrundwerte für anorganische und organische Stoffe in Oberböden Nordrhein-Westfalens. Landesumweltamt Nordrhein-Westfalens, Düsseldorf. [http://www.lanuv.nrw.de/boden/bodenschutz/HGW\\_Internet\\_2003-3.pdf](http://www.lanuv.nrw.de/boden/bodenschutz/HGW_Internet_2003-3.pdf). Last accessed May 10, 2013.
- Li P, Feng XB, Qiu GL, Shang LH, Li ZG (2009) Mercury pollution in Asia: a review of the contaminated sites. *J Hazard Mater* 168:591-601.
- Li YC, Ge Y, Zhang CH, Zhou QS (2010a) Mechanisms for high Cd activity in a red soil from southern China undergoing gradual reduction. *Aust J Soil Res* 48:371-384.
- Li ZG, Feng X, Li P, Liang L, Tang SL, Wang SF, Fu XW, Qiu GL, Shang LH (2010b) Emissions of air-borne mercury from five municipal solid waste landfills in Guiyang and Wuhan, China. *Atmos Chem Phys* 10: 3353-3364.
- Lindberg SE, Zhang H, Gustin M, Vette A, Marsik F, Owens J, Casimir A, Ebinghaus R, Edwards G, Fitzgerald C, Kemp J, Kock HH, London J, Majewski M, Poissant L, Pilote M, Rasmussen P, Schaedlich F, Schneeberger D, Sommar J, Turner R, Wallschläger D, Xiao Z (1999) Increases in mercury emissions from desert soils in response to rainfall and irrigation. *J Geophys Res* 104:21879-21888.
- Liu G, Cabrera J, Allen M, Cai Y (2006) Mercury characterization in a soil sample collected nearby the DOE Oak Ridge Reservation utilizing sequential extraction and thermal desorption method. *Sci Total Environ* 369:384-392.
- Maggi C, Berducci MT, Bianchi J, Giani M, Campanella L (2009) Methylmercury determination in marine sediment and organisms by Direct Mercury Analyser. *Anal Chim Acta* 641:32-36.
- Manceau A, Drits VA, Silvester E, Bartoli C, Lanson B (1997) Structural mechanism of  $\text{Co}^{2+}$  oxidation by the phyllo-manganate buserite. *Am Mineral* 82:1150-1175.

- Mansfeldt T (2003) In situ long-term redox potential measurements in a dyked marsh soil. *J Plant Nutr Soil Sci* 166:210-219.
- Mansfeldt T (2004) Redox potential of bulk soil and soil solution concentration of nitrate, manganese, iron, and sulfate in two Gleysols. *J Plant Nutr Soil Sci* 167:7-16.
- Mansfeldt T, Overesch M (2013) Arsenic mobility and speciation in a Gleysol with petroglycic properties: A field and laboratory approach. *J Environ Qual* 42:1130-1141.
- Martell A, Smith R, Motekaitis R (2004) NIST critically selected stability constants of metal complexes. 1st edn. National Institute of Standards and Technology, Gaithersburg.
- Masscheleyn PH, Delaune RD, Patrick WH (1991) Effect of redox potential and pH on arsenic speciation and solubility in a contaminated soil. *Environ Sci Technol* 25:1414-1419.
- Massmann G, Greskowiak J, Dunnbier U, Zuehlke S, Knappe A, Pekdeger A (2006) The impact of variable temperatures on the redox conditions and the behaviour of pharmaceutical residues during artificial recharge. *J Hydrol* 328:141-156.
- McLaren RG, Lawson DM, Swift RS (1986) Sorption and desorption of cobalt by soils and soil components. *J Soil Sci* 37:413-426.
- Meers E, Unamuno VR, Du Laing G, Vangronsveld J, Vanbroekhoven K, Samson R, Diels L, Geebelen W, Ruttens A, Vandegheuchte M, Tack FMG (2006) Zn in the soil solution of unpolluted and polluted soils as affected by soil characteristics. *Geoderma* 136:107-119.
- Mehra OP, Jackson ML (1960) Iron oxide removal from soils and clays by a dithionite-citrate system buffered with sodium bicarbonate. *Clays Clay Miner* 7:317-327.
- Mirlean N, Roisenberg A, Chies JO (2007) Metal contamination of vineyard soils in wet subtropics (southern Brazil). *Environ Poll* 149:10-17.
- Mitsunobu S, Harada T, Takahashi Y (2006) Comparison of antimony behaviour with that of arsenic under various soil redox conditions. *Environ Sci Technol* 40:7270-7276.
- Mitsunobu S, Takahashi Y, Terada Y (2010) *u*-XANES Evidence for the reduction of Sb(V) to Sb(III) in soil from Sb mine tailing. *Environ Sci Technol* 44:1281-1287.

- Morel FMM, Kraepiel AML, Amyot M (1998) The chemical cycle and bioaccumulation of mercury. *Ann Rev Ecol Systemat* 29:543-566.
- Murray JW, Dillard JG (1979) The oxidation of cobalt(II) adsorbed on manganese dioxide. *Geochim Cosmochim Acta* 43:781-787.
- Olivie-Lauquet G, Gruau G, Dia A, Riou C, Jaffrezic A, Henin O (2001) Release of trace elements in wetlands: Role of seasonal variability. *Water Res* 35:943-952.
- Onstott TC, Chan E, Polizzotto ML, Lanzon J, DeFlaun MF (2011) Precipitation of arsenic under sulfate reducing conditions and subsequent leaching under aerobic conditions. *Appl Geochem* 26:269-285.
- Oremland RS, Stolz JF (2005) Arsenic, microbes and contaminated aquifers. *Trends Microbiol* 13:45-49.
- Oscarson DW, Huang PM, Hammer UT, Liaw WK (1983) Oxidation and sorption of arsenite by manganese-dioxide as influenced by surface-coatings of iron and aluminium-oxides and calcium-carbonate. *Water Air Soil Poll* 20:233-244.
- Overesch M, Rinklebe J, Broll G, Neue H-U (2007) Metals and arsenic in soils and corresponding vegetation at Central Elbe river floodplains (Germany). *Environ Poll* 145:800-812.
- Patrick WH (1966) Apparatus for controlling the oxidation-reduction potential of waterlogged soils. *Nature* 212:1278-1279.
- Patrick WH, Williams BG, Moraghan JT (1973) Simple system for controlling redox potential and pH in soil suspension. *Soil Sci Soc Am J* 37:331-332.
- Patrick WH, Jugsujinda A (1992) Sequential reduction and oxidation of inorganic nitrogen, manganese, and iron in flooded soil. *Soil Sci Soc Am J* 56:1071-1073.
- Paul EA, Clark FE (1996) *Soil microbiology and biochemistry*, 2 edn. Academic Press, San Diego.

- Pelfrêne A, Gassama N, Grimaud D (2009) Mobility of major-, minor- and trace elements in solutions of a planosolic soil: Distribution and controlling factors. *Appl Geochem* 24:96-105.
- Rabenhorst MC (2005) Biologic zero: A soil temperature concept. *Wetlands* 25:616-621.
- Rabenhorst MC, Castenson KL (2005) Temperature effects on iron reduction in a hydric soil. *Soil Sci* 170:734-742.
- Rai D, Sass BM, Moore DA (1987) Chromium(III) hydrolysis constants and solubility of chromium(III) hydroxide. *Inorg Chem* 26:345-349.
- Ravenscroft P, Brammer H, Richards KS (2009) *Arsenic pollution: A global synthesis*. 1st edn. Wiley-Blackwell, Chichester.
- Reddy KR, Delaune RD (2008) *Biogeochemistry of Wetlands: Science and applications*. CRC Press, Boca Raton, London, New York.
- Rennert T, Mansfeldt T (2005) Iron-cyanide complexes in soil under varying redox conditions: speciation, solubility and modelling. *Eur J Soil Sci* 56:527-536.
- Rinklebe J, Doring A, Overesch M, Wennrich R, Stark HJ, Mothes S, Neue H-U (2008) Optimization of a simple field method to determine mercury volatilization from soils- Examples of 13 sites in floodplain ecosystems at the Elbe River (Germany). *Ecol Eng* 35:319-328.
- Rinklebe J, Doring A, Overesch M, Du Laing G, Wennrich R, Stärk H-J, Mothes S (2010) Dynamics of mercury fluxes and their controlling factors in large Hg-polluted floodplain areas. *Environ Poll* 158:308-318.
- Rogers RD (1979) Volatility of Hg from soils amended with various Hg compounds. *Soil Sci Soc Am J* 43:289-291.
- Rogers RD, McFarlane JC (1979) Factors influencing the volatilization of mercury from soil. *J Environ Qual* 8:255-260.
- Schenk R (1994) *Verteilung und Dynamik von Schwermetallen in Sedimenten der Wupper*. Dissertation an der Universität Düsseldorf, Düsseldorf.

- Schlüter K (2000) Review: evaporation of mercury from soils. An integration and synthesis of current knowledge. *Environ Geol* 39:249-271.
- Schulz-Zunkel C, Krueger F (2009) Trace metal dynamics in floodplain soils of the river Elbe: A review. *J Environ Qual* 38:1349-1362.
- Schuster E (1991) The behavior of mercury in the soil with special emphasis on complexation and adsorption processes - A review of the literature. *Water Air Soil Poll* 56:667-680.
- Schwab AP, Lindsay WL (1983) The effect of redox on the solubility and availability of manganese in a calcareous soil. *Soil Sci Soc Am J* 47:217-220.
- Schwertmann U (1964) Differenzierung der Eisenoxide des Bodens durch photochemische Extraction mit saurer Ammoniumoxalatlösung. *Z Pflanzenernaehr Düng Bodenkd* 105:194-202.
- Shams KM, Tichy G, Sager M, Peer T, Bashar A, Jozic M (2009) Soil contamination from tannery wastes with emphasis on the fate and distribution of tri- and hexavalent chromium. *Water Air Soil Poll* 199:123-137.
- Shi J, Liang L, Jiang G, Jin X (2005) The speciation and bioavailability of mercury in sediments of Haihe River, China. *Environ Int* 31:357-365.
- Simpson SL, Rosner J, Ellis J (2000) Competitive displacement reactions of cadmium, copper, and zinc added to a polluted, sulfidic estuarine sediment. *Environ Toxicol Chem* 19:1992-1999.
- Skylberg U, Qian J, Frech W, Xia K, Bleam WF (2003) Distribution of mercury, methyl mercury and organic sulphur species in soil, soil solution and stream of a boreal forest catchment. *Biogeochemistry* 64:53-76.
- Smedley PL, Kinniburgh DG (2002) A review of the source, behaviour and distribution of arsenic in natural waters. *Appl Geochem* 17:517-568.
- Smith RM, Martell AE (1976) *Critical stability constants: Inorganic complexes*. 4th edn. Plenum Press, New York.



- Song X, Van Heyst B (2005) Volatilization of mercury from soils in response to simulated precipitation. *Atmos Environ* 39:7494-7505.
- Takahashi Y, Ohtaku N, Mitsunobu S, Yuita K, Nomura M (2003) Determination of the As(III)/As(V) ratio in soil by X-ray absorption near-edge structure (XANES) and its application to the arsenic distribution between soil and water. *Anal Sci* 19:891-896.
- van der Geest HG, León Paumen M (2008) Dynamics of metal availability and toxicity in historically polluted floodplain sediments. *Sci Total Environ* 406:419-425.
- Vaughan KL, Rabenhorst MC, Needelman BA (2009) Saturation and temperature effects on the development of reducing conditions in soils. *Soil Sci Soc Am J* 73:663-667.
- Viollier E, Inglett PW, Hunter K, Roychoudhury AN, Van Cappellen P (2000) The ferrozine method revisited: Fe(II)/Fe(III) determination in natural waters. *Appl Geochem* 15:785-790.
- Wallschläger D, Hintelmann H, Evans RD, Wilken RD (1995) Volatilization of demethylmercury and elemental mercury from river Elbe floodplain soils. *Water Air Soil Poll* 80:1325-1329.
- Wallschläger D, Desai MVM, Wilken R-D (1996) The role of humic substances in the aqueous mobilization of mercury from contaminated floodplain soils. *Water Air Soil Poll* 90:507-520.
- Wallschläger D, Kock HH, Schroeder WH, Lindberg SE, Ebinghaus R, Wilken RD (2000) Mechanism and significance of mercury volatilization from contaminated floodplains of the German river Elbe. *Atmos Environ* 34:3745-3755.
- Wallschläger D, Kock HH, Schroeder WH, Lindberg SE, Ebinghaus R, Wilken RD (2002) Estimating gaseous mercury emissions from contaminated floodplain soils to the atmosphere with simple field measurement techniques. *Water Air Soil Poll* 135:39-54.
- Wan X-M, Tandy S, Hockmann K, Schulin R (2013) Changes in Sb speciation with water-logging of shooting range soils and impacts on plant uptake. *Environ Poll* 172:53-60.
- Wang G, Staunton S (2006) Evolution of water-extractable copper in soil with time as a function of organic matter amendments and aeration. *Eur J Soil Sci* 57:372-380.

- Warner KA, Roden EE, Bonzongo J-C (2003) Microbial mercury transformation in anoxic freshwater sediments under iron-reducing and other electron-accepting conditions. *Environ Sci Technol* 37:2159–2165.
- Wasserman JC, Amouroux D, Wasserman MAV, Donard OFX (2002) Mercury speciation in sediments of a tropical coastal environment. *Environ Technol* 23:899-910.
- Weber F-A, Voegelin A, Kretzschmar R (2009) Multi-metal contaminant dynamics in temporarily flooded soil under sulfate limitation. *Geochim Cosmochim Acta* 73:5513-5527.
- Weber F-A, Hofacker AF, Voegelin A, Kretzschmar R (2010) Temperature dependence and coupling of iron and arsenic reduction and release during flooding of a contaminated soil. *Environ Sci Technol* 44:116-122.
- Weigand H, Mansfeldt T, Baumler R, Schneckenburger D, Wessel-Bothe S, Marb C (2010) Arsenic release and speciation in a degraded fen as affected by soil redox potential at varied moisture regime. *Geoderma* 159:371-378.
- Wichard T, Mishra B, Myneni SCB, Bellenger J-P, Kraepiel AML (2009) Storage and bioavailability of molybdenum in soils increased by organic matter complexation. *Nature Geosci* 2:625-629.
- Wightwick AM, Mollah MR, Partington DL, Allinson G (2008) Copper fungicide residues in Australian vineyard soils. *J Agricult Food Chem* 56:2457-2464.
- Wilson SC, Lockwood PV, Ashley PM, Tighe M (2010) The chemistry and behaviour of antimony in the soil environment with comparisons to arsenic: A critical review. *Environ Poll* 158:1169-1181.
- WRB and IUSS Working Group (2006) World reference base for soil resources. A framework for international classification, correlation and communication. World soil resources reports 103. FAO, Rome.
- Xu N, Christodoulatos C, Braida W (2006) Adsorption of molybdate and tetrathiomolybdate onto pyrite and goethite: Effect of pH and competitive anions. *Chemosphere* 62:1726-1735.

- Yu X, Li H, Pan K, Yan Y, Wang WX (2012) Mercury distribution, speciation and bioavailability in sediments from the Pearl River Estuary, Southern China. *Mar Pollut Bull* 64:1699-1704.
- Zachara JM, Fredrickson JK, Smith SC, Gassman PL (2001) Solubilization of Fe(III) oxide-bound trace metals by a dissimilatory Fe(III) reducing bacterium. *Geochim Cosmochim Acta* 65:75-93.
- Zeien H, Brümmer GW (1989) Chemische Extraktion zur Bestimmung von Schwermetallbindungsformen in Böden. *Mitt Dtsch Bodenkdl Ges* 59:505-510.
- Zhang H, Lindberg SE (1999) Processes influencing the emission of mercury from soils: A conceptual model. *J Geophys Res* 104:21889-21896.
- Zhang H, Lindberg S, Gustin M, Xu X (2003) Toward a better understanding of mercury emissions from soils. In: Cai Y, Braids OC (ed) *Biogeochemistry of Environmentally Important Trace Elements*, 1st edn. ACS Symposium Series San Diego, pp 246-261.
- Zhi-Guang L (1985) Oxidation-Reduction Potential. In: Tian-ren Y (ed) *Physical chemistry of paddy soils*. 1st edn. Springer Verlag, Berlin, pp 1-26.

## **Erklärung**

Ich versichere, dass ich die von mir vorgelegte Dissertation selbständig angefertigt, die benutzten Quellen und Hilfsmittel vollständig angegeben und die Stellen der Arbeit – einschließlich Tabellen, Karten und Abbildungen –, die anderen Werken im Wortlaut oder dem Sinn nach entnommen sind, in jedem Einzelfall als Entlehnung kenntlich gemacht habe; dass diese Dissertation noch keiner anderen Fakultät oder Universität zur Prüfung vorgelegen hat; dass sie – abgesehen von unten angegebenen Teilpublikationen – noch nicht veröffentlicht worden ist sowie, dass ich eine solche Veröffentlichung vor Abschluss des Promotionsverfahrens nicht vornehmen werde. Die Bestimmungen der Promotionsordnung sind mir bekannt. Die von mir vorgelegte Dissertation ist von Prof. Dr. Tim Mansfeldt betreut worden.

Nachfolgend genannte Teilpublikationen wurden veröffentlicht:

- Hindersmann I., Mansfeldt T. (2014): Trace element solubility in a multi metal-contaminated soil as affected by redox conditions. *Water, Air, and Soil Pollution*, DOI. 10.1007/s11270-014-2158-8.
- Hindersmann I., Hippler J., Hirner A. V., Mansfeldt T. (2014): Mercury volatilization from a floodplain soil during a simulated flooding event. *Journal of soil and sediments*, 14: 1549-1558.

Lindlar, den 10.10.2014

Iris Hindersmann

## **Lebenslauf**

### **Persönliche Angaben**

---

Name Iris Hindersmann, geb. Bördgen  
Geburtstag/-ort 27.08.1982 in Lindlar  
Nationalität Deutsch  
Familienstand verheiratet, 1 Kind

### **Schulbildung**

---

08/1993 Realschule Lindlar  
- 07/1995  
08/1995 St. Angela Gymnasium Wipperfürth  
- 07/2002  
Schulabschluss Abitur am 29.06.2002 (Note 2,2)

### **Studium**

---

Studiengang 10/2002 - 09/2008  
Diplom Geographie an der Universität zu Köln  
Nebenfächer Geologie, Volkswirtschaftslehre und Verkehrswissenschaften  
Abschluss Diplom Geographie am 19.09.2008 (Note 1,9)  
Diplomarbeit Staubfilterung durch Straßenbäume - Ahorn-, Linden- und Ginkgo-  
blättern als Zwischenspeicher staubgebundener Metallimmissionen

### **Praktika**

---

07/ 2002 Schönauer GmbH Marienheide  
- 08/2002 *Übersetzungen, Aktenarchivierung, weitere Bürotätigkeiten*  
08/2005 Bundesanstalt für Straßenwesen  
- 09/2005 *Mitarbeit am Projekt „Staubbelastung an Bundesautobahnen“ und  
Auswertung von Verkehrsdaten*

## Lebenslauf

---

10/2006  
- 12/2006  
Stadt Köln, Abteilung für Verkehrstechnik  
*Datenerfassung für die Projekte Bike & Ride und Park & Ride, Mitarbeit an Projekten „Verkehrliche Umgestaltung der Altstadt Köln“ und „Umgestaltung Neusserstraße Köln“, eigenes Projekt „Erweiterung der des Park & Ride Parkplatzes in Weiden-West“*

## Nebentätigkeit

---

11/2005  
- 05/2008  
studentische Hilfskraft am Lehrstuhl Prof. Dr. U. Radtke  
*Laborarbeit mit Probenvorbereitung und Probenanalyse mit AAS, ICP-MS und C/N-Analysator; Betreuung von Studenten bei Diplomarbeiten*

07/2008  
- 09/2008  
studentische Hilfskraft am Lehrstuhl Prof. Dr. T. Mansfeldt  
*Laborarbeit mit Probenvorbereitung und Probenanalyse mit AAS, ICP-MS und C/N-Analysator; Mitarbeit am Projekt „Ermittlung und Beurteilung des Mobilisierungspotenzials von Arsen in Böden“*

## Berufstätigkeit

---

10/2008  
- 07/2009  
wissenschaftliche Hilfskraft am Lehrstuhl Prof. Dr. T. Mansfeldt  
*Laborarbeit mit Probenvorbereitung und Probenanalyse mit AAS, ICP-MS und Photometer; Betreuung von Studenten bei Diplomarbeiten und Praktika, Antragsstellung für Forschungsmittel zum Thema „Ausgasung von Quecksilber“ bei der Deutschen Forschungsgemeinschaft und der RheinEnergieStiftung*

10/2009  
- 09/2012  
wissenschaftliche Mitarbeiterin am Lehrstuhl Prof. Dr. T. Mansfeldt  
*Vorbereitung einer Promotion zum Thema „Quecksilberausgasung aus Böden“, Betreuung von Diplom- und Bachelorarbeiten und Leitung eines Seminars zum Thema „Relief und Boden,“ Mitorganisation des Kongresses "International Geographical Congress 2012"*

10/2012  
- 04/2013  
Arbeitssuchend und Abschlussarbeiten an meiner Promotion

seit 05/2013  
Elternzeit